

**Spatial Analysis of Emergency Medical Service Calls
and Extreme Heat in King County, WA**

Aubrey DeVine

A thesis
submitted in partial fulfillment of the
requirements for the degree of

Master of Science

University of Washington

2017

Committee:

Tania Busch Isaksen

Michael Yost

Edmund Seto

Program Authorized to Offer Degree:

Environmental Health

©Copyright 2017

Aubrey DeVine

University of Washington

Abstract

Spatial Analysis of Emergency Medical Service Calls and Extreme Heat in King County, WA

Aubrey DeVine

Chair of the Supervisory Committee:

Lecturer Tania Busch Isaksen PhD, MPH

Department of Environmental and Occupational Health Sciences

Background: Climate change is increasing allergens and environmental degradation, changing vector ecology, and intensifying severe weather and extreme heat (Center for Disease Control, 2016). Average global temperatures are steadily rising, along with the number and intensity of extreme heat events. Extreme heat has significant human health effects such as heat exhaustion, heat stress, and heatstroke. It is well known that morbidity, mortality, and hospitalizations increase during extreme heat events (Busch Isaksen et al., 2016; Medina-Ramon et al., 2006), but this research analyzed the relationship between extreme heat and Emergency Medical Service (EMS) calls.

Objective: Building off the previous research of Calkins et al. (2016) who found increased relative risks for both Basic Life Support (BLS) calls and Advanced Life Support (ALS) calls on a King County-wide extreme heat day compared to a non-heat day, this study redefined the spatial scale of analysis to 4km x 7.5km grid cells. Additionally, it looked at county-wide

temporal variations in EMS calls as well as examined the relationship of local extreme heat relative risk with community-level grid cell variables: percent tree canopy, percent impervious surfaces, total population, percent of population by age groups, percent development, percent water, average median income, and percent poverty.

Methods: Using previously collected EMS data from Emergency Medical Technicians (EMT) of Seattle and King County Division of the Department of Public Health and meteorological data from the Climate Impacts Group, this study analyzed the spatial relationship between extreme heat and EMS calls in King County, WA. EMS data from the summer months of May 1st to September 30th, 2007 to 2012, was evaluated by calculating local crude relative risks for both BLS and ALS calls in each grid cell using a poisson regression and an *a priori* extreme heat threshold from Calkins et al. (2016). The more precise spatial scale in this analysis portrayed the spatial variation of heat risk in King County.

Results: For both BLS and ALS calls, there were increased estimated relative risks of an EMS call on an extreme heat day compared to a non-heat day during peak humidex hours (3-6pm) and after peak humidex hours (6-10pm). Crude relative risks varied in grid cells across the county; significant increases in relative risk for BLS call volumes ranged from 1.05 (95% CI: 1.01, 1.09) to 4.13 (95% CI: 1.65, 10.32), while significant increases in relative risk for ALS call volumes ranged from 1.21 (95% CIs: 1.11, 1.32) to 6.50 (95% CIs: 1.06, 40.03). The results of regression models between relative risk and predictor variables showed negative correlations with grid cell percent impervious surface and positive correlations with grid cell percent canopy.

Conclusion: The spatial distribution of EMS calls showed crude relative risks significantly vary across King County. Due to the strong negative relationship with impervious surfaces, we hypothesized BLS calls may be caused by recreational activities on extreme heat days. On the other hand, ALS calls were more severe ambulance calls and may be more driven by the presence of chronic health conditions. Further research and more patient specific variables need to be collected in order to confirm these hypotheses.

Table of Contents

Abstract.....	3
Acknowledgements.....	12
Dedication.....	13
Background and Significance.....	14
Specific Aims.....	22
Methods.....	24
Exposure Data.....	24
EMS Data Preparation.....	25
Social and Environmental Data Preparation.....	31
Data Analysis.....	33
Temporal Analysis.....	33
Relative Risk Analysis.....	34
Analysis of Community-Level Predictors.....	36
Results.....	40
Temporal Analysis.....	40
Relative Risk Analysis.....	45
Analysis of Community-Level Predictors.....	52
Discussion.....	80
Limitations and Further Research.....	91

Conclusion.....	95
References.....	96
Appendix.....	102
1. Data Cleaning and Preparation.....	105
2. Data Cleaning and Preparation ArcGIS Instructions.....	110
3. Data Cleaning and Preparation R Markdown.....	113
4. Methods Temporal Analysis.....	134
5. Methods + Results Temporal Analysis R Markdown.....	136
6. Methods Relative Risk Analysis.....	137
7. Methods + Results Relative Risk R Markdown.....	139
8. Methods Analysis of Community-Level Predictors.....	148
9. Methods + Results Analysis of Community-Level Predictors R Markdown.....	151

List of Tables

Table 1: EMS Call Volume Descriptive Statistics for Spatial Analysis.....	27
Table 2: Tally of Peak Humidex Times.....	42
Table 3: ALS and BLS Call Counts by Time Block on All Days.....	42
Table 4: BLS Call Rates per Average Heat/Non-Heat Day and Time Block.....	44
Table 5: ALS Call Counts per Average Heat/Non-Heat Day and Time Block.....	44
Table 6: BLS Categorical Ranges.....	55
Table 7: BLS Median Income Results.....	56
Table 8: BLS Percent Impervious Surface Results.....	58
Table 9: BLS Percent Canopy Results.....	60
Table 10: BLS Percent Poverty Results.....	61
Table 11: BLS Log Population Results.....	63
Table 12: BLS Age Group Results.....	64
Table 13: BLS Model Subset Selection 1 Results with Total Population of Grid Cell.....	66
Table 14: BLS Model Subset Selection 2 Results with Age Group Population of Grid Cell.....	67
Table 15: ALS Variable Categorical Ranges.....	68
Table 16: ALS Median Income Results.....	69
Table 17: ALS Percent Impervious Surface Results.....	70
Table 18: ALS Percent Canopy Results.....	72
Table 19: ALS Percent Poverty Results.....	74
Table 20: ALS Log Population Results.....	75
Table 21: ALS Age Group Results.....	76
Table 22: ALS Model Subset Selection 1 Results with Total Population of Grid Cell.....	77
Table 23: ALS Model Subset Selection 2 Results with Age Group Population of Grid Cell.....	78
Table 24: Moran’s I Spatial Autocorrelation Results.....	78
Table 25: Grid Cells Above Calkins et al. (2016) BLS Crude Relative Risk Estimate.....	80

Table 26: Grid Cells Above Calkins et al. (2016) ALS Crude Relative Risk Estimate.....81

Appendix Tables:

Table 3.1: BLS Call Counts per Hour.....116

Table 6.1: BLS Call Counts by Time Block.....136

Table 6.2: BLS Call Counts by Time Block and Heat/Non-Heat Day.....136

Table 8.1: BLS RR and Predictor Variables by Grid Cell.....141

Table 8.2: ALS RR and Predictor Variables by Grid Cell.....144

List of Figures

Figure 1: ALS and BLS Call Counts per Geocode.....	28
Figure 2: ALS and BLS Call Counts per Grid Cell.....	29
Figure 3: ALS Call Counts by Grid Cell Quartiles.....	30
Figure 4: BLS Call Counts by Grid Cell Quartiles.....	30
Figure 5: Seattle Weather Station Humidex Every 10 Days.....	40
Figure 6: Seattle Weather Station Extreme Heat Days.....	41
Figure 7: SeaTac Weather Station Extreme Heat Days.....	41
Figure 8: BLS Crude Relative Risks per Grid Cell.....	46
Figure 9: Histogram of BLS Relative Risks.....	47
Figure 10: ALS Crude Relative Risks per Grid Cell.....	48
Figure 11: Histogram of ALS Relative Risks.....	49
Figure 12: Average ALS and BLS Call Counts per Heat Day.....	51
Figure 13: Correlation Coefficient Plots.....	54
Figure 14: BLS Median Income Quartiles.....	57
Figure 15: BLS Percent Impervious Surface Quartiles.....	59
Figure 16: BLS Percent Canopy Quartiles.....	60
Figure 17: BLS Percent Poverty Quartiles.....	62
Figure 18: BLS Log Population Quartiles.....	63
Figure 19: ALS Median Income Quartiles.....	69
Figure 20: ALS Percent Impervious Surface Quartiles.....	71
Figure 21: ALS Percent Canopy Quartiles.....	73
Figure 22: ALS Percent Poverty Quartiles.....	74
Figure 23: ALS Log Population Quartiles.....	75
Figure 24: BLS Crude RR with City Labels.....	83
Figure 25: ALS Crude RR with City Labels.....	84

Appendix Figures:

Figure 3.1: BLS Quadratic Relationship.....	121
Figure 3.2: Histogram of BLS Call Count Frequency.....	121
Figure 3.3: Histogram of BLS RR without Grid Cell Exclusion.....	123
Figure 3.4: Histogram of BLS RR with Grid Cell Exclusion.....	124
Figure 3.5: Correlation Coefficients.....	126
Figure 3.6: BLS RR and Log Population.....	127
Figure 3.7: BLS RR and Percent Age Younger than 5.....	127
Figure 3.8: BLS RR and Percent Age 5-14.....	128
Figure 3.9: BLS RR and Percent Age 15-44.....	128
Figure 3.10: BLS RR and Percent Age 45-64.....	129
Figure 3.11: BLS RR and Percent Age 65-84.....	129
Figure 3.12: BLS RR and Percent Age Older than 85.....	130
Figure 3.13: BLS RR and Percent Water Quartiles.....	130
Figure 3.14: BLS RR and Percent Development Quartiles.....	131
Figure 3.15: BLS RR and Percent Canopy Quartiles.....	131
Figure 3.16: BLS RR and Percent Impervious Surface Quartiles.....	132
Figure 3.17: BLS RR and Median Income Quartiles.....	132
Table 3.18: BLS RR and Percent Poverty Quartiles.....	133
Figure 8.1: King County Grid Cell ID Labels.....	147

ACKNOWLEDGEMENTS

A huge thank you should be given to everyone on the author's thesis committee including Dr. Tania Busch Isaksen, Dr. Michael Yost, and Dr. Edmund Seto. Each one of these professionals contributed their time, guidance, and expertise to the final product of this thesis project. In particular, the author would like to thank her advisor Tania Busch Isaksen for her constant involvement and support throughout this entire process. Furthermore, Dr. Paul Sampson from the statistics department and biostatistics PhD student Phuong Vu provided endless support and guidance through the data analysis process.

Public Health Seattle, King County Division of Emergency Medical Services, and The Climate Impacts Group were crucial to the completion of this thesis providing complete and accurate data. Additionally, the author thanks the University of Washington School of Public Health Department of Environmental and Occupational Health Sciences for the excellent education, support, and funding.

Other thanks go out to Brian High for technical support, Miriam Calkins for guidance, as well as the patience and praise of the author's family members and friends.

DEDICATION

This thesis is dedicated to my grandparents,
Richard and Clare DeVine and Dorothy and Frank Jones,
for their constant encouragement and support to pursue my higher education

BACKGROUND AND SIGNIFICANCE

Climate Change

According to the United States Climate and Health Assessment, the US average temperatures are predicted to rise 3°F to 10°F by the end of the century (U.S. Global Change Research Program, 2016). With this temperature increase, will come more frequent and intense heat waves along with harmful effects to human health. Scientists predict that for every doubling of carbon dioxide, there will be at least a 1.9-4.5°C increase in temperature (Roe & Baker, 2007; Knutti & Hegerl, 2008) with chances of a 7.1°C to 12°C increase (Meinshausen 2009; Montenegro et al. 2007). Sherwood and Huber (2010), argued that a global mean increase of 7°C would begin to limit the habitability in some regions of the world. Areas which expose humans to 35°C for extended periods of time will induce hyperthermia due the inability for dissipation of metabolic heat to occur (Sherwood & Huber, 2010). As climate change increases global temperatures, an increase in heat exposure is reasonably expected to increase heat-related morbidity and mortality.

Heat and Health Effects

Extreme temperatures make it difficult for the body to regulate its internal temperature giving heat the potential to cause many illnesses such as heatstroke and heat exhaustion along with negative consequences on chronic cardiovascular disease, respiratory disease and diabetes-related conditions (U.S. Global Change Research Program, 2016). However, temperature alone is not an accurate measure of human thermal comfort. In fact, heat effects

on human health result from a combination of air temperature, wind speed, air humidity, and radiation (Hoppe, 1999). Therefore, many studies define heat through other measurements such as heat index (or apparent temperature), heat islands, or humidex (Wong et al., 2016; Golden et al., 2008; Alessandrini et al., 2011; Bassil, et al., 2011; Kue & Dyer, 2013). Humidex, a measure of temperature, humidity, and vapor pressure, was used to measure heat for this analysis.

There are many studies analyzing the morbidity and mortality of extreme heat; nearly all concluded that extreme heat does, in fact, increase the risk of death, hospitalizations, and other illnesses, especially related to the cardiovascular and respiratory systems (Busch Isaksen et al., 2014; Busch Isaksen et al., 2016; Medina-Ramon et al., 2006). Furthermore, researchers have also observed the effects of heat on ambulance calls. Studies vary in their measurement of heat and study design, but most found increased call volumes during heat event compared to non-heat events or increased call counts per degree increase in heat (Kue & Dyer, 2013; Golden et al., 2008; Alessandrini et al., 2011; Bassil et al., 2011; Dolney & Sheridan, 2006). Specifically, Bassil et al. (2011) concluded, on average, there was a 16% increase in heat related illness calls for every one point increase in humidex. Furthermore, and Dolney & Sheridan (2006) calculated a 10% increase in ambulance calls on heat days compared to non-heat days. Additionally, Dolney & Sheridan (2006) observed spatial variations in call volumes; while the urban core experienced the greatest increase in call counts, industrial and recreational areas had the greatest percent call volume increases on hot days.

Temporal Effects of Heat Stress

To further assess the increase in health effects related to heat, some research has found temporal variations in heat burden and health outcomes throughout the day. As one would expect, Davis et al. (2003) observed mortality rates were significantly correlated to peak temperatures. In addition, Golden et al. (2008) discovered the time between peak solar irradiation and maximum diurnal temperature had the greatest volume of medical dispatches in Phoenix, AZ. Based on these trends, we also hypothesize that EMS call volumes in King County would be greatest during peak humidex hours.

Environmental and Social Vulnerability

There are impending effects on health from climate change temperature increases for everyone worldwide. However, research shows that there are many environmental and social factors which can influence heat burden in the general population. Environmental predictors such as altitude, distance to water, vegetation, and impervious surfaces are all effect modifiers which can have significant impacts on local temperature. In addition, socioeconomic factors are potential confounders which may impact an individual's thermal comfort and overall health.

Environmental factors which influence local temperatures include buildings, open space, population density, normalized vegetation index (NDVI), vegetation, impervious surface, bare soil, and water (Buyantuyev & Wu, 2010; Yuan & Bauer, 2007; Laing & Weng, 2008; Weng et al., 2006; Weng & Yang, 2004). The amount of shade from vegetation cover, is strongly correlated with ground and air temperatures (Buyantuyev & Wu, 2010; Jenerette et al., 2011; Zhang et al.,

2011; Johnson & Wilson, 2009; Huang et al., 2011). As a result, increased vegetation is also associated with decreased heat stress and heat-related deaths (Johnson & Wilson, 2009; Harlan et al., 2006; Johnson et al., 2012). Water is another important parameter for temperature. There are numerous Swedish studies that show distance to large water bodies greatly influence urban temperature patterns with temperature decreasing as distance decreases (Carrega, 1995; Tveito & Førland, 1999; Lindqvist, 1970; Svensson et al., 2002). According to Kestens et al. (2011), land cover and NDVI are the two most important predictors for surface temperature. More specifically, Elaiou and Svensson (2003) used both environmental factors and weather patterns in its analysis, concluding that on cloudy days, altitude and percent impervious surfaces/build-up are the two most important environmental factors explaining temperature variations, while on clear, calm days, distance from water explains most of the temperature variation, with sky-view factor, percent impervious surfaces, and percent vegetation as additional variables.

Furthermore, many studies analyzed political, economic and social factors that contribute to environmental inequity. The highest extreme heat related morbidity and mortality occur in cities and upon marginalized groups such as the poor, minority and elderly populations (Congressional Black Caucus Foundation, 2004; Center for Disease Control, 2004; International Federation of Red Cross, 2003). Socioeconomic factors associated with heat mortality include ethnic minorities, poverty, poor education, elderly (≥ 65 years), crime, and living alone (Harlan et al., 2006; Huang et al., 2011; Klinenberg, 2002; Semenza et al., 1996;

Ghumman & Horney, 2016; Wong et al., 2016). Low income and minority groups are more likely to live in neighborhoods with high densities, sparse vegetation, and little open space which significantly increases their exposure to heat stress (Harlan et al., 2006). To further exacerbate socioeconomic heat burden disparities, low income and minority communities generally do not have the same access to protective resources such as air conditioning, which many claim to be the most effective heat stress prevention factor (Naughton et al., 2002; Kilbourne, 2002; Rogot et al., 1992). Income level can affect the patient's health status and ability to treat/manage pre-existing health conditions making them more susceptible to heat illness. For example, diabetes was shown to have a strong correlation with low income or below the poverty line households (Kolpak and Wang, 2017) in addition to a strong correlation with extreme heat vulnerability (U.S. Global Change Research Program, 2016; Calkins et al., 2016). Drug or alcohol use and the ability to seek help is another confounding factor correlated to both low socioeconomic status (Huang et al., 2011) and increased risk of an EMS call in an extreme heat event (Calkins et al. 2016). It is important to consider these socioeconomic factors when comparing spatial distributions of extreme heat risk. This research accounted for a number of social and environmental predictors for heat vulnerability including impervious surfaces, development, water, tree canopy, and neighborhood-level median income, and percent poverty.

Pacific Northwest Vulnerability

In particular, the Pacific Northwest is susceptible to the health effects of extreme heat.

Research by Curriero et al. (2002) determined that while cold temperatures have a greater effect on mortality in certain southern cities, heat exacerbated mortality in the northern cities. Since southern cities generally experience more extreme heat than the colder climates of northern cities, neither region adapts well to opposite extreme temperatures. Reid et al. (2009) specifically pointed out the Pacific Coast as one of the most vulnerable regions to extreme heat due to four factors: social and environmental vulnerability from education, race, and green space; social isolation; air conditioning prevalence; and the proportion of elderly and diabetes in the population. As a northern county near the Pacific Coast, research indicates that King County may be vulnerable to the health impacts of the increasing extreme heat events. Given these concerns, it is unclear how well King County is prepared for increases in extreme heat due to climate change. If the county is not prepared, there may be elevated heat related health effects on extreme heat days. As climate change increases the number and duration of extreme heat events in the Pacific Northwest, the general public, public officials, and medical professionals need to take steps to mitigate and adapt to these impacts.

King County EMS System

The EMS dataset was obtained from EMT personnel of Seattle and King County Division of the Department of Public Health. Between the summer months, defined as May 1st to September 30th, of 2007-2012, 6 Advanced Life Support (ALS) agencies responded to 121,794 King County Emergency Medical Service calls and 30 Basic Life Support (BLS) agencies responded to 441,119 King County Emergency Medical Service calls. On average, that was

around 165,000 BLS calls per year and 45,000 ALS calls per year. The call classification was determined by the dispatcher based on the level of care they believed the patient needed from the information provided over the phone. BLS units sent out emergency medical technician-trained firefighters who could aid in non-invasive care, while ALS units were equipped with paramedics authorized for advanced patient care such as intubation, manual defibrillation, and intravenous medications.

Preliminary Studies

Previous published studies by Tania Busch Isaksen and Miriam Calkins have shown there are heat related health effects in King County, WA (Busch Isaksen et al. 2014; Busch Isaksen et al. 2016; Calkins et al. 2016). Busch Isaksen et al. (2014 and 2016) discovered an increase in morbidity and mortality during high humidex days. Calkins et al. (2016) used the same EMS and meteorological datasets as this analysis, and also concluded there was a county-wide increase in EMS calls on extreme heat days in King County. Specifically, Calkins et al. (2016) found the best fit model to be an extreme heat threshold at the 95th percentile humidex value (29.7°C) for BLS calls and at the 99th percentile humidex value (36.7°C) for ALS calls. This threshold was determined from the maximum likelihood best-fit of the model based on the Akaike Information Criterion (AIC). Although data analysis was only done on summer months, the threshold incorporated full year humidex values. On a county-wide extreme heat day, basic Life Support (BLS) calls increased by 8% (99th humidex threshold) and Advanced Life Support (ALS) calls increased by 14% (95th humidex threshold) compared to a county-wide non-heat day. The

analysis discovered an increased risk of EMS calls on a heat day for abdominal/genito-urinary, alcohol/drug, anaphylaxis/allergy, cardiovascular, metabolic/endocrine, diabetes, neurological, heat illness and dehydration, and psychological conditions.

Calkin et al. (2016) found a daily average of all the max humidex values interpolated in King County to define a heat day and a non-heat day as well as county-wide call volumes. However, when the distribution of humidex values and call volumes were spatially mapped in the county, the western side had much higher call volumes and higher humidex values compared to the eastern half. Therefore, a county-wide humidex average may have biased the results because it could lower humidex values for calls in the western half of the county and increase humidex values for calls in the eastern half of King County. In order to improve the spatial accuracy of the relationship between extreme heat days and EMS calls, this analysis used the 4 km by 7.5 km meteorological grid block scale where temperature data was interpolated to find a local relative risk of EMS calls on extreme heat days compared to non-heat days. This helped reduce the type II error in misclassification of EMS calls due to extreme heat in King County and aid the EMS division in planning for EMS call volumes on local extreme heat days. Using the BLS and ALS extreme heat threshold for EMS calls, this study built on Calkins et al. (2016) by evaluating the relative risk of EMS calls on local heat days vs non-heat days throughout each grid cell in King County, WA. In addition, it looked at the relationship of the risk with community-level variables.

SPECIFIC AIMS

The goal of this project was to assist the Emergency Medical Service (EMS) Division in preparing for extreme heat days by closely examining the effects of extreme heat on EMS call volumes in different areas of King County, in addition to analyzing the effects of environmental and social predictors of local heat risks. Moreover, it described statistics on the county-wide temporal variation of BLS and ALS call volumes at different times of the day. The research expanded on a previous study by Calkins et al. (2016) by re-defining the spatial scale of the analysis from the county-wide scale to 4 km by 7.5 km grid cells where temperature data was interpolated throughout King County. Calkins et al. (2016) used the same EMS and meteorological datasets, but performed her analysis on a county-wide scale with county averages of daily heat and EMS call volumes. It defined extreme heat days as days with a county-wide average humidex above the 95th and 99th percentile of year round humidex values in King County for BLS and ALS calls, respectively. This analysis used Calkins et al.'s (2016) extreme heat thresholds for BLS and ALS calls, but refined the spatial scale from the entire county to 4 km by 7.5 km grid cells to find a local relative risk of EMS calls on local extreme heat days compared to non-heat days for each grid cell. Furthermore, this research analyzed potential community-level variables which could influence local relative risk variations. Based on previous research in other regions of the US, areas with high percent vegetation, low percent impervious surfaces, low elderly populations, and high economic statuses were correlated with lower heat burdens. Therefore, we also hypothesized these factors would be

significant predictors for the risk of an EMS call in extreme heat. Additionally, we hypothesized the greatest call volumes would occur during the peak humidex hours. This was innovative research that had never been explored in King County, WA, and was very practical information for the Emergency Medical Services department. Based on this detailed analysis, EMS Divisions in King County can better plan and organize for local extreme heat events.

METHODS

This research utilized MySQL Workbench, ESRI ArcGIS, and RStudio. MySQL was used for EMS and Meteorological data storage, ArcGIS mapped EMS call locations and matched them to grid cell attributes, while RStudio ran the analysis.

Exposure Data

The University of Washington's Climate Impacts Group provided all of the meteorological data from a historical (1915-2012) meteorological dataset. This dataset was based on Parameter-elevation Relationships of Independent Slopes Model (PRISM) (Maurer et al. 2002). The climate data from the National Oceanic and Atmospheric Administration's Global Historic Climate Network-Daily (GHCN) database was modeled on a 4 km by 7.5 km (1/16th resolution) block grid from land surface stations throughout the world and was developed at Oregon State University. Each grid block point included daily minimum, maximum, and average temperature; relative humidity; and precipitation. From this, a minimum, maximum, and average humidex value for each day was calculated using the following equation.

$$f(T,H) = T + (5/9) * (v - 10); v = (6.112 * 10^{(7.5T)/(237.7+T)}) * H / 100$$

T=temperature (Celsius); H=humidity (%); V=vapor pressure

Humidex was a temperature index that better described the human perception of heat by taking the effects of humidity into account as well as air temperature. It portrayed a more accurate measure of heat burden than temperature alone (Santee, 2005).

EMS Data Preparation

The EMT personnel of Seattle and King County Division of the Department of Public Health prepared, de-identified, and supplied the University of Washington researchers with Emergency Medical Service call data. These data included information on EMS calls from the mid-1990s until 2012, but this research focused on six recent years: 2007-2012. These years contained the most accurate and well documented information due to King County EMS' transition to electronic data collection. These EMS data included two datasets depending on the severity of the call, one for BLS calls and another for ALS calls. However, despite whether an ALS unit responded, all calls in King County received a BLS response, so this was the main dataset of the analysis. Each dataset included a wide range of information for each EMS call including date, location, patient age and sex, diagnosis type, the level of care the patient received, and transportation needs.

For the temporal analysis, data preparation excluded calls with missing location variable and missing notified call times. The calls were grouped into four time blocks: low humidex (4-7am), before peak humidex (7am-3pm), peak humidex (3-6pm), and after peak humidex (6-10pm) based on hourly Weather Underground data (hourly humidex were not available in the Climate Impacts Group's dataset). Overnight hours were excluded from this analysis; extreme heat was not an important factor during overnight hours and including calls overnight would only increase the potential for bias from non-heat related calls, such as late night exhaustion or alcohol induced accidents. Data exclusion decreased the number of BLS calls from 441,119 to

351,208 and ALS calls from 121,794 to 97,052.

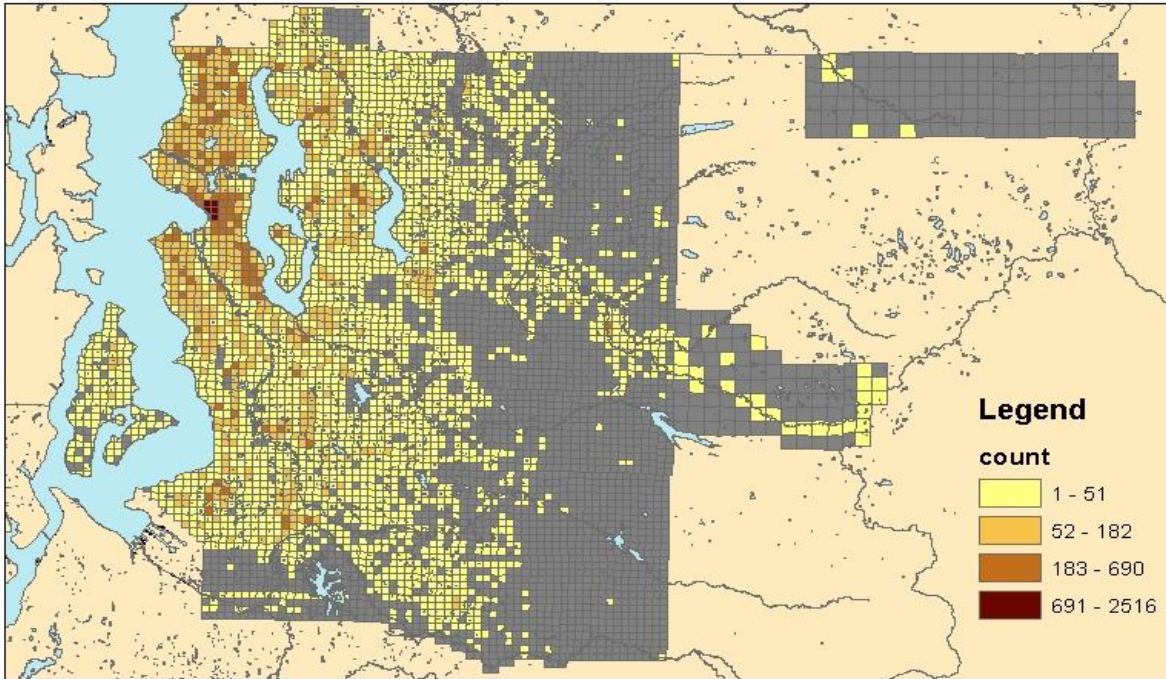
Before the spatial analysis, all EMS calls were mapped based on their geocode (Figure 1), and all geocodes were assigned to a 4km by 7.5km grid cell. The grid cells were the spatial unit for this analysis. Nearly all grid cells had a center point, where daily temperature, humidity, and vapor pressure data were interpolated in order to calculate a daily humidex value for the grid cell. However, a handful of grids in King County were missing land surface stations because they were located over water. The few with missing center points were matched to the meteorological data from the nearest bordering center point. Based on this gridded model, each of the 221 grid cells in King County had a maximum humidex value for every day in the study time frame, and each day in every grid cell was classified as a local heat day or non-heat day based on if the humidex value was above or below the extreme heat threshold (29.7 °C for BLS calls and 36.7 °C for ALS calls) determined *a priori* from Calkins et al. (2016). Data preparation excluded calls with a missing geocode (location) variable, calls located on the outer border of the grid cell map, and calls in grid cells with 5 or less total calls for the entire study period. BLS call counts decreased from 441,119 to 434,853 and ALS call counts decreased from 121,794 to 120,638.

Table 1: EMS Call Volume Descriptive Statistics for Spatial Analysis

	BLS	ALS
Total Calls	441,119	121,794
Total Calls After Data Preparation	434,853	120,638
Average Number of Calls Per Day	474	131
Number of Grid Cells with >5 Total EMS Calls	124	116
Average Number of Calls Per Day Per Grid Cell	3.82	1.13
Average Number of Local Heat Days Per Grid Cell	149	28
Average Number of Local Non-Heat Days Per Grid Cell	769	890
Average Number of Calls Per Heat Day Per Grid Cell	4.10	1.27
Average Number of Calls Per Non-Heat Day Per Grid Cell	3.77	1.13

Figure 1: ALS and BLS Call Counts per Geocode

ALS Calls Per Geocode



BLS Calls Per Geocode

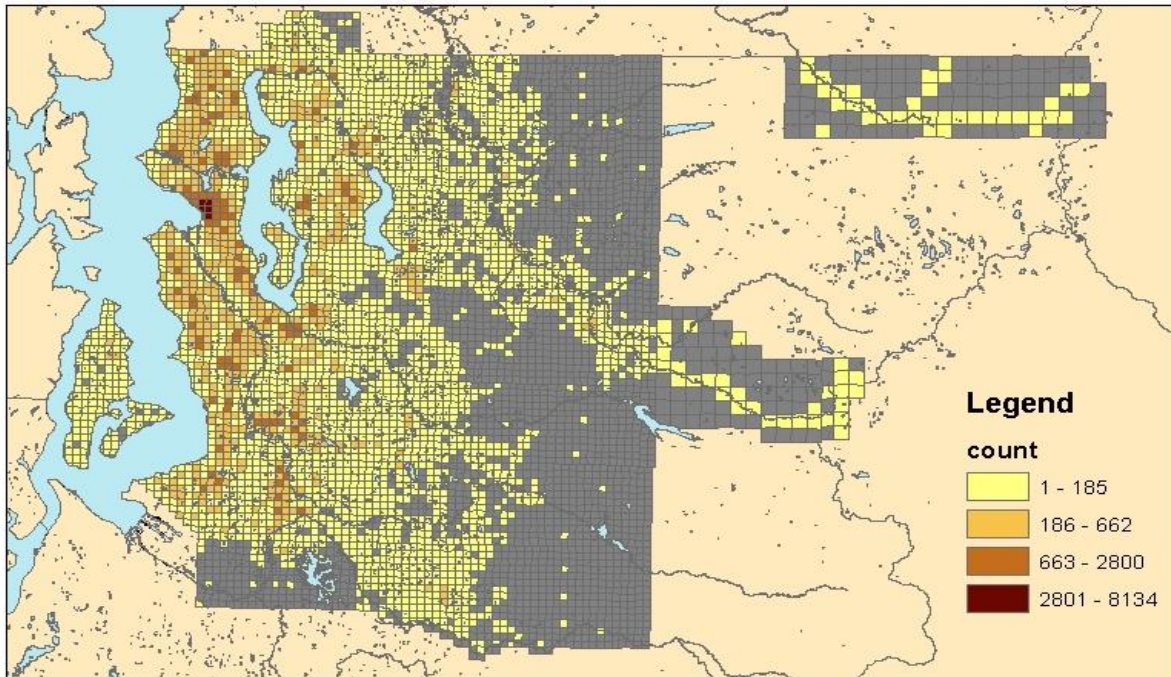
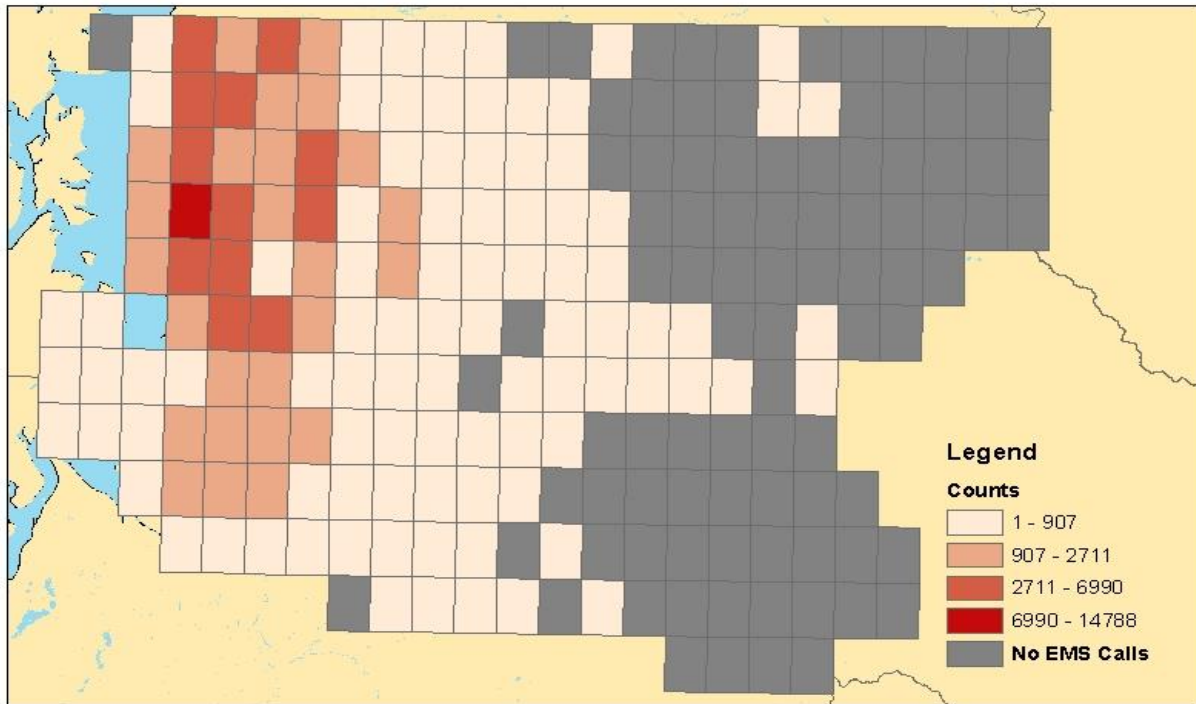


Figure 2: ALS and BLS Call Counts per Grid Cell

ALS Calls Per Grid Cell



BLS Calls Per Grid Cell

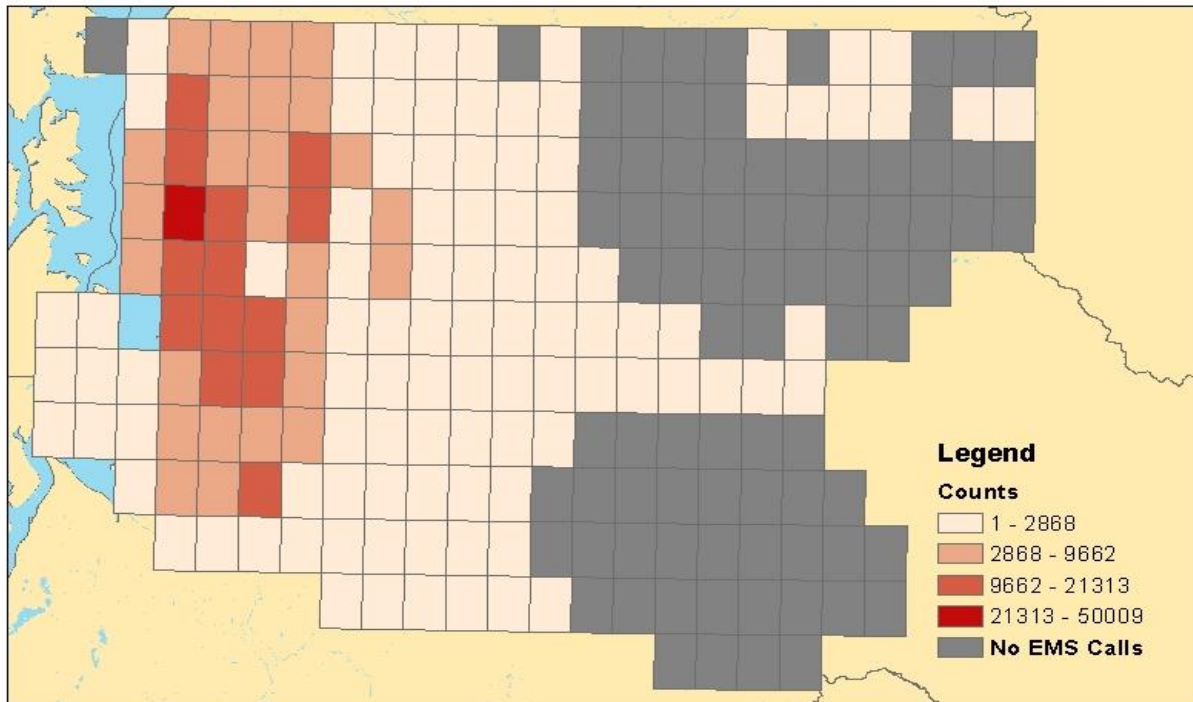


Figure 3: ALS Call Counts by Grid Cell Quartiles

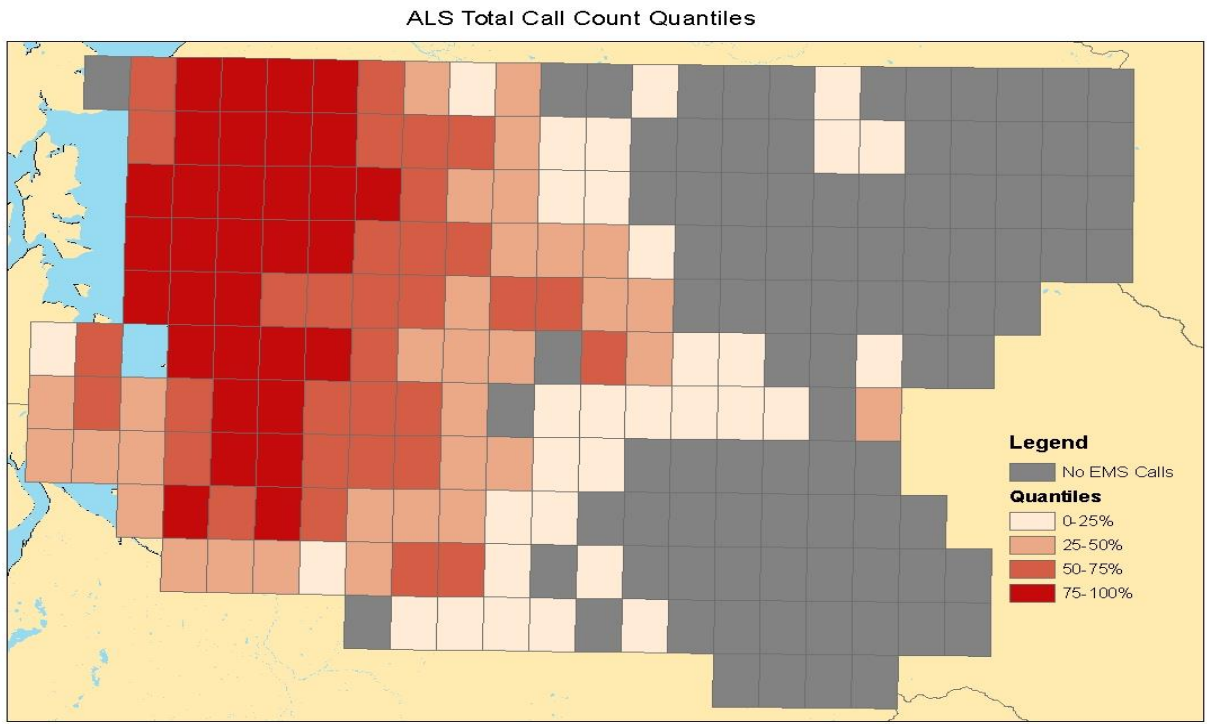
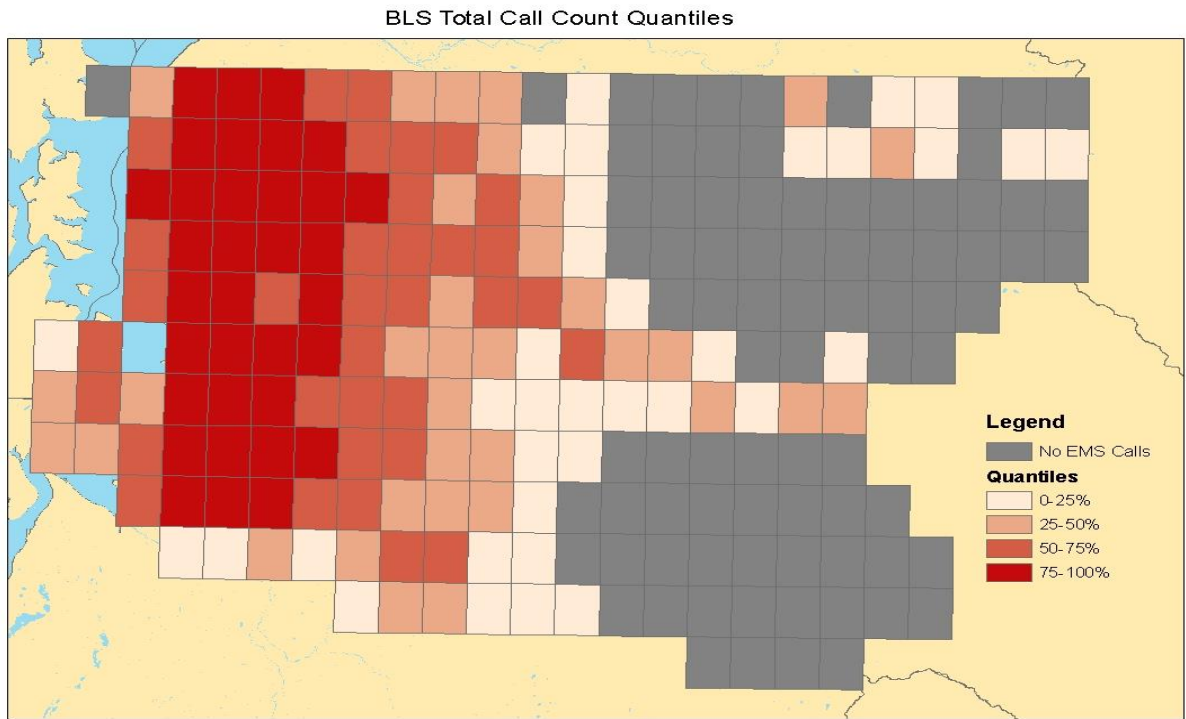


Figure 4: BLS Call Counts by Grid Cell Quartiles



Population and Socioeconomic Data

Population data by age (U.S. Census Bureau, *Age Groups and Sex: 2010*, 2010), median household income (U.S. Census Bureau, *2010 Income in the Past 12 Months*, 2010), and population below poverty (U.S. Census Bureau, *2010 Poverty Status in the Past 12 Months by Sex and Age*, 2010) were downloaded from the US Census Bureau American Fact Finder database. These data were downloaded on the census tract level in Washington State for 2010. In order to extrapolate estimates to the grid cell scale, the intersect tool in ArcGIS found the percent of each census tract inside a given grid cell. These percentages were used as weights to find approximated population (total and by age groups) and poverty population for each grid cell. The estimated total population in each intersected area between census tracts and grid cells aided in finding a weighted median income for each grid cell. The authors did not think it was necessary to collect data for more than one year; there was already some uncertainty with the data due to extrapolation from census tract level to the grid cell scale, and the study frame was a short six year time period. Lastly, poverty and median income data were categorized into four quartiles in order to compare the risk of an EMS call on an extreme heat day compared to a non-heat day between grid cells with the lowest and highest economic status.

Environmental Data

The environmental factors, tree canopy, impervious surfaces, and land cover were all downloaded from the Washington State Department of Ecology as raster data from remote sensing imagery techniques (Department of Ecology and NOAA, 2016). The tree canopy and

impervious surface data was from 2006, and included a percentage value for each pixel in the county. After the data was uploaded into ArcGIS, the zonal statistics as table tool estimated the average percent tree canopy and percent impervious surfaces for each grid cell. While the land cover data was collected in a more recent year (2011), this data classified each pixel as a certain land type instead of a percentage. These land types included High Intensity Development, Medium Intensity Development, Low Intensity Development, and Open Water. The high, medium, and low development pixels were based on vegetation and percent impervious surface. In order to find percent water and percent developed areas, raster values for water and developed land were separately reclassified from the land cover raster dataset as 0 (not water or not developed land) and 1 (water or developed land) using the reclassify tool in spatial analyst tools of ArcCatalog. Then, zonal statistics was utilized with the newly reclassified data in order to find the percent of the grid cell that was water and the percent that was developed land. Because percent development was based off of the percent impervious surface data, these two datasets were highly correlated. In addition, percent impervious surface and percent canopy were more accurate data sets because they use a percentage scale per pixel instead of classifying the pixel as developed or not developed. As a result, we made the decision not to use the percent development or percent water datasets in this analysis. Finally, grid cells were categorized into quartiles for each environmental trait in order to compare grids with the lowest percent environmental trait to the grid cells with highest percentages.

Temporal Analysis

The first specific aim was to describe the temporal variations in BLS and ALS calls throughout King County. Due to limitations in statistical power for the grid cell spatial scale, this aim simply looked at county-wide temporal variations. Based on previous research, we hypothesized call volumes would be related to the time of day when humidex was the highest. Our meteorological dataset only included daily max, min, and average temperature values. Therefore, in order to analyze temporal variations in call volumes, it was necessary to collect historical hourly meteorological data from Weather Underground (Weather Underground, 2007-2012).

There were two meteorological stations in King County from Weather Underground: Seattle and SeaTac. Data was collected from both of these stations for hourly temperature, humidity, and vapor pressure every 10 days as well as for all 23 county-wide extreme heat days defined by Calkins et al. (2016). An hourly humidex value was calculated using the same humidex equation from the Climate Impact Group's meteorological dataset, and graphs of humidex and time were plotted to show daily fluctuations of heat. The data from every 10 days throughout the study period were compared to data from extreme heat days in order to observe any temporal humidex differences between extreme heat days and an average non-heat day. In addition, the two stations were compared to see if there were any variations in peak temperature based on location in the county. The hottest hours of the day were determined based on these graphs.

After the peak humidex time block was determined, countywide EMS call counts were compared between the peak time of day and other non-peak time blocks. Descriptive statistics were calculated for call counts on all days in each time block as well as call counts in each time block on heat and non-heat days. The calls were classified as calls on a heat day or non-heat day based on their local grid cell humidex value. Because each grid cell had a different number of heat and non-heat days, we were unable to calculate a formal relative risk. However, an estimation of the risk of a call in each time block on a heat day compared to a non-heat day was calculated based on the average number of heat days and non-heat days for grid cell with EMS calls across the county.

Relative Risk Analysis

A crude relative risk (RR) using poisson regression estimated the relationship between extreme heat and EMS call counts. It estimated the difference of expected EMS call counts on heat days compared to non-heat days. It was calculated for both BLS and ALS calls in each grid cell, and included calls of all causes and ages. The RR was estimated through the regression model of the log-transformed call counts as follows:

$$\log(\mu_j) = \beta_0 + \beta_1 I_j\{\text{humidex} > \text{threshold}\} + B_2(\text{time}) + B_3(\text{weekend/day of week})$$

Where j indexes the day, μ_j is the expected call count on day j , $I_j\{\text{humidex} > \text{threshold}\}$ is the indicator of a heat day, defined as whether its humidex exceeds a threshold, time is an overall time trend variable for all days in the study period, and $\text{weekend/day of the week}$ is a time trend variable adjusting for differences in call volumes on the weekend or on every day of

the week.

In order to classify days as extreme heat days or non-heat days, this research used a threshold chosen *a priori* based on the research of Calkins et al. (2016). Calkins et al. (2016), used the same meteorological dataset and the Akaike Information Criterion (AIC) to determine the maximum likelihood best fit in the model between the 90th, 95th, and 99th percentile full year humidex values. For the BLS data, the AIC best fit threshold was the 95th percentile humidex value or 29.7 °C, and for the ALS data, the best fit threshold was the 99th percentile humidex value or 36.7 °C. For both BLS and ALS datasets, days with a daily maximum humidex above their respective thresholds were considered extreme heat days.

A generalized linear regression for each grid cell fit the daily call counts by the predictor of interest, heat or non-heat day. The quasi-poisson model with a log link function allowed for flexibility in the mean-variance relationship, accepting over or under dispersion. Because this dataset had many grid cells with 0 calls per day, it was not realistic to assume the variance was always equal to the mean. For statistical power purposes, any grid cell with 5 or fewer total calls during the six year study period was eliminated from the analysis. This excluded 15 grid cells for the BLS dataset and 14 grid cells for the ALS dataset. For each grid cell relative risk, the 95% confidence interval was calculated using the Huber-White sandwich estimate of the standard error. This approach helped correct for heteroscedasticity that could occur from a wide range of variability across the predictor variable (Long and Ervin 2000; White 1980).

Furthermore, this dataset was collected over a period of six years, meaning temporal

correlations in the observations were likely. In order to account for this, the model included some functions of time based on trends in the aggregated data. These functions were determined by fitting a generalized linear model to the overall EMS data. An overall time trend variable was adjusted for in addition to adjusting for certain days of the week. Although this research only looked at the summer months May to September, the time functions were determined from full year trends. These temporal functions were not chosen on time trends in each individual grid cell because of the inefficiency and difficulty to compare relative risks across grid cells if each included different mean models.

Analysis of Community-Level Predictors

LINEAR REGRESSION MODELS:

In order to evaluate the relationship between predictor variables and relative risk variations, each predictor variable was assessed individually in addition to performing a formal model selection process. The model selection process used a combination of best subset selection and cross-validation to identify a single best fit model for BLS and ALS grid cell relative risks. The potential predictors for model selection were grid cell log population, population younger than 5 years old, population 5 to 14 years, population 15-44 years, population 45-64 years, population 65-84 years, and population over 85 years; median household income; percent poverty; percent canopy; percent development; percent water; and percent impervious surface. Models with each predictor variable gave a basic picture of their individual relationship with grid cell relative risk, while a formal model selection process helped assess the

collinearity and interaction between the grid cell predictors and relative risk. The formal model selection built a model that optimally described the data and was predictive for future data using cross-validation to help with the selection procedure.

The best subset selection procedure was a more thorough method than forward and backward stepwise selection, where a separate least square regression was fit for all combinations of the p predictors. Two R programs were considered for the model selection process: Bestglm and Leaps. Using a cross-validated selection process, the best model of all 2^p possibilities was chosen by the statistical program in two stages (James et al., 2013). First, the statistical program fit all $\binom{p}{k}$ models that contained exactly k predictors and identified the models among the $\binom{p}{k}$ models that have the lowest RSS or equivalently highest R^2 . Next, it used the cross-validated prediction error, AIC criterion, to pick the single best fit model.

Again, the potential community-level predictors for this analysis were log population, percent younger than 5, percent 5-14, percent 14-44, percent 45-64, percent 65-84, percent older than 85, percent canopy, percent impervious surfaces, percent below poverty line, percent development, percent water, and median household income for each grid cell. Although, some information was lost when categorizing variables, percent canopy, percent impervious surfaces, percent development, percent water, percent poverty, and percent median income were grouped into quartiles. This categorization compared the differences in mean relative risks between grid cells with the lowest percentages of traits and grid cells with the highest percentages. In addition, plots, descriptive statistics, and correlation coefficients

described and explored the relationships between variables and their effect on relative risk.

Because the grid cell age group variables were a more detailed look at log population, the first model selection did not include the age group populations in order to analyze the overall effect of predictor variables. However, previous extreme heat research did show that age had a significant effect on health and one's vulnerability to extreme heat (Naughton, 2002; Naughton, 2008). Therefore, a second model selection analysis also included the age group variables to see if the age make-up of the community was an important predictive factor for relative risk of an EMS call and how these variables changed the results of the previous model.

SPATIAL AUTOCORRELATION

After the final model selection process, the residuals from each regression were tested for spatial autocorrelation using the Moran's I test. Spatial autocorrelation measured how similar one object was to other nearby objects. It was important to test for because neighboring grids were more likely to have similar attributes than grid cells that were across the county. However, spatially correlated grid cells would violate the statistical assumption that observations were independent from one another. The Moran's I Index Value was calculated from the equation below and significance was assessed through its p-value.

$$I = \frac{N}{\sum_i \sum_i w_{ij}} \frac{\sum_i \sum_i w_{ij} (X_i - \bar{X})(X_j - \bar{X})}{\sum_i (X_i - \bar{X})^2}$$

Where N is the number of number of features indexed by i and j , X is the variable of interest, \bar{X} is the mean of X , and w_{ij} is the spatial weight between feature i and j .

The values of the Moran's index ranged from -1 to +1 and indicated different types of spatial patterns. A value of 0 indicated random dispersion, a value of negative 1 indicated a perfectly spaced checker board, and a value of positive 1 would have a clustered pattern.

RESULTS

Temporal Analysis

Based on Figures 5, 6, and 7, as well as Table 2, 3-6pm were the common hours for peak humidex in the summer months in King County, WA (Weather Underground, 2007-2012).

Harlan et al. (2006) also found this time period was a popular time for people to be outdoors while getting off work or going out for their evening activities. As a result, we expected EMS call volumes in King County to be greatest during this time.

Figure 5: Seattle Weather Station Humidex Every 10 Days

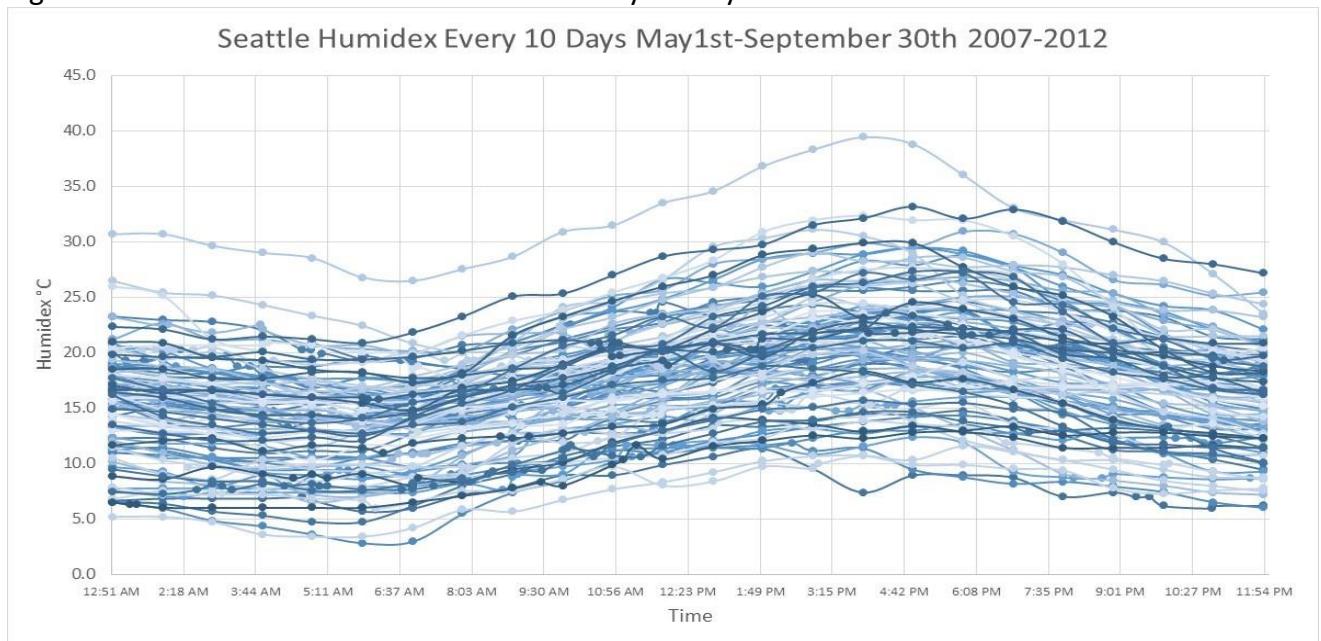


Figure 6: Seattle Weather Station Extreme Heat Days

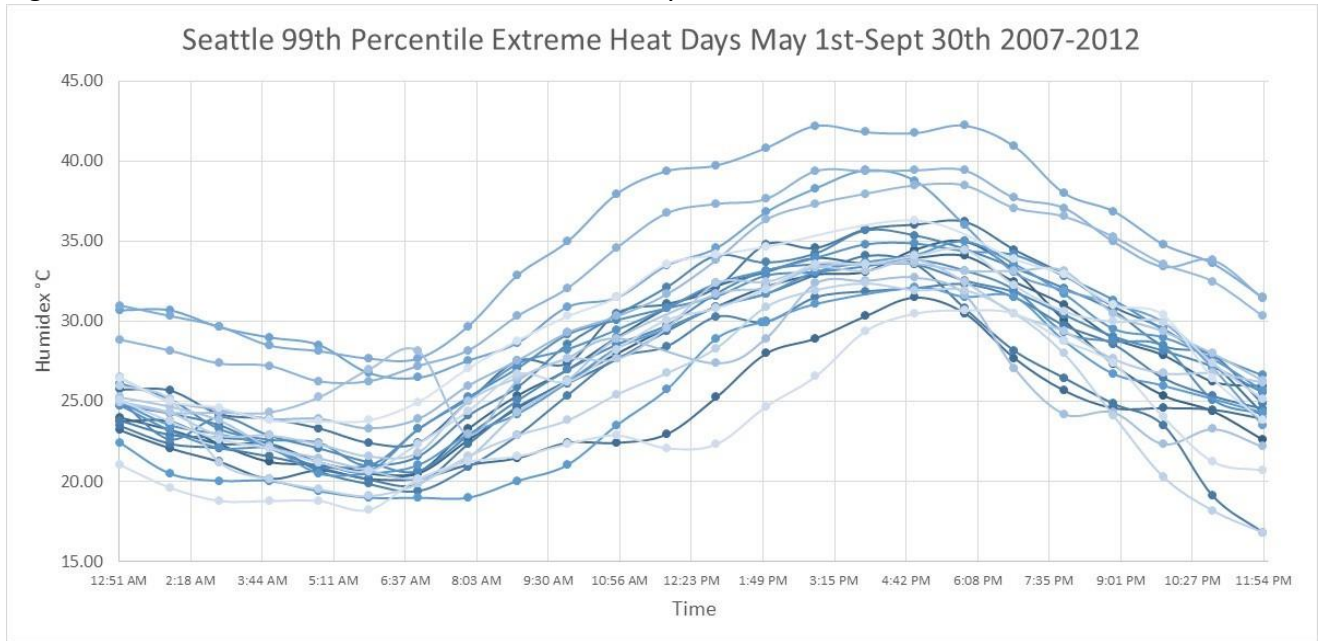


Figure 7: SeaTac Weather Station Extreme Heat Days

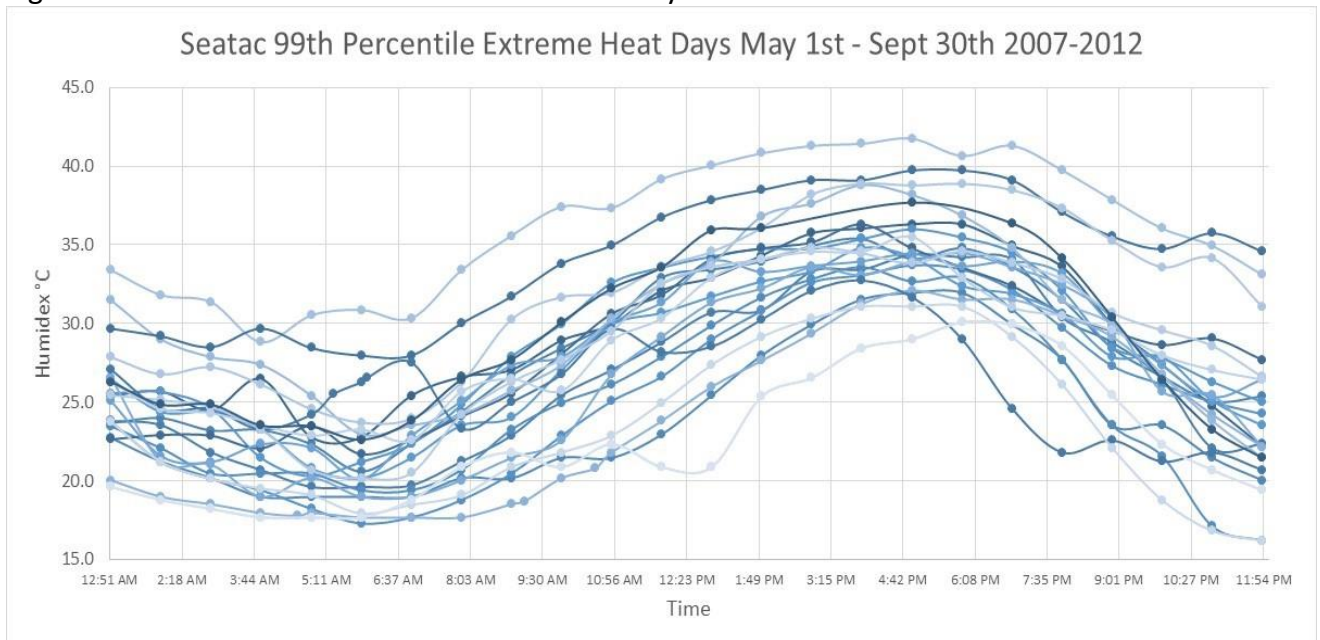


Table 2: Tally of Peak Humidex Times

Time	Every 10 days Seattle	Extreme Heat Seattle	Extreme Heat Seatac
1pm	1	0	0
2pm	6	0	0
3pm	13 (10%)	3 (9%)	1 (3%)
4pm	24 (20%)	8 (25%)	8 (24%)
5pm	38 (31%)	11 (34%)	13 (38%)
6pm	30 (25%)	10 (31%)	10 (29%)
7pm	5	0	2
8pm	2	0	0

Table 3 shows exploratory total call counts for BLS and ALS data for all days. These call counts were not location specific and included all EMS calls in King County. Heat days and non-heat days were not distinguished.

Table 3: ALS and BLS Call Counts by Time Block on All Days

Time Block	BLS	ALS
Morning (6:00am-11:59am)	107,553	31,921
Afternoon (12:00pm-5:59pm)	147,180	39,034
<i>Early Afternoon (12pm-3pm)</i>	<i>72,497</i>	<i>19,933</i>
<i>Late Afternoon (3pm-6pm)</i>	<i>74,683</i>	<i>19,101</i>
Evening (6:00pm-11:59pm)	122,721	32,659
Overnight (12:00am-5:59am)	63,537	18,174

After the 3-6pm time block was identified as the peak extreme heat time block based on hourly Weather Underground data, three other time blocks were set to compare call volumes on an extreme heat day compared to a non-heat day. Based on the graphs of hourly humidex, 4-7am were the hours of the day with the lowest humidex values in King County, and therefore were designated as a low humidex time block. Before Peak Heat and After Peak Heat time blocks were distinguished as 7am-3pm and 6pm-10pm, respectively. Again, overnight hours were excluded to reduce bias from non-heat related EMS calls, such as those from exhaustion or alcohol. Table 4 and 5 distinguished BLS and ALS call counts in each time block on a heat day and non-heat day. These call counts were location specific because each call was classified as a heat day call or a non-heat day call based on its local, grid cell daily humidex value. Relative risks were not calculated for every time block in every grid cell because of problems with statistical power. However, we did calculate a rough relative risk estimate for each time block based on county-wide call counts and the average number of grid cell heat days and non-heat days. First, the total call counts for each time block were divided by the average number of heat days and non-heat days for all grid cells: 149 extreme heat days and 769 non-heat days for the BLS threshold; 28 extreme heat days and 890 non-heat days for the ALS threshold (reference Table 1). Then, the average number of calls per heat day was divided by the average number of calls per non-heat day for each time block to find a simple relative risk estimate. For the Low Humidex and Before Peak Heat time blocks, there were slightly reduced or equal call volumes on a heat day compared to a non-heat day. However, call volumes were 1.06 and 1.05

times higher on extreme heat days compared to non-heat days in the Peak Heat time block for BLS and ALS calls, respectively. Interestingly, the After Peak Heat hours had greater estimated relative risks than the Peak Heat time block of 1.10 and 1.08 for BLS and ALS calls, respectively.

Table 4: BLS Call Rates per Average Heat/Non-Heat Day and Time Block

	Low Humidex (4am-7am)	Before Peak Heat (7am-3pm)	Peak Heat (3pm-6pm)	After Peak Heat (6pm-10pm)
Non-Heat Day	22,515/769 = 29.28	139,997/769 = 182.05	60,984/769 = 79.3	72,210/769 = 93.9
Heat Day	4,240/149 = 28.46	27,073/149 = 181.70	12,557/149 = 84.28	15,353/149 = 103.04
All Days	26,755/918 = 29.14	167,070/918 = 181.99	73,541/918 = 80.11	87,563/918 = 95.38
Simple Relative Risk Estimate	0.97	1.00	1.06	1.10

Table 5: ALS Call Counts per Average Heat/Non-Heat Day and Time Block

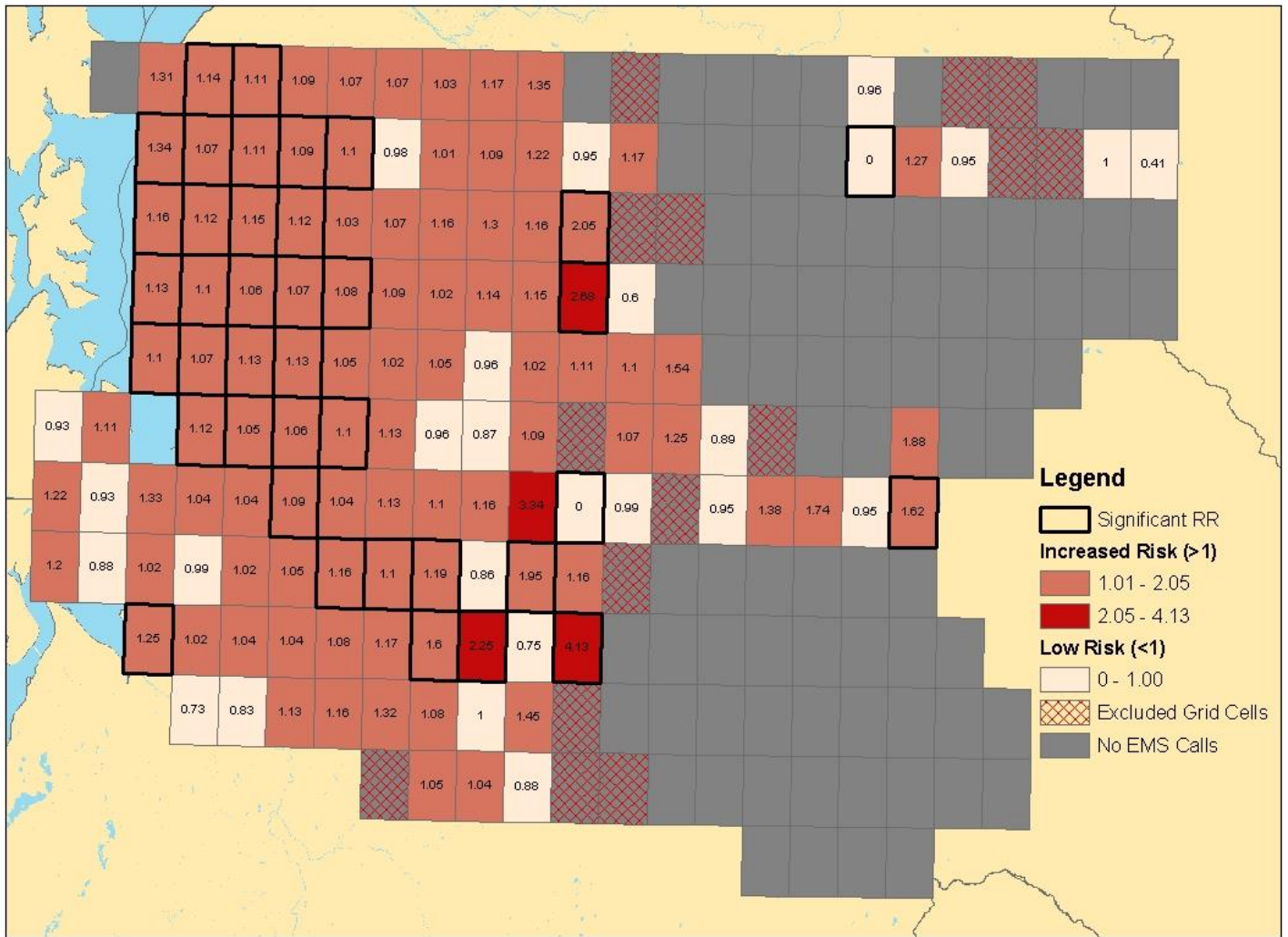
	Low Humidex (4am-7am)	Before Peak Heat (7am-3pm)	Peak Heat (3pm-6pm)	After Peak Heat (6pm-10pm)
Non-Heat Day	7,893/890 = 8.87	46,954/890 = 52.76	18,314/890 = 20.58	22,488/890 = 25.27
Heat Day	211/28 = 7.54	1,352/28 = 48.29	603/28 = 21.54	765/28 = 27.32
All Days	8,104/918 = 8.83	48,306/918 = 52.62	18,917/918 = 20.61	23,253/918 = 25.33
Simple Relative Risk Estimate	0.85	0.92	1.05	1.08

Relative Risk Analysis

In order to adjust for temporal correlations, each dataset included some functions of time based on full year time trends. Both BLS and ALS datasets had a strong correlations with an overall time trend function, so this variable was adjusted for in each relative risk analysis. The BLS data also showed a strong quadratic relationship, so a square of the overall time trend variable was also included in the BLS relative risk model. Looking at days of the week, the ALS dataset showed correlations with Saturday and Sunday, while the BLS data showed correlations with Sunday and Tuesday. A weekend time function was created and adjusted for in the ALS relative risk, while the BLS relative risk adjusted for all days of the week.

The BLS and ALS relative risks for all King County grid cells with EMS calls are shown in Figure 8 and Figure 10, respectively. Because there were no EMS calls in a number of grids in eastern King Co, we were unable to calculate a relative risk for every grid cell. There were 139 grid cells with BLS calls and 130 grid cells with ALS calls. However, for statistical power, grid cells with 5 or less total calls were excluded from the analysis. This reduced the number of grid cells to 124 for BLS calls and 116 for ALS calls. These were crude relative risks for EMS calls of all ages and all causes during the summer months (May 1st - September 30th) 2007-2012.

Figure 8: BLS Crude Relative Risks per Grid Cell



For the BLS dataset, there were BLS calls in 139 King County grids, but 15 of these grid cells were excluded because they had 5 or fewer total calls. 98 grid cells observed call increases on local 95th (29.7°C) percentile humidex extreme heat days compared to non-heat days with a relative risk greater than 1, and 34 of these grid cells had statistically significant results.

Statistically significant increases in BLS calls range from an increase of 1.05 (95% CI: 1.01, 1.09)

to 4.13 (95% CI: 1.65, 10.32) times the number of calls on a local heat day compared to a non-heat day. 26 grid cells had relative risks less than 1, meaning there were less BLS calls on an extreme heat day compared to a non-heat day; 2 of these grid cells had statistically significant results with a relative risk of 0 because there were no BLS calls made on an extreme heat day.

Figure 9: Histogram of BLS Relative Risks

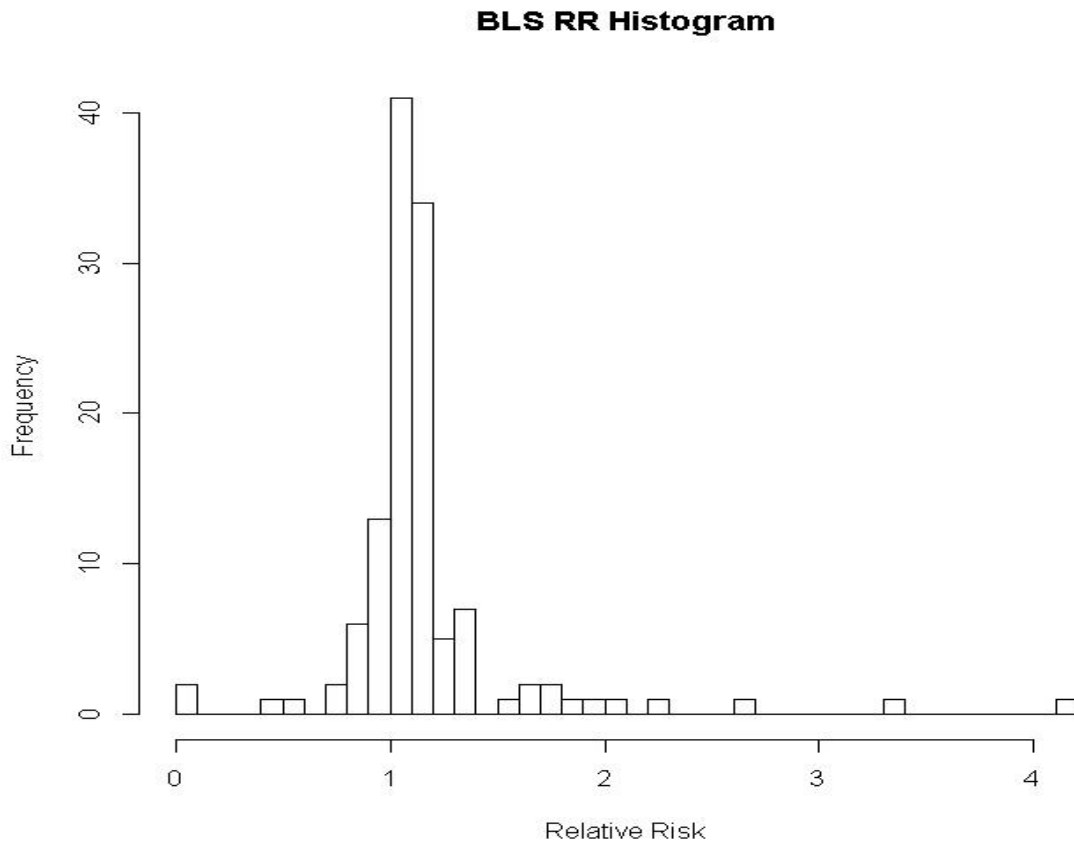
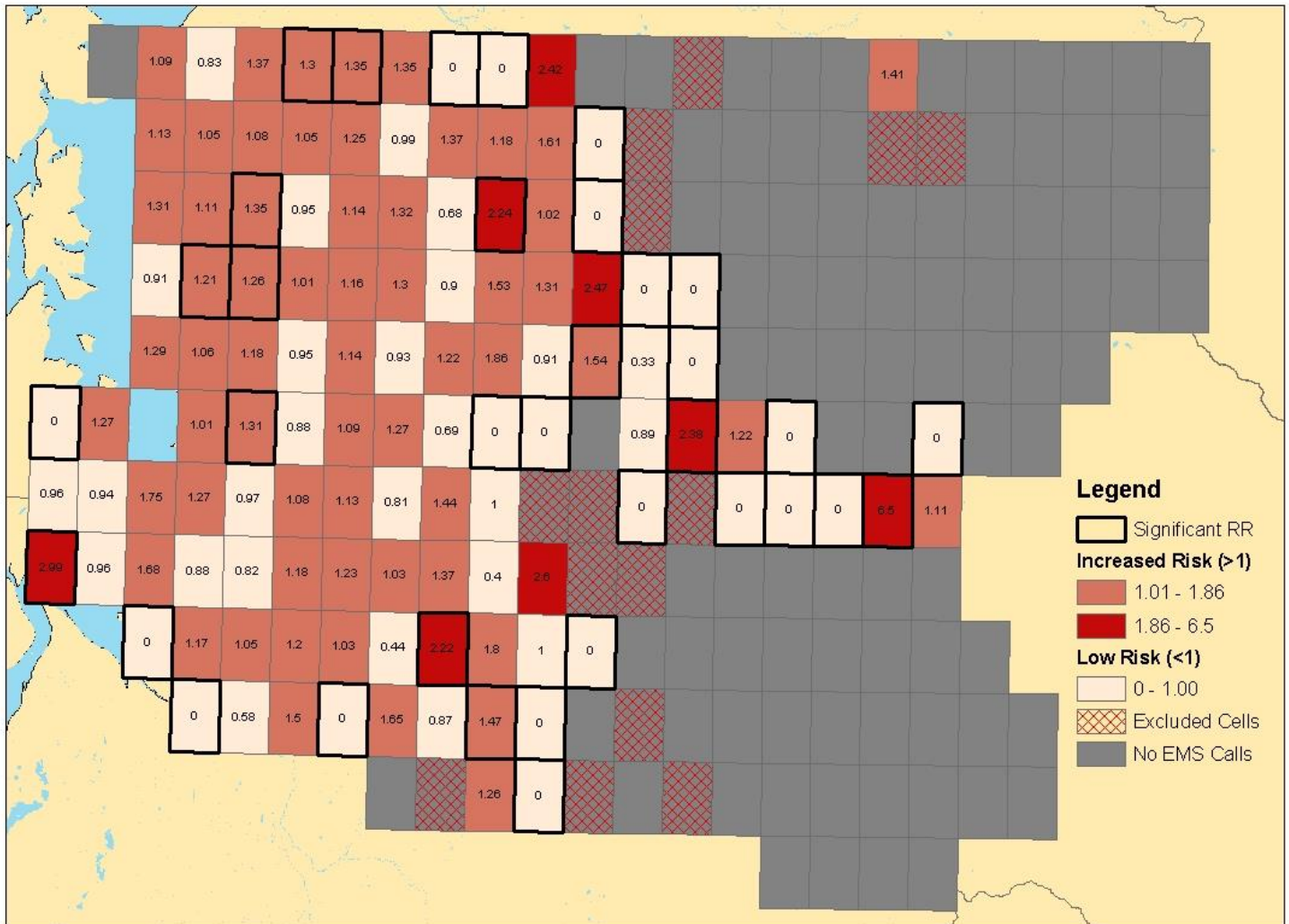


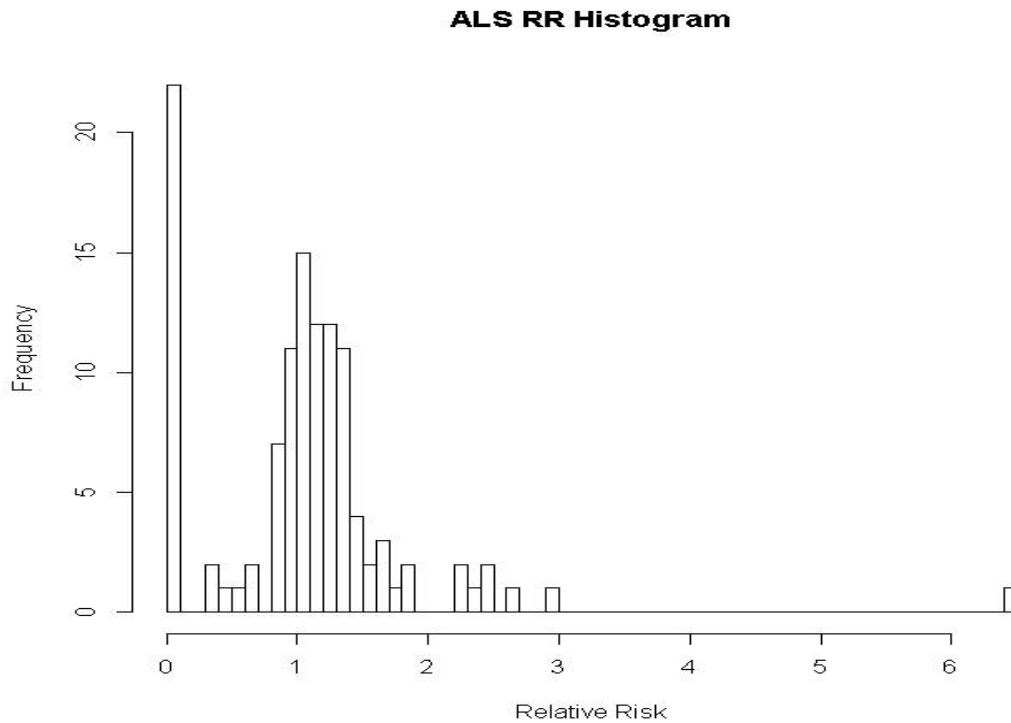
Figure 10: ALS Crude Relative Risks per Grid Cell



There were 14 ALS grid cells that were excluded from this analysis because their total call volume was less than or equal to 5 EMS calls for the entire 6 year period. Out of the other 116 grid cells with relative risks for ALS calls, 68 grid cells had a relative risk above 1, indicating there was an increase in ALS calls on local 99th (36.7 °C) percentile humidex heat days compared to non-heat days. However, only 13 of these grid cell relative risks were statistically

significant. Of the 13 significant increases in relative risk, ALS call volumes ranged from 1.21 (95% CIs: 1.11, 1.32) to 6.50 (95% CIs: 1.06, 40.03) times the number of calls on an extreme heat day compared to a non-heat day. All of these statistically significant relative risks were greater than the county-wide crude relative risk estimate of 1.14 (95% CI: 1.09, 1.2) from Calkins et. al. (2016). 22 grid cells had statistically significant low relative risks (<1) on an extreme heat day compared to a non-heat days indicating they were protective in the case of extreme heat.

Figure 11: Histogram of ALS Relative Risks

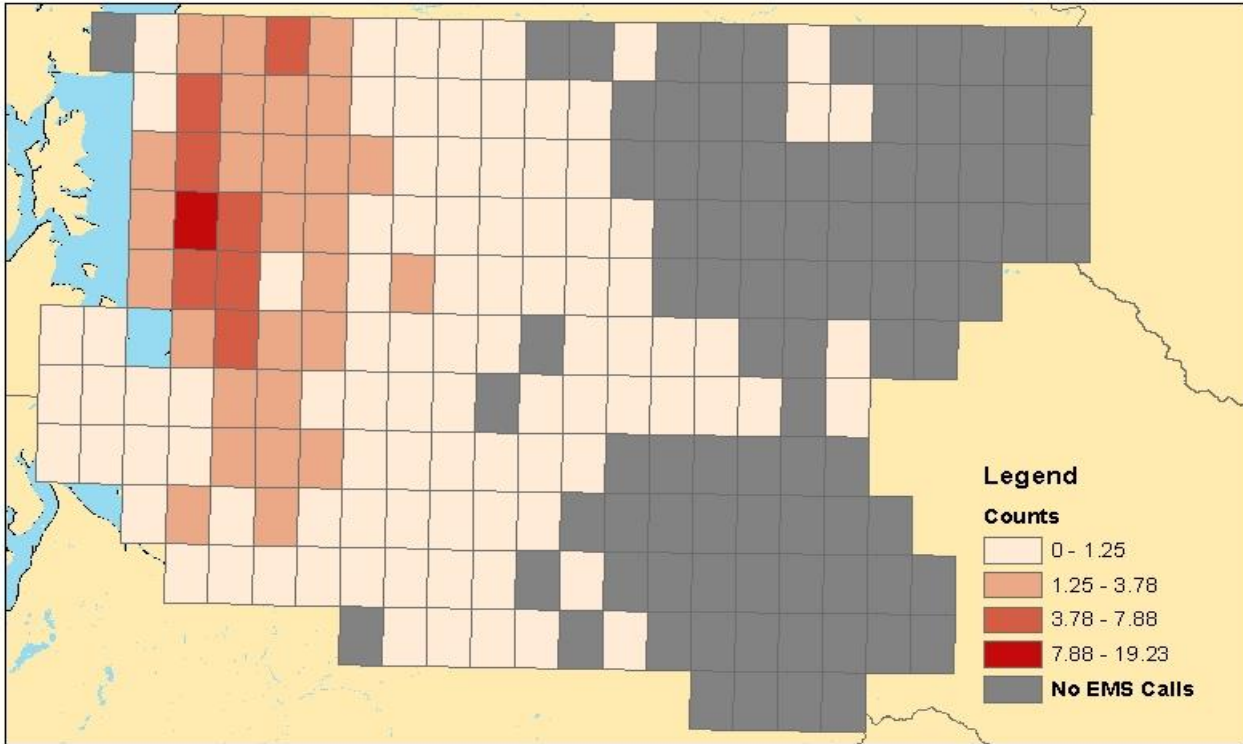


STUDY POWER:

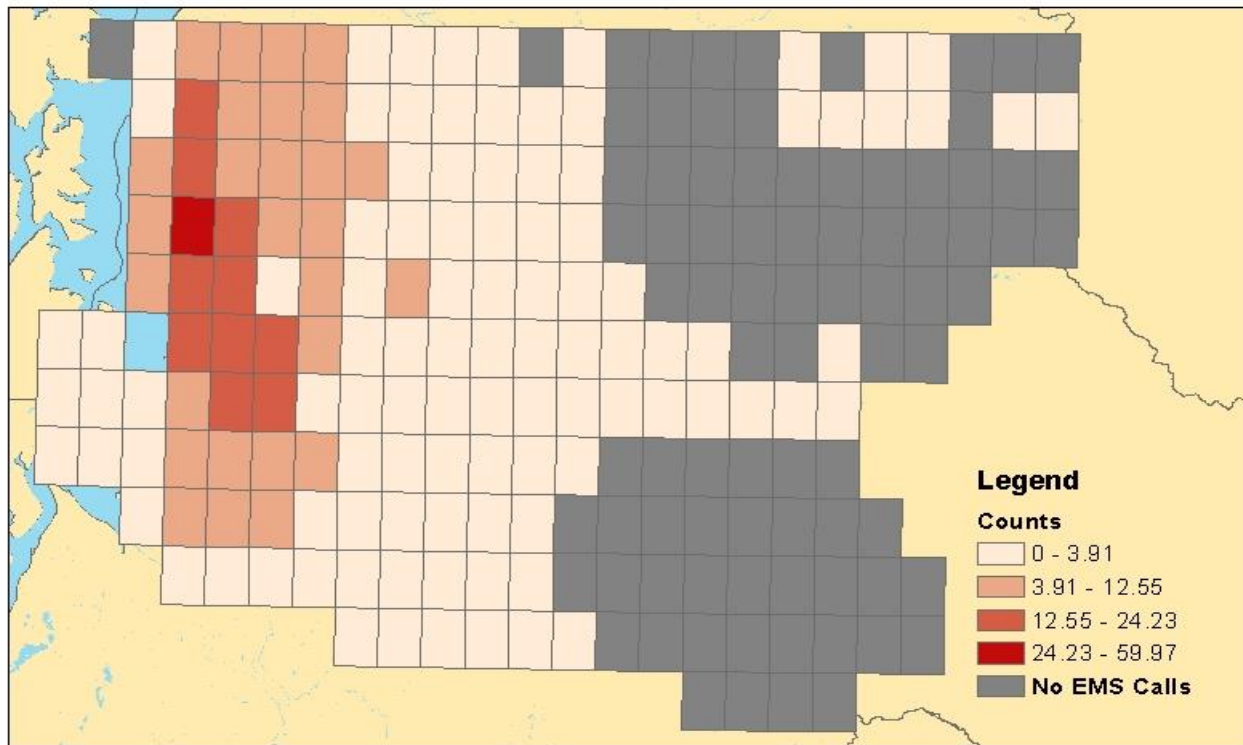
There were a total of 918 days in the study period with an average of 394 BLS calls per day and 103 ALS calls per day. However, the grid split the call volumes into 116 grids for ALS calls and 124 grids for BLS calls. This means there was an average total number of calls per day per grid cell of 3.82 and 1.13 for BLS and ALS, respectively. Figure 12 visualizes the range in the average number of calls per heat day across all grid cells. The average number of calls per heat day in each grid cell was only 4.10 and 1.27 for BLS and ALS data, respectively, while the average calls per non-heat day was 3.77 and 1.13 for BLS and ALS data, respectively. In fact, many grid cells had 0 calls on all local heat days combined. Although grid cells with less than 5 total calls were eliminated, study power was definitely a limiting factor in this analysis. Only 36 grids were significant results for BLS calls (34 increases and 2 decreases), while 35 grids had statistically significant results for ALS calls (13 increases and 22 decreases). This difference was likely due to the difference in sample size between BLS and ALS data sets as well as the difference in extreme heat thresholds.

Figure 12: Average ALS and BLS Call Counts per Heat Day

ALS Avg Call Counts Per Heat Day



BLS Avg Call Counts per Heat Day



Analysis of Community-Level Predictors:

LINEAR REGRESSION MODELS:

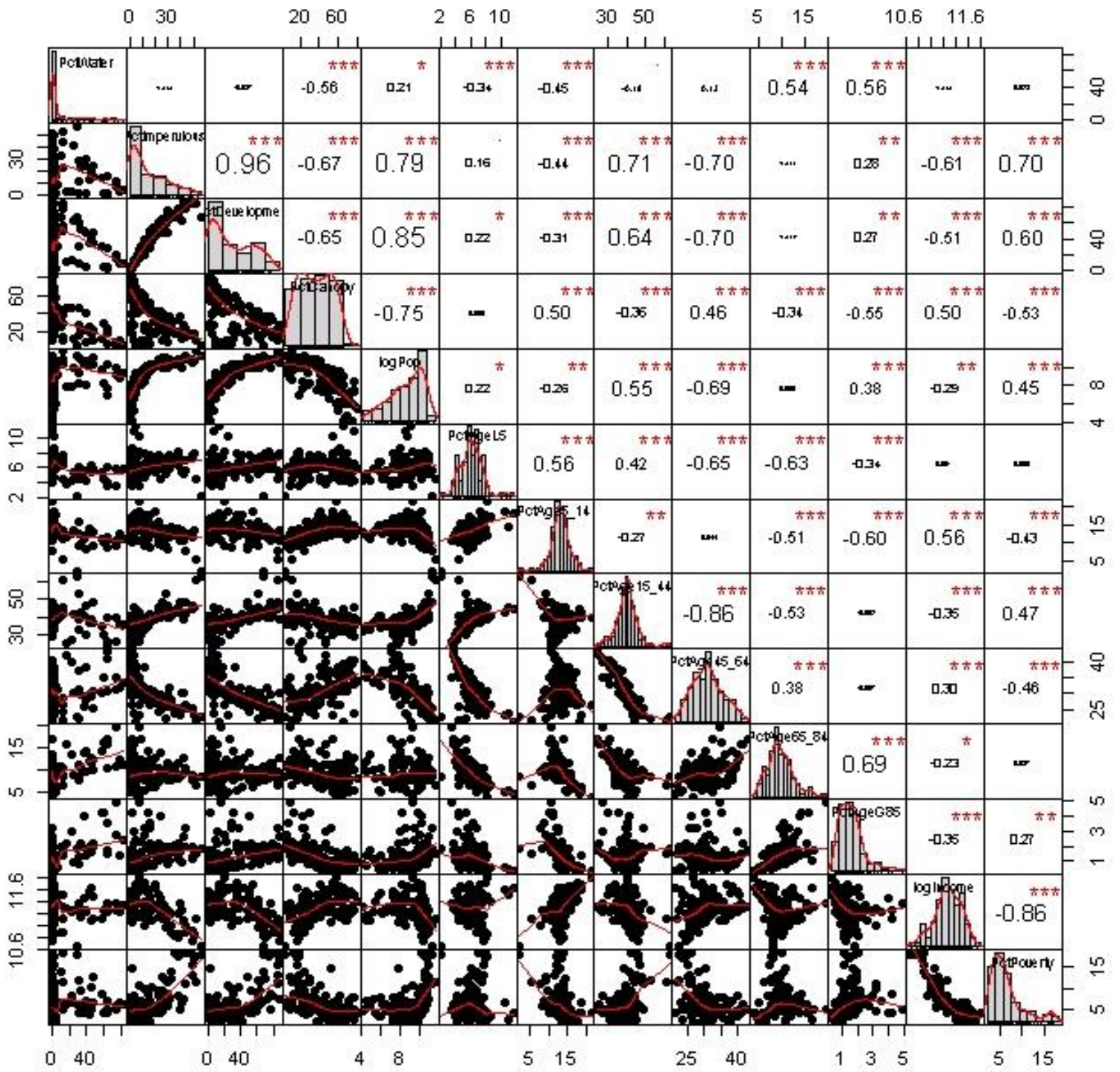
The goal of this final aim was to determine the relationship between relative risk and grid cell predictors. Potential community level indicators were log population, percent younger than 5, percent age 5-14, percent age 14-44, percent age 45-64, percent age 65-84, percent older than 85, percent canopy, percent impervious surfaces, percent development, percent water, percent below poverty, and median household income for each grid cell.

In order to assess the relationship of each individual predictor, I ran linear regression models for each individual variable. However, because these variables could have significant confounding relationships with each other and the grid cell relative risk, a formal model selection process was used to identify the best combination of variables to predict grid cell relative risk. Both R packages, Bestglm and Leaps, were considered for formal model selection analysis. Bestglm used an AIC criteria, while Leaps used a similar criterion, Cp. In the end, each program reported similar variables in their results. However, we chose to use Bestglm because it did not create dummy variables from the categorical data.

Based on the results of a correlation analysis shown in Figure 13, there were many variables which were very highly correlated. Particularly, percent development, percent impervious surfaces, and log population had correlation coefficients ranging from 0.93 to 0.98. As population in a grid cell increased, so did the percent impervious surface and the percent development. In addition, median income and percent poverty had a high -0.86 correlation

coefficient meaning that as the median income for the grid cell increased, the percent of the population below the poverty line decreased. Due to the extremely high correlation coefficient between percent development and percent impervious surfaces (0.98), these two variables were nearly the same and may compete with each other in a regression model. Furthermore, the difference in the data collection of percent impervious surface versus percent development led to the conclusion that percent impervious surface was a more accurate variable to include. A raster file of percent impervious surface had a percentage for each raster pixel in order to calculate the average percent impervious surface for the grid cell. On the other hand, development percentages were determined from a land use raster file and each pixel was classified strictly as developed or not-developed to find the percent of the grid cell that was developed land. Water was also collected in this less precise manner. As a result, we made the decision not to include the development and water variables in the model.

Figure 13: Correlation Coefficient Plots



In order to analyze the specific relationship between relative risk and each predictor, a linear regression model ran each predictor variable individually with BLS and ALS grid cell relative risk. All grid cell population variables were continuous variables, while percent canopy, percent impervious surface, percent poverty, and median income were categorized into four equal quartiles. For the categorical variables, the mean relative risks of quartile two, three, and four grid cells, were compared to the mean relative risk of the lowest quartile of grid cells. The true ranges for each quartile are found in Table 6 (BLS) and Table 15 (ALS).

In addition, a formal model selection process, using a best subset selection with cross-validation in the R package Bestglm with AIC criterion, choose predictor variables to include in a single best fit model of the BLS and ALS data sets. The first overall best subset model selection results, included the variables for log population, median income, percent poverty, percent impervious surface, and percent canopy of each grid cell. Next, a second best subset model selection ran the model including the continuous grid cell age group variables as well.

Table 6: BLS Categorical Ranges

	Quartile 1: 0-25th	Quartile 2: 25th-50th	Quartile 3: 50th-75th	Quartile 4: 75th-100th
Percent Canopy	[3.97-23.3%]	(23.3-42.1%)	(42.1-62.6%)	(62.6-86.2%)
Percent Impervious Surfaces	[0.229-1.66%]	(1.66-7.62%)	(7.62-24.2%)	(24.2-56.7%)
Median Income	[\$42,000-\$70,100]	(\$70,100-\$81,100]	(\$81,100-\$97,000]	(\$97,000-\$136,000]
Percent Poverty	[1.95-4.12%]	(4.12-5.78%)	(5.78-7.87%)	(7.87-18.5%)

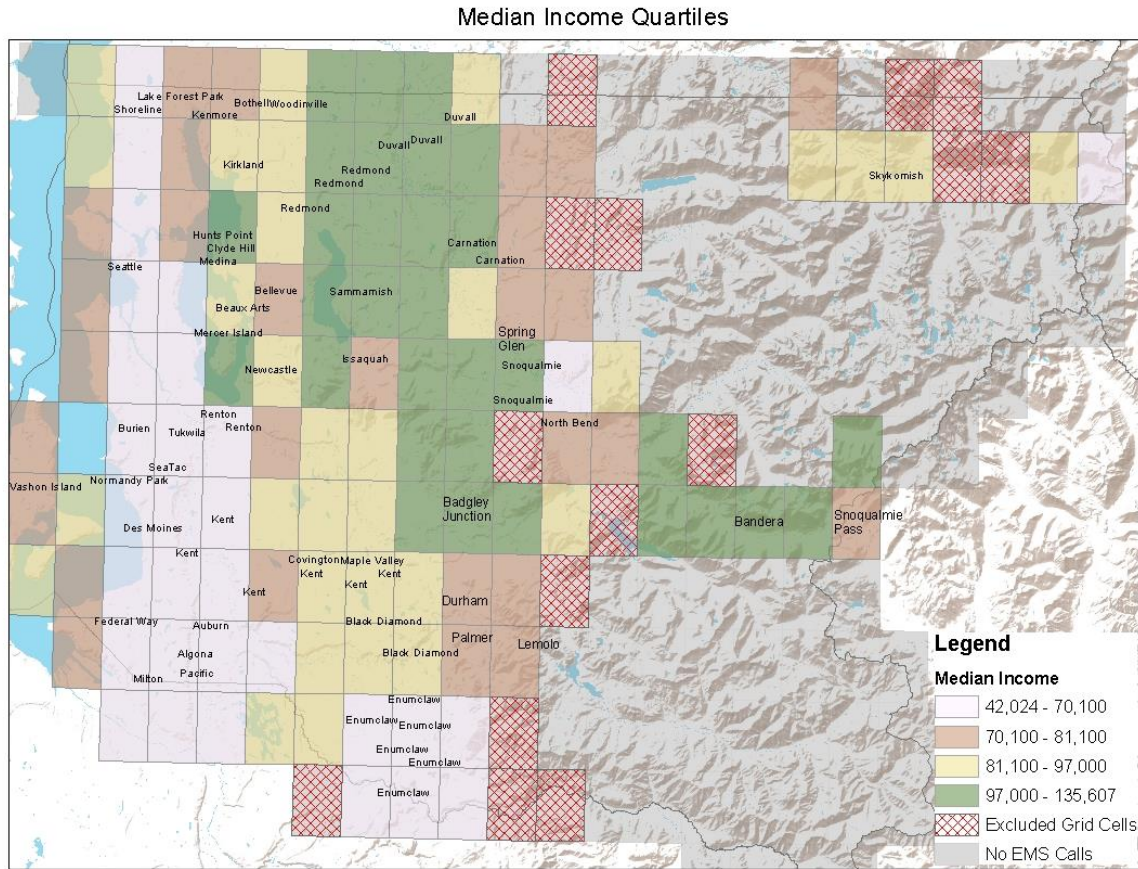
BLS Median Household Income

Table 7 displays the results for the relationship between BLS median household income quartiles and relative risk, while Figure 14 maps the grid cells in each median income quartile. The mean relative risk for the lowest quartile of median income [\$42,000-\$70,100] was 1.04 (95% CI: 0.98, 1.11), meaning that an average relative risk of all the quartile one grid cells showed a 4% increase in BLS call volumes on a 95th percentile humidex heat day compared to a non-heat day. There was a statistically significant increase of BLS relative risk by 0.25 (95% CI: 0.02, 1.11) in the mean relative risk of quartile two for median income (\$70,100-\$81,100] compared to the mean relative risk of quartile one. Quartile two grid cells had a mean increase of 1.3 (95% CI: 1.06, 1.53) times the number of BLS calls on a 95th percentile local humidex heat day compared to a non-heat day. The third (\$81,100-\$97,000] and fourth (\$97,000-\$136,000] quartile of median income had a mean relative risk of 1.146 and 1.165 respectively, but neither increase was a statistically significant compared to the mean relative risk of the lowest quartile of median income grid cells.

Table 7: BLS Median Income Quartile Results

Variables	Quartile Percentages	Estimate	Estimate 95% CI	P-Value	Mean RR	Mean RR 95% CI
Intercept – Q1 Median Income	[\$42,000-\$70,100]	1.04268	(0.98,1.11)	1.26e-02*	1.04268	(0.98,1.11)
Q2 Median Income	(\$70,100-\$81,100]	0.25703	(0.02, 0.49)	0.034*	1.29971	(1.06, 1.53)
Q3 Median Income	(\$81,100-\$97,000]	0.10398	(-0.03, 0.24)	0.129	1.14666	(1.01,1.28)
Q4 Median Income	(\$97,000-\$136,000]	0.12235	(-0.06, 0.31)	0.195	1.16503	(0.98,1.35)

Figure 14: BLS Median Income Quartiles



BLS Percent Impervious Surface

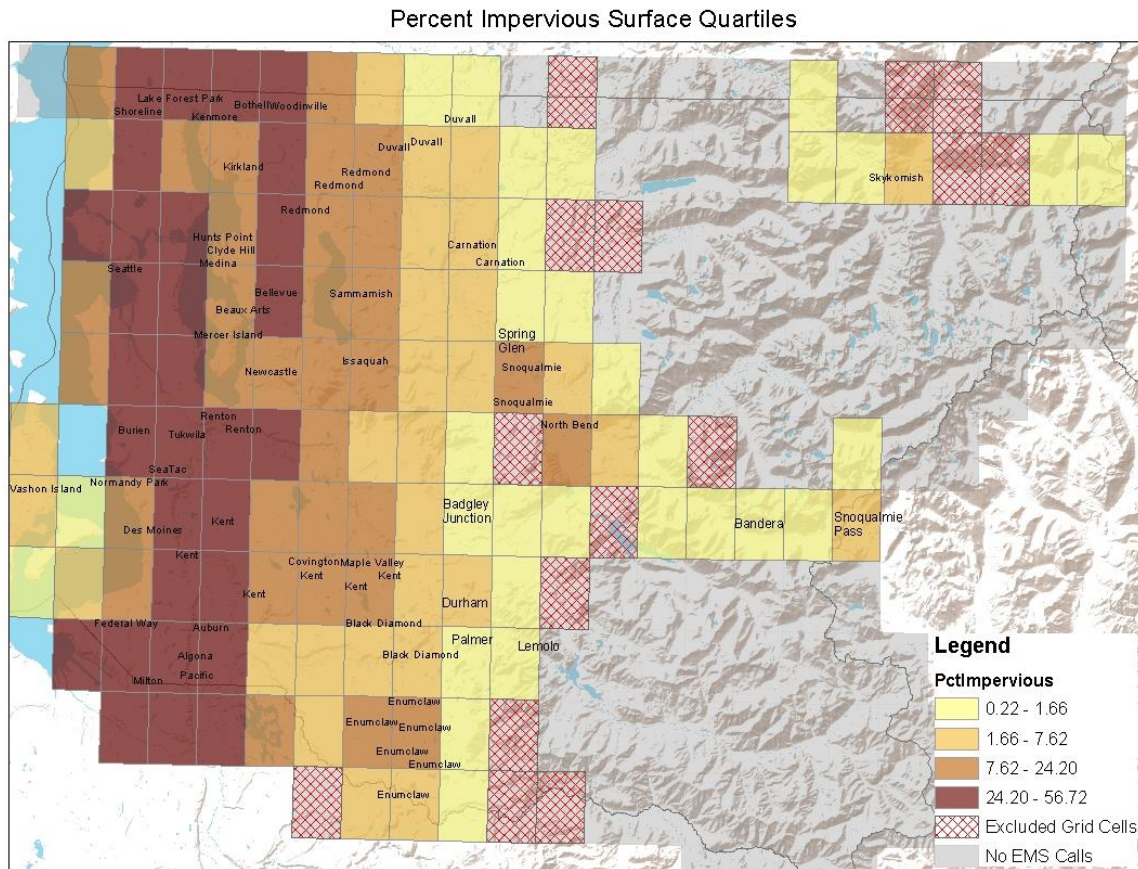
Table 8 and Figure 15 display the results from a linear regression with percent impervious surface and BLS data. In the lowest quartile of percent impervious surface, there was a statistically significant mean relative risk of 1.3 (95% CI: 1.01, 1.6); this relative risk indicates that BLS call volumes were 1.3 times higher on a 95th percentile local heat day compared to a non-heat day when averaging the relative risks of the lowest quartile of percent impervious surface. Furthermore, the model showed a clear trend of decreasing mean relative

risk as percent impervious surface quartiles increased. The mean relative risk of the second quartile (1.66%-7.62%) decreased by 0.11 (95% CI: -0.43, 0.20) compared to the lowest quartile, while the mean relative risk of the third (7.62%-24.2%) and fourth (24.2%-56.7%) quartiles decreased by 0.21 (95% CI: -0.51, 0.084) and 0.23 (95% CI: -0.53, 0.061), respectively, compared to the mean relative risk of quartile one. None of these results were statistically significant, but the increasing negative trend in mean relative risk was clear.

Table 8: BLS Percent Impervious Surface Results

Variables	Quartile Percentages	Estimate	Estimate 95% CI	P-Value	Mean RR	Mean RR 95% CI
Intercept – Q1 Percent Impervious Surface	[0.229-1.66%]	1.30326	(1.01, 1.6)	3.98e-18*	1.30326	(1.01, 1.6)*
Q2 Percent Impervious Surface	(1.66-7.62%)	-0.11264	(-0.43, 0.20)	0.481	1.19062	(0.87,1.5)
Q3 Percent Impervious Surface	(7.62-24.2%)	-0.21153	(-0.51, 0.084)	0.160	1.09173	(0.79,1.38)
Q4 Percent Impervious Surface	(24.2-56.7%)	-0.23480	(-0.53, 0.061)	0.120	1.06846	(0.77, 1.36)

Figure 15: BLS Percent Impervious Surface Quartiles



BLS Percent Canopy

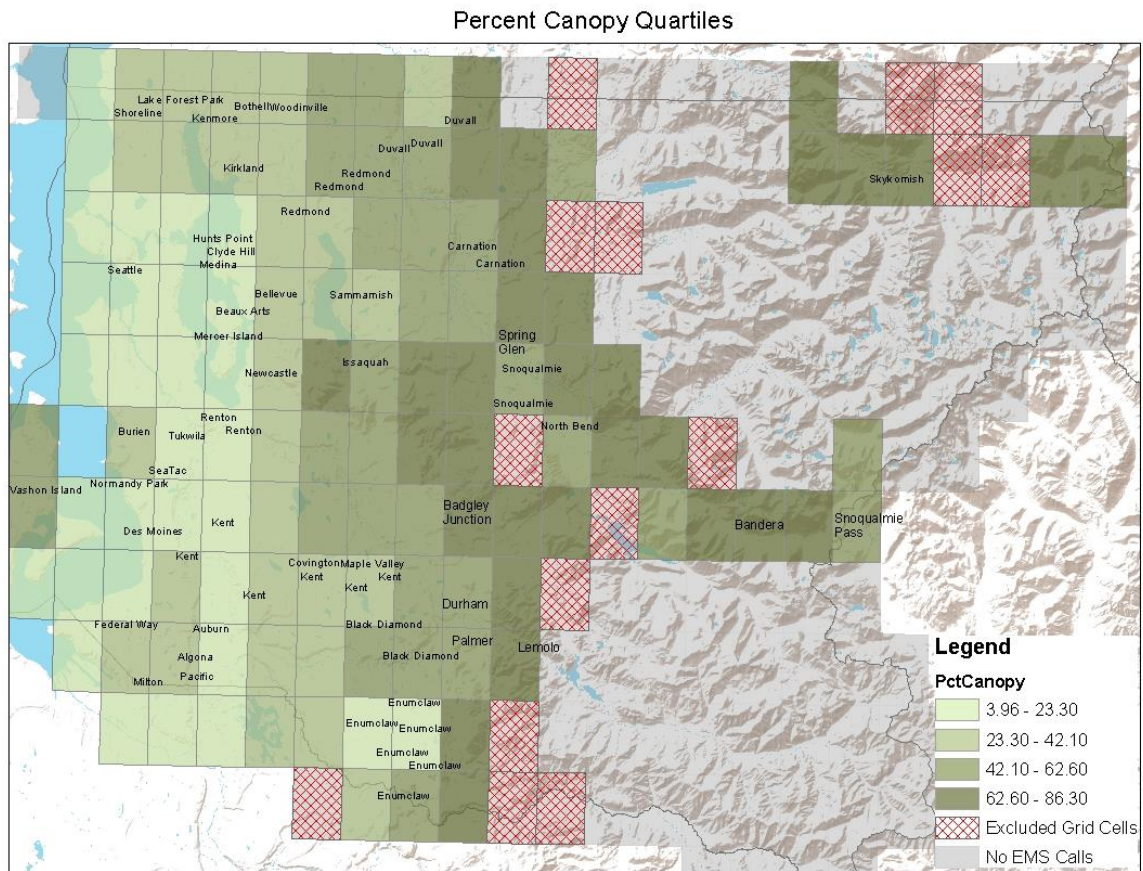
Next, the results of a linear regression with BLS relative risk and percent canopy quartiles are shown in Table 9 and the quartiles are mapped in Figure 16. The mean relative risk of the lowest quartile of percent canopy [3.97-23.3%] was 1.08 (95% CI: 1.04, 1.13), which had a statistically significant increase in BLS calls on an extreme heat day compared to a non-heat day. Conversely from percent impervious surface quartiles, as percent canopy increased, the relative risk of a BLS call on a 95th percentile heat day also increased. Although it showed

another clear trend with the grid cell relative risks, none of the results were statistically significant.

Table 9: BLS Percent Canopy Results

Variables	Quartile Percentages	Estimate	Estimate 95% CI	P-Value	Mean RR	Mean RR 95% CI
Intercept – Q1 Percent Canopy	[3.97-23.3%]	1.08490	(1.04,1.13)	0.00*	1.0849	(1.04,1.13)*
Q2 Percent Canopy	(23.3-42.1%)	0.02108	(-0.03, 0.07)	0.409	1.10598	(1.05, 1.15)*
Q3 Percent Canopy	(42.1-62.6%)	0.10559	(-0.02, 0.23)	0.096	1.19049	(1.06, 1.31)*
Q4 Percent Canopy	(62.6-86.2%)	0.18782	(-0.11, 0.48)	0.212	1.27272	(0.97,1.56)

Figure 16: BLS Percent Canopy Quartiles



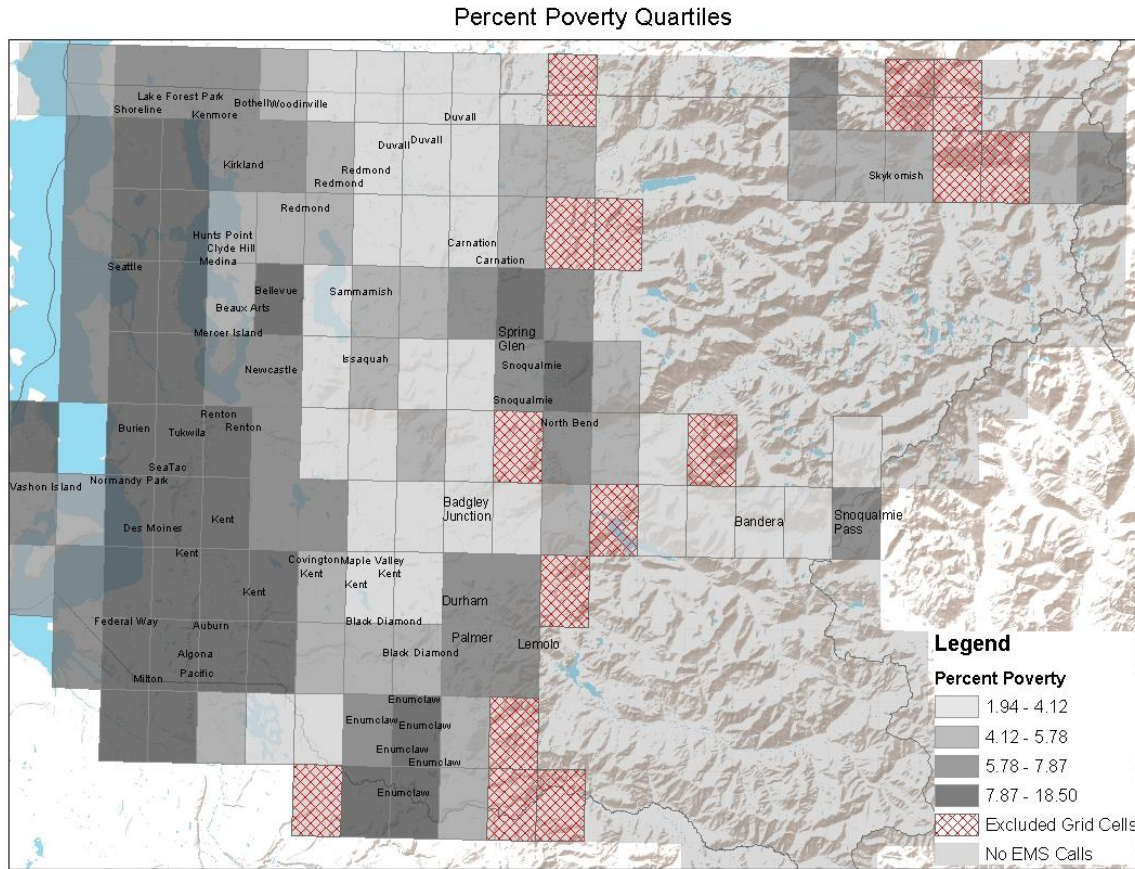
BLS Percent Poverty

A linear regression with quartiles of percent poverty also did not show any statistically significant results when comparing the mean relative risk of quartile two, three, and four with the mean relative risk of quartile one. There was also no clear trend between percent poverty quartiles and BLS relative risk. In quartile one, there was a statistically significant mean grid cell increase of 1.19 (95% CI: 1.01, 1.36) times the number of BLS calls on a 95th percentile heat day compared to non-heat day.

Table 10: BLS Percent Poverty Results

Variables	Quartile Percentages	Estimate	Estimate 95% CI	P-Value	Mean RR	Mean RR 95% CI
Intercept – Q1 Percent Poverty	[1.95-4.12%]	1.18563	(1.01, 1.36)	4.33e-41	1.18563	(1.01, 1.36)*
Q2 Percent Poverty	(4.12-5.78%]	-0.01901	(-0.24, 0.20)	0.865	1.16662	(0.95,1.39)
Q3 Percent Poverty	(5.78-7.87%]	0.01111	(-0.26, 0.28)	0.936	1.19674	(0.93,1.47)
Q4 Percent Poverty	(7.87-18.5%]	-0.08053	(-0.28, 0.12)	0.436	1.1051	(0.91,1.31)

Figure 17: BLS Percent Poverty Quartiles



BLS Log Population

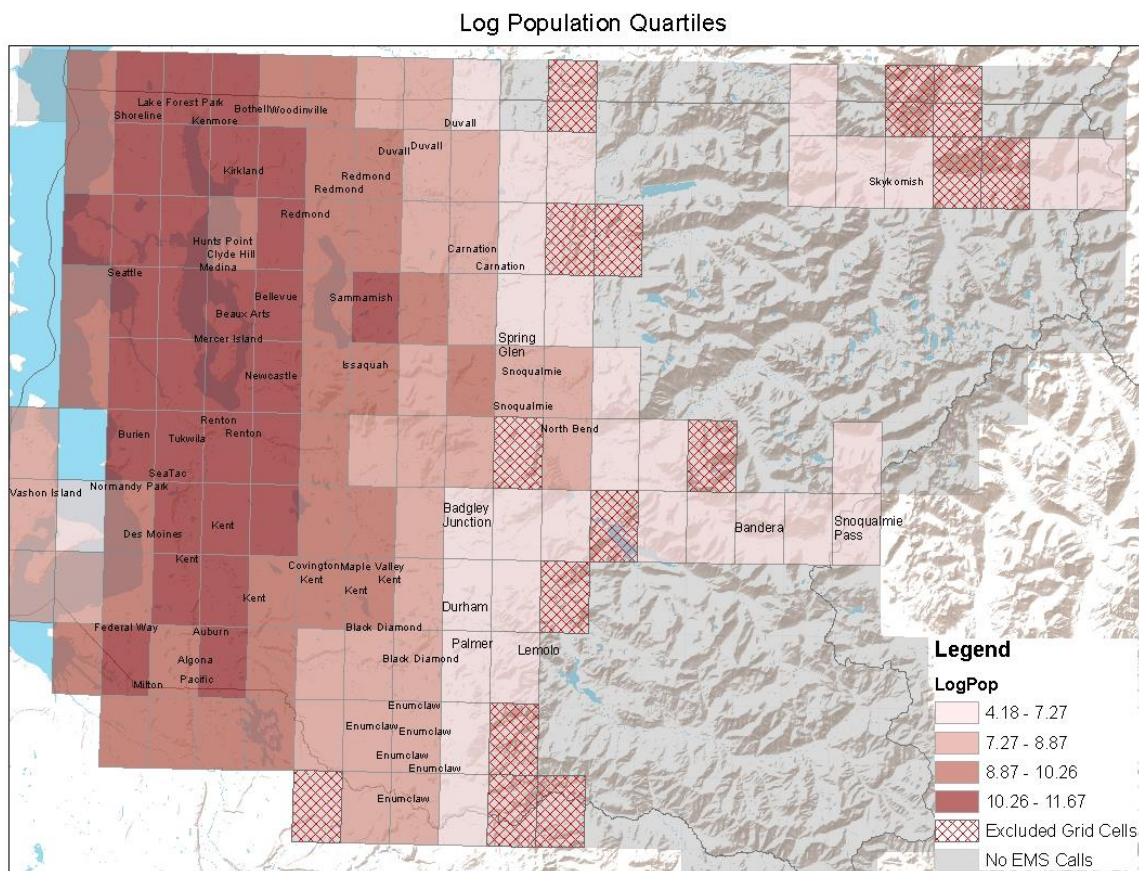
The linear regression of log population and relative risk of a BLS call on a 95th percentile local heat day compared to a non-heat day suggested a negative trend in relative risk with increasing population. For every unit increase in log population of a grid cell, there was a decrease of 0.03 (95% CI: -0.08, 0.02) in relative risk. This result was not statistically significant (p-value =0.218). In this model, the intercept had no scientific meaning. Theoretically, it was the relative risk of a grid cell with a log population of 0 (a population of 1); however, there were

no BLS grid cells in this model with a population of 1. Even though, log population was a continuous variable, Figure 18 displays BLS log population quartiles to help visualize the spatial distribution of population throughout the county.

Table 11: BLS Log Population Results

Variables	Estimate	Estimate 95% CI	P-Value
Intercept	1.42474	(0.94,1.91)	1.03e-08*
Log Population	-0.03050	(-0.08, 0.02)	0.218

Figure 18: BLS Log Population Quartiles



BLS Grid Cell Population Age Groups

Finally, Table 12 has the results of a linear regression model of BLS relative risk with percent of the grid cell population in each designated age group. Percent younger than 5, percent 15-44, percent 65-84, and percent older than 85 showed decreases in relative risk for every one percent increase in age group population. Age groups 5-14 and 45-64 had an increase in relative risk with each percent increase in age group. None of the age group results were statistically significant on the 0.05 level. Again the intercept values of each model did not have scientific meaning because the percent of each age group was never 0.

Table 12: BLS Age Group Results

Variables	Estimate	Estimate 95% CI	P-Value
Percent Younger than 5			
Intercept	1.29341	(0.87, 1.72)	2.55e-09*
Percent Younger than 5	-0.02163	(-0.08, 0.04)	0.482
Percent Age 5-14			
Intercept	1.02702	(0.83, 1.23)	5.63e-24*
Percent Age 5-14	0.01028	(-0.004, 0.02)	0.147
Percent Age 15-44			
Intercept	1.320402	(0.85, 1.79)	3.43e-08
Percent 15-44	-0.004061	(-0.01, 0.006)	0.449
Percent Age 45-64			
Intercept	0.821572	(0.29, 1.35)	0.0022*
Percent Age 45-64	0.010933	(-0.008, 0.03)	0.260
Percent Age 65-84			
Intercept	1.30339	(1.09, 1.51)	2.97e-34*
Percent Age 65-84	-0.01486	(-0.03, 0.005)	0.137
Percent Older than 85			
Intercept	1.24655	(1.08, 1.42)	2.35e-46*
Percent Older than 85	-0.05941	(-0.13, 0.01)	0.115

BLS Model Selection 1

For the BLS dataset, the first best subset selection model included quartiles of percent impervious surface, median income, and log population in its single best fit model. The results are shown in Table 13. When comparing grid cells with similar log population and quartiles of median income, the mean relative risk of a BLS call on a 95th percentile extreme heat day compared to a non-heat day decreased by 0.20 between the lowest quartile of percent impervious surface and the second quartile (p-value=0.30). The mean relative risk between the lowest quartile of percent impervious surface and the third quartile of percent impervious surface decreased by 0.39 when comparing grid cells with similar log population and median income (p-value of 0.108). Finally, when in grid cells with similar log population and median income quartiles, the mean relative risk between the highest quartile of percent impervious surfaces and the lowest quartile of percent impervious surfaces decreased the relative risk of a BLS call on a 95th percentile extreme heat day compared to a non-heat day by 0.44 (p-value=0.111). Since the mean relative risk of the lowest quartile of impervious surface [0.229%-1.66%] was 1.30, this means that the second quartile of impervious surface grid cells (1.66%-7.62%) had a mean relative risk of 1.10, the third quartile of percent impervious surface grid cells (7.62%-24.2%) had a mean relative risk of 0.89, and the fourth quartile of percent impervious surface grid cells (24.2%-56.7%) had a mean relative risk of 0.80 when accounting for grid cell log population and median income. This trend for a decrease in relative risk as impervious surface increases was the same trend seen when percent impervious surface was

run in a model alone, but the magnitude of the decrease was larger when log population and median income were adjusted for in the model.

Median household income also had the same trend in this model comparing grid cells with similar percent impervious surface and log population as it did when it was put in a model alone. However, the magnitude of change between mean relative risks of the second, third and fourth quartile of median income compared to the mean relative risk of the lowest quartile median income was smaller than the magnitude when the variable was in the model alone. When comparing grid cells with similar percent impervious surface and median income, log population had an insignificant positive increase in relative risk which was the converse of its effect in a model alone.

Table 13: BLS Model Subset Selection 1 Results with Total Population of Grid Cell

Variables	Quartile Percentages	Estimate	Estimate 95% CI	P-Value
Intercept	NA	0.88760	(0.34, 1.44)	1.52e-03*
Q2 Percent Impervious Surface	(1.66-7.62%]	-0.20542	(-0.59, 0.18)	0.300
Q3 Percent Impervious Surface	(7.62-24.2%]	-0.39100	(-0.87, 0.09)	0.108
Q4 Percent Impervious Surface	(24.2-56.7%]	-0.44432	(-0.99, 0.10)	0.111
Log Pop	NA	0.05412	(-0.03, 0.14)	0.225
Q2 Median Income	(\$70,100-\$81,100]	0.19071	(-0.0003 0.38)	0.050*
Q3 Median Income	(\$81,100-\$97,000]	0.06171	(-0.09,0.22)	0.435
Q4 Median Income	(\$97,000-\$136,000]	0.03806	(-0.16, 0.24)	0.710

BLS Model Selection 2

In the second best subset model selection process which included age group percentages of each grid cell, the BLS best fit model only resulted with age group variables: percent younger than 5, percent 15-44, and percent 65-84. According to the model, percent of the population aged 65-84 had a nearly statistically significant negative relationship with grid cell relative risk; when grid cells with similar percentages of population younger than 5 and age 15-44 were compared, the relative risk of a BLS call on a 95th percentile local extreme heat day compared to a non-heat day decreased by 0.04 (95% CI: -0.085, 0.0002) for each percent increase in population aged 65-84 (p-value=0.051).

Table 14: BLS Model Subset Selection 2 Results with Age Group Population of Grid Cell

Variables	Estimate	Estimate 95% CI	P-Value
Intercept	2.229852	(0.96, 3.5)	5.9e-04*
Percent Age Younger than 5	-0.05681	(-0.14, 0.03)	0.206
Percent Age 15-44	-0.008340	(-0.018 0.002)	0.104
Percent Age 65-84	-0.042818	(-0.085, 0.0002)	0.051.

Moving on to ALS model results, Table 15 below shows the category ranges for each predictor variable.

Table 15: ALS Variable Categorical Ranges

	Quartile 1: 0-25th	Quartile 2: 25th-50th	Quartile 3: 50th-75th	Quartile 4: 75th-100th
Percent Canopy	[3.97,22.6]	(22.6,41.3]	(41.3,60.8]	(60.8,81.2]
Percent Impervious Surfaces	[0.0763,2.49]	(2.49,8.57]	(8.57,25.1]	(25.1,56.7]
Median Income	[42,000,70,100]	(70,100,81,100]	(81,100,98,600]	(98,600,136,000]
Percent Poverty	[2.06,4.09]	(4.09,5.84]	(5.84,7.94]	(7.94,18.5]

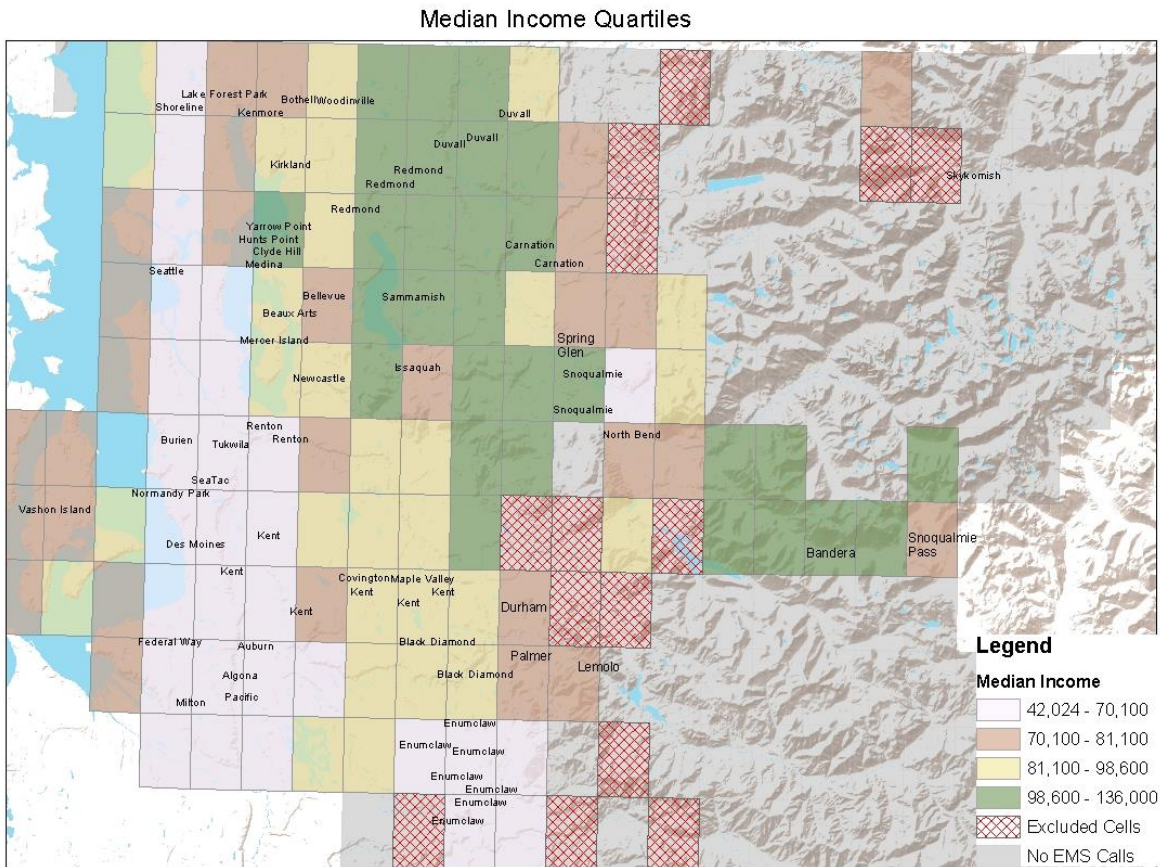
ALS Median Household Income

The relationship between ALS grid cell relative risks and quartiles of median household income is presented in Table 16, and Figure 19 maps the ALS median household income quartiles in King County. There was a mean relative risk of 0.95 (95% CI: 0.80, 1.09) in the lowest quartile [\$42,000-\$70,100] of ALS median income grid cells. When this mean relative risk of quartile one grid cells was compared to the mean relative risk of quartile two (\$70,100-\$81,100] grid cells, there was an increase of 0.19 (95% CI: -0.13, 0.51) in mean relative risk for quartile two. Quartile three (\$81,100-\$98,600] and quartile four (\$98,600-\$136,000] of median income also had an increase in mean relative risk compared to the lowest quartile, but no results were statistically significant.

Table 16: ALS Median Income Results

Variables	Quartile Percentages	Estimate	Estimate 95% CI	P-Value	Mean RR	Mean RR 95% CI
Intercept – Q1 Median Income	[\$42,000-\$70,100]	0.9493009	(0.80, 1.09)	1.94e-37*	0.9493009	(0.8, 1.09)
Q2 Median Income	(\$70,100-\$81,100]	0.1888856	(-0.13, 0.51)	0.244	1.138187	(0.82, 1.46)
Q3 Median Income	(\$81,100-\$98,600]	0.1131845	(-0.15, 0.38)	0.400	1.062485	(0.8, 1.34)
Q4 Median Income	(\$98,600-\$136,000]	0.0989014	(-0.37, 0.56)	0.678	1.048202	(0.58, 1.51)

Figure 19: ALS Median Income Quartiles



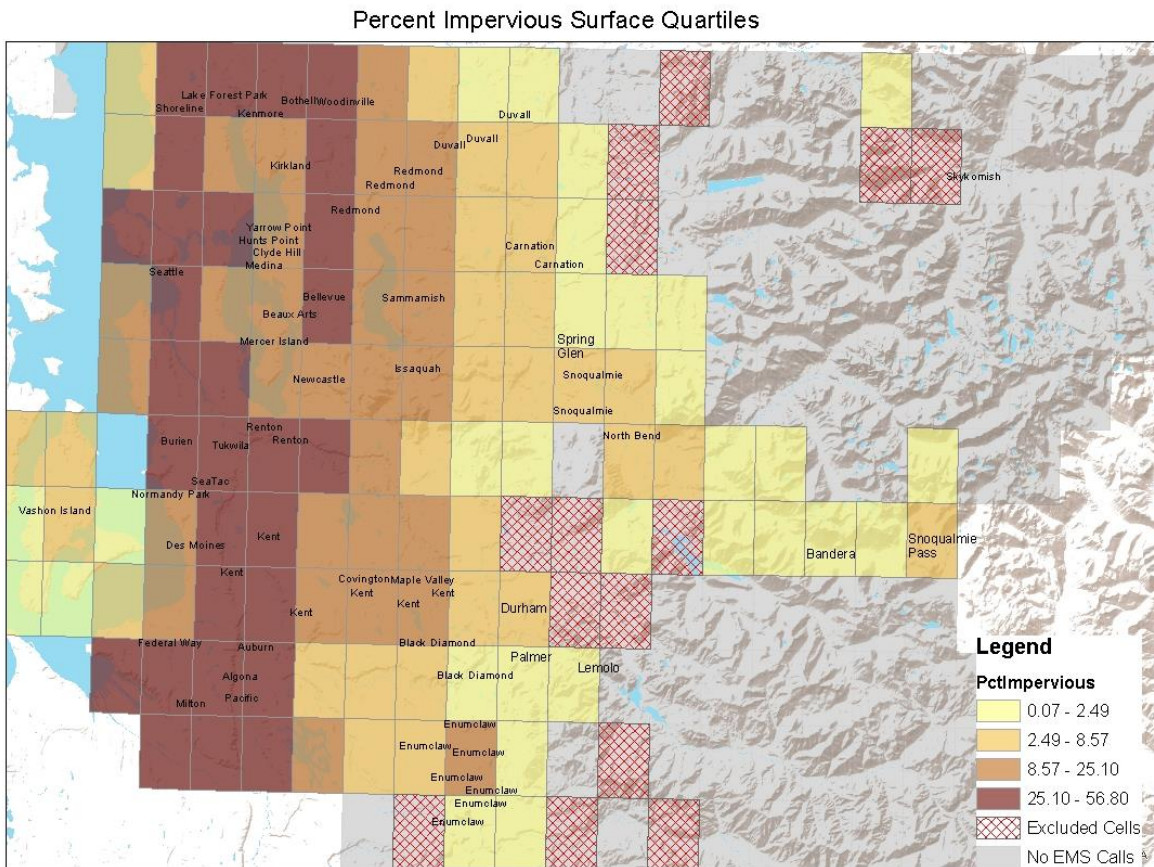
ALS Percent Impervious Surface

Table 17 presents the results for a linear model of ALS relative risk and quartiles of percent impervious surface. Quartile two of percent impervious surface (2.49%-8.57%) had the highest mean relative risk, and contrary to the BLS results, the lowest quartile of percent impervious surface [0.0763%-2.49%] had the lowest mean relative risk. After quartile two, there was a decreasing trend in mean relative risk of an ALS call, on a 99th percentile local extreme heat day compared to non-heat day, as the quartile of percent impervious surface increased. However, none of these quartiles had statistically significant results at the 0.05 level. The ALS quartile distribution of percent impervious surfaces can be viewed in Figure 20

Table 17: ALS Percent Impervious Surface Results

Variables	Quartile Percentages	Estimate	Estimate 95% CI	P-Value	Mean RR	Mean RR 95% CI
Intercept – Q1 Percent Impervious Surface	[0.0763-2.49%]	0.8531333	(0.35, 1.36)	9.7e-04*	0.8531333	(0.35, 1.36)
Q2 Percent Impervious Surface	(2.49-8.57%)	0.3500875	(-0.21, 0.91)	0.220	1.203221	(0.64, 1.76)
Q3 Percent Impervious Surface	(8.57-25.1%)	0.2368371	(-0.28, 0.75)	0.370	1.08997	(0.57, 1.60)
Q4 Percent Impervious Surface	(25.1-56.7%)	0.1987172	(-0.32, 0.72)	0.456	1.051851	(0.53, 1.57)

Figure 20: ALS Percent Impervious Surface Quartiles



ALS Percent Canopy

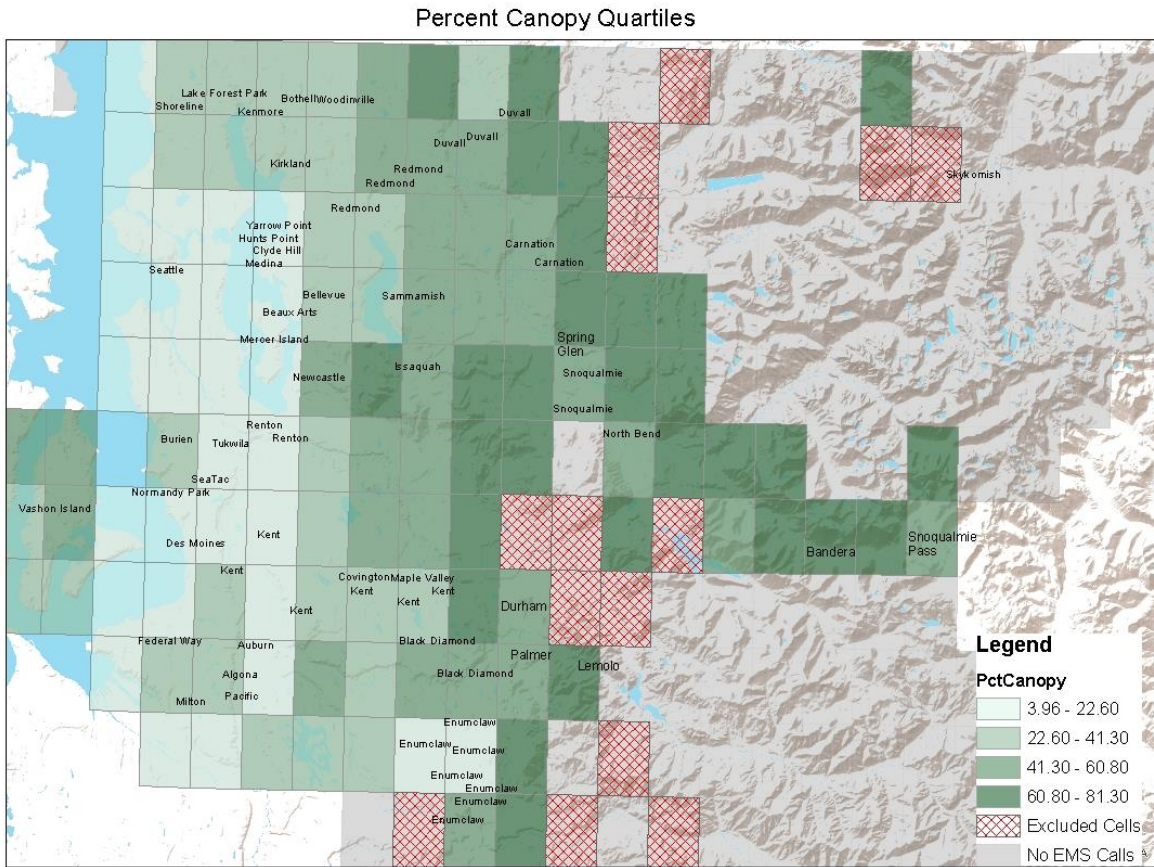
The linear regression model of ALS relative risk and percent canopy per grid cell also did not deliver any significant results as shown in Table 18. The mean relative risk of the lowest quartile of percent canopy [3.97%-22.6%] had a mean relative risk in ALS call volume of 1.06 (95% CI: 1, 1.12) times the number of ALS calls on a 99th percentile local extreme heat day compared to a non-heat day. The mean relative risk in quartile two of percent canopy increased by 0.06 (95% CI: -0.17, 1.2) compared to quartile one and quartile three increased by

0.13 (95% CI: -0.11, 0.37) compared to quartile one, but the mean relative risk of quartile four decreased by 0.26 (95% CI: -0.77, 0.25) compared to quartile one. These results were similar to the ALS percent impervious surface results because grid cell quartiles of percent impervious surface and percent canopy were strongly correlated. The grid cells with the highest percent canopy or the lowest percent impervious surface had the lowest risk of an ALS call on a local extreme heat day.

Table 18: ALS Percent Canopy Results

Variables	Quartile Percentages	Estimate	Estimate 95% CI	P-Value	Mean RR	Mean RR 95% CI
Intercept – Q1 Percent Canopy	[3.97-22.6%]	1.0662602	(0.93, 1.20)	5.33e-53*	1.0662602	(0.93, 1.20)
Q2 Percent Canopy	(22.6-41.3%]	0.0581601	(-0.17, 0.29)	0.620	1.12442	(0.90, 1.36)
Q3 Percent Canopy	(41.3-60.8%]	0.1333109	(-0.11, 0.37)	0.281	1.199571	(0.96, 1.44)
Q4 Percent Canopy	(60.8-81.2%]	-0.2583365	(-0.77, 0.25)	0.323	0.807924	(0.3, 1.32)

Figure 21: ALS Percent Canopy Quartiles



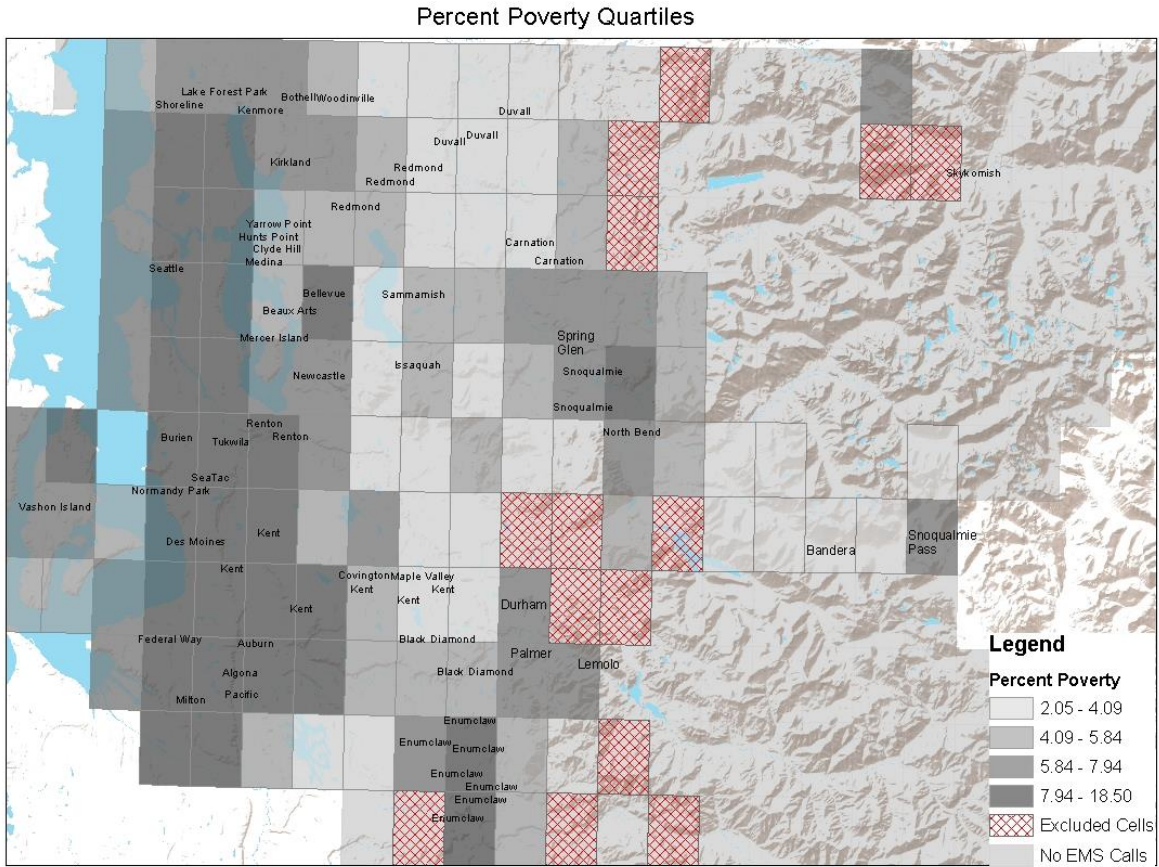
ALS Percent Poverty

The model results of the percent poverty regression with ALS grid cell relative risks are presented in Table 19 while the grid cell quartiles are mapped in Figure 22. Similar to the relationship with BLS relative risks, quartiles of percent poverty did not have any significant results or clear trends with the ALS relative risks.

Table 19: ALS Percent Poverty Results

Variables	Quartile Percentages	Estimate	Estimate 95% CI	P-Value	Mean RR	Mean RR 95% CI
Intercept – Q1 Percent Poverty	[2.06-4.09%]	1.0859750	(0.63, 1.54)	3.02e-06*	1.0859750	(0.63, 1.54)
Q2 Percent Poverty	(4.09-5.84%)	-0.0990506	(-0.64, 0.44)	0.718	0.986924	(0.45, 1.53)
Q3 Percent Poverty	(5.84-7.94%)	-0.0097926	(-0.51, 0.49)	0.970	1.076182	(0.58, 1.58)
Q4 Percent Poverty	(7.94-18.5%)	-0.0368818	(-0.51, 0.43)	0.877	1.049093	(0.58, 1.52)

Figure 22: ALS Percent Poverty Quartiles



ALS Log Population

Grid cell log population had a positive relationship with ALS relative risk, as shown in

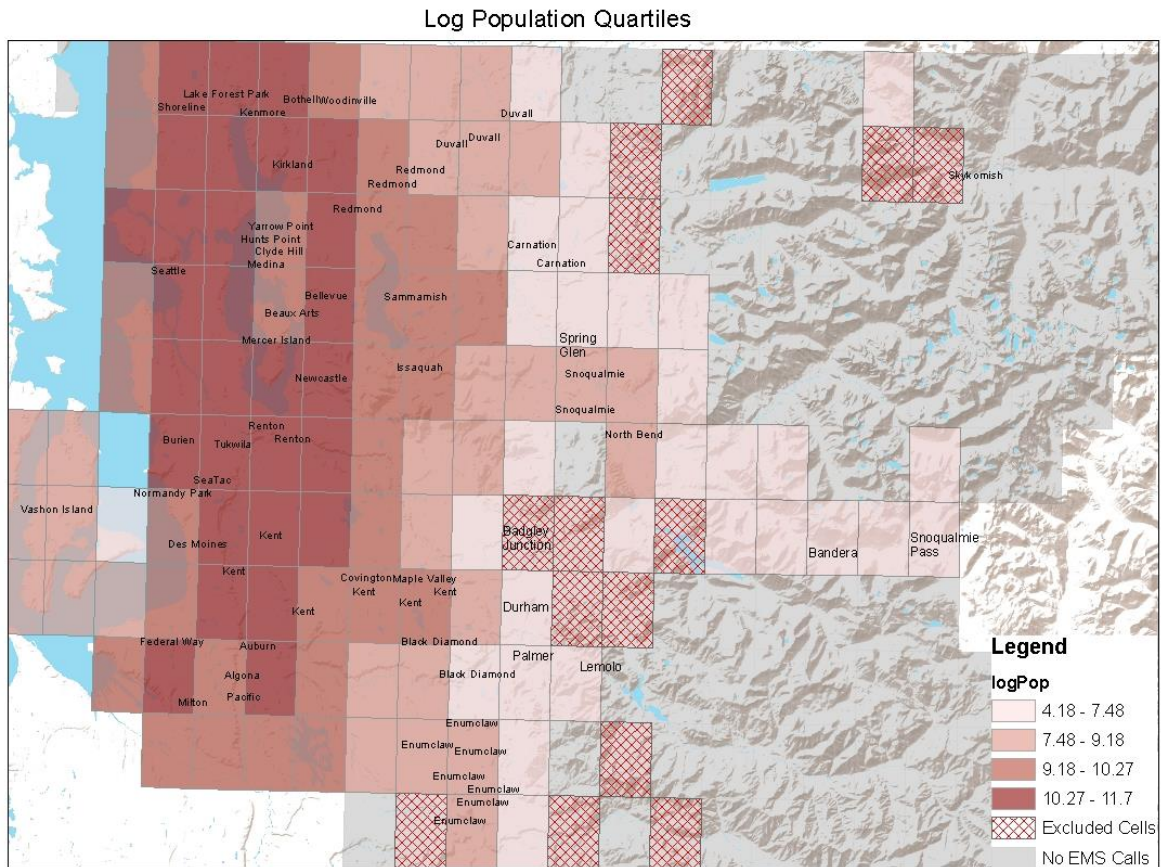
Table 20. When there was a one unit increase in log population, relative risk increased by 0.016

(95% CI: -0.04, 0.16) on a 99th percentile heat day compared to a non-heat day. However, this was not a statistically significant finding. Although the variable was continuous, quartiles of log population in King County can be seen in Figure 23 for visual grid cell comparison purposes. Again, the intercept did not have scientific meaning because there were no grid cells with a population of 1 person.

Table 20: ALS Log Population Results

Variables	Estimate	Estimate 95% CI	P-Value
Intercept	0.54113901	(-0.46, 1.54)	0.289
Log Population	0.05806516	(-0.04, 0.16)	0.255

Figure 23: ALS Log Population Quartiles



ALS Grid Cell Population Age Groups

Finally, each age group variable for percent of the grid cell population was modeled with ALS relative risk and the results are printed in Table 21. There was a negative relative risk relationship with grid cell population percent 45-64 and percent 65-84. Percent of the population younger than 5, percent 5-14, 15-44, and percent older than 85 had a positive association meaning that as percent of population in the age group increased, so did the relative risk of an ALS call on a 99th percentile local heat day compared to a non-heat day. The percent younger than 5 and percent age 45-64 had statistically significant results. For each one percent increase in the grid cell population younger than 5, there was an increase of 0.08 (95% CI: 0.002, 0.16) in relative risk of an ALS call on an extreme heat day compared to a non-heat day (p-value=0.044). The risk of an ALS call decreased by 0.026 (95% CI: -0.049, -0.002) for each one percent increase in population age 45-64 (p-value = 0.033).

Table 21: ALS Age Group Results

Variables	Estimate	Estimate 95% CI	P-Value
Percent Younger than 5			
Intercept	0.5384707	(0.024, 1.05)	0.040*
Percent Younger than 5	0.0834264	(0.002, 0.16)	0.044*
Percent Age 5-14			
Intercept	0.9387118	(0.44, 1.43)	2.04e-04*
Percent Age 5-14	0.0083393	(-0.033, 0.049)	0.690
Percent 15-44			
Intercept	0.6314104	(-0.10, 1.37)	0.0925
Percent 15-44	0.0107090	(-0.007, 0.028)	0.231
Percent Age 45-64			
Intercept	1.8418428	(1.19, 2.49)	2.7e-08*
Percent Age 45-64	-0.025725	(-0.049,-0.002)	0.033*

Percent Age 65-84			
Intercept	1.1031438	(0.41, 1.80)	1.87e-03*
Percent Age 65-84	-0.005751	(-0.07, 0.06)	0.864
Percent Older than 85			
Intercept	0.9250989	(0.56, 1.29)	5.18e-07*
Percent Older than 85	0.0876053	(-0.09, 0.27)	0.344

ALS Model Selection 1

The following tables show the best fit model for the ALS dataset selected by the Bestglm package using the best subset model selection process. Model 1 in Table 22 was the model selected when the predictor variables percent impervious surface, percent canopy, log population, percent poverty, and median income were included. The single best fit model included only log population, but it was not a statistically significant result (p-value=0.255). A one unit increase in log population had a positive 0.06 (95% CI: -0.042, 0.16) increase in relative risk on a local 99th percentile extreme heat day compared to a non-heat day.

Table 22: ALS Model Subset Selection 1 Results with Total Population of Grid Cell

Variables	Estimate	Estimate 95% CI	P-Value
Intercept	0.541139	(-0.46, 1.54)	0.289
Log Pop	0.058065	(-0.042, 0.16)	0.255

ALS Model Selection 2

However, when percent of the population in designated age groups were included in the model selection process, grid cell population percent younger than 5 and percent older than 85 appeared in the single best fit model. When comparing grid cells with similar percent of the population older than 85, a one unit increase in percent of the population younger than

5 had a positive 0.11 (95% CI: 0.035, 0.19) increase in relative risk on a local 99th percentile extreme heat day compared to a non-heat day. This was a statistically significant result with a p-value of 0.004. When comparing grid cells with similar percent of the population younger than 5, a one unit increase in percent of the population older than 85 had a positive 0.15 (95% CI: -0.034, 0.34) increase in relative risk on a local 99th percentile extreme heat day compared to a non-heat day.

Table 23: ALS Model Subset Selection 2 Results with Age Group Population of Grid Cell

Variables	Estimate	95% CI	P-Value
Intercept	0.130074	(-0.55, 0.81)	0.707
Percent Younger than 5	0.114879	(0.035, 0.19)	4.6e-03*
Percent Older than 85	0.151858	(-0.034, 0.34)	0.109

SPATIAL AUTOCORRELATION:

The Moran’s I test looking for spatial autocorrelation in the best fit model concluded there was no clustering or dispersion patterns between grid cell locations and residual model values. The Moran’s I test results of each best fit model are displayed in Table 24.

Table 24: Moran’s I Spatial Autocorrelation Results

Model	Moran’s I Index Value	P-Value
BLS Model 1: All Age Pop	4.23e-05	0.437
BLS Model 2: Age Group Pop	0.003	0.414
ALS Model 1: All Age Pop	-0.023	0.613
ALS Model 2: Age Group Pop	-0.052	0.802

None of the p-values were statistically significant, so we could not reject the null hypothesis that there was no spatial auto-correlation in the values. The results indicated that it was more likely the spatial distribution of grid cells and their values were randomly spaced.

STUDY POWER:

Study power was definitely of concern in this analysis. There were already some limitations to study power when finding the relative risk of each grid cell due to the division of EMS calls into more spatially accurate grid cells. Because this section of the analysis heavily depended on the accuracy of relative risk in the first section, the robustness of the results were questionable. The lack of significant findings and slightly varying results in the various linear regressions could indicate that more EMS data was needed in addition to a wider spatial range of grid cells.

DISCUSSION

Previous research by Calkins et al. (2016) found an 8% (RR of 1.08; 95% CI: 1.06, 1.09) increase of BLS calls and a 14% (RR of 1.14; 95% CI: 1.09, 1.2) increase of ALS calls on extreme heat days compared to non-heat days in King County, WA. When this data was redefined on a more spatially precise grid scale, the results varied across the county. BLS relative risks ranged from 0 to 4.13 (95% CI: 1.65, 10.32) and ALS relative risks ranged from 0 to 6.50 (95% CIs: 1.06, 40.03), both excluded grid cells with 5 or less total calls over the six year study period. In order to compare the crude county-wide relative risk results from Calkins et al. (2016) with the grid cell relative risks, Table 25 and Table 26 show the number and percent of grid cells which were above the results from Calkins et al. (2016), as well as the number and percent of grid cells that were 10%, 25%, 50% and 100% higher. About 56% of grid cells were above the county-wide estimate for BLS calls, and 44% of grid cells were above the county-wide estimate for ALS calls.

Table 25: Grid Cells Above Calkins et al. (2016) BLS Crude Relative Risk Estimate

	Number of Grids	Percent of Grids
Above or equal to 1.08	69	55.64%
10% greater than 1.08 (1.188)	26	20.97%
25% greater than 1.08 (1.35)	14	11.29%
50% greater than 1.08 (1.62)	9	7.26%
100% greater than 1.08 (2.16)	4	3.23%

Table 26: Grid Cells Above Calkins et al. (2016) ALS Crude Relative Risk Estimate

	Number of Grids	Percent of Grids
Above or equal to 1.14	51	43.97%
10% greater than 1.14 (1.254)	38	32.76%
25% greater than 1.14 (1.425)	19	16.38%
50% greater than 1.14 (1.71)	11	9.48%
100% greater than 1.14 (2.28)	7	6.03%

These results showed large variation in relative risk across the county. As one can observe from the relative risk BLS and ALS maps with city labels (Figure 24 and Figure 25), grids with the highest increase in risk were mostly located in central King County with a few towards eastern King County. However, grid cells in eastern King County often ran into problems with statistical power likely because population counts and call counts were low on this side of the county; the grids with statistically significant increases in risk were generally in the more populated regions.

Theoretically, according to the urban heat island effect, an increase in percent impervious surface and percent development in urban cores lead to an increase in temperatures. Akbari (2005) claimed that heat given off from impervious surfaces such as pavement increased temperatures in cities up to 5.5°C (22°F) compared to rural areas nearby. Conversely, an increase in tree canopy was shown to have cooler air temperatures during an extreme heat event (Buyantuyev & Wu, 2010; Jenerette et al., 2011; Zhang et al., 2011;

Johnson & Wilson, 2009; Huang et al., 2011). Based on this, we predicted that increased tree canopy would have a protective factor on the relative risks of an EMS call on a local extreme heat day compared to non-heat day in King County, and that increased impervious surface would increase the risk of an EMS call on an extreme heat day in King County. However, the overall trend of these results showed the opposite effect. As impervious surface increased and tree canopy decreased, relative risk of an EMS calls decreased. The highest relative risks were in grid cells located in or near small towns such as Carnation, Durham, Black Diamond, and outside North Bend and Snoqualmie. While Seattle had some significant increases in the risk of an EMS call on a BLS or ALS extreme heat day compared to non-heat days, these results were not the highest risks.

Figure 24: BLS Crude RR with City Labels

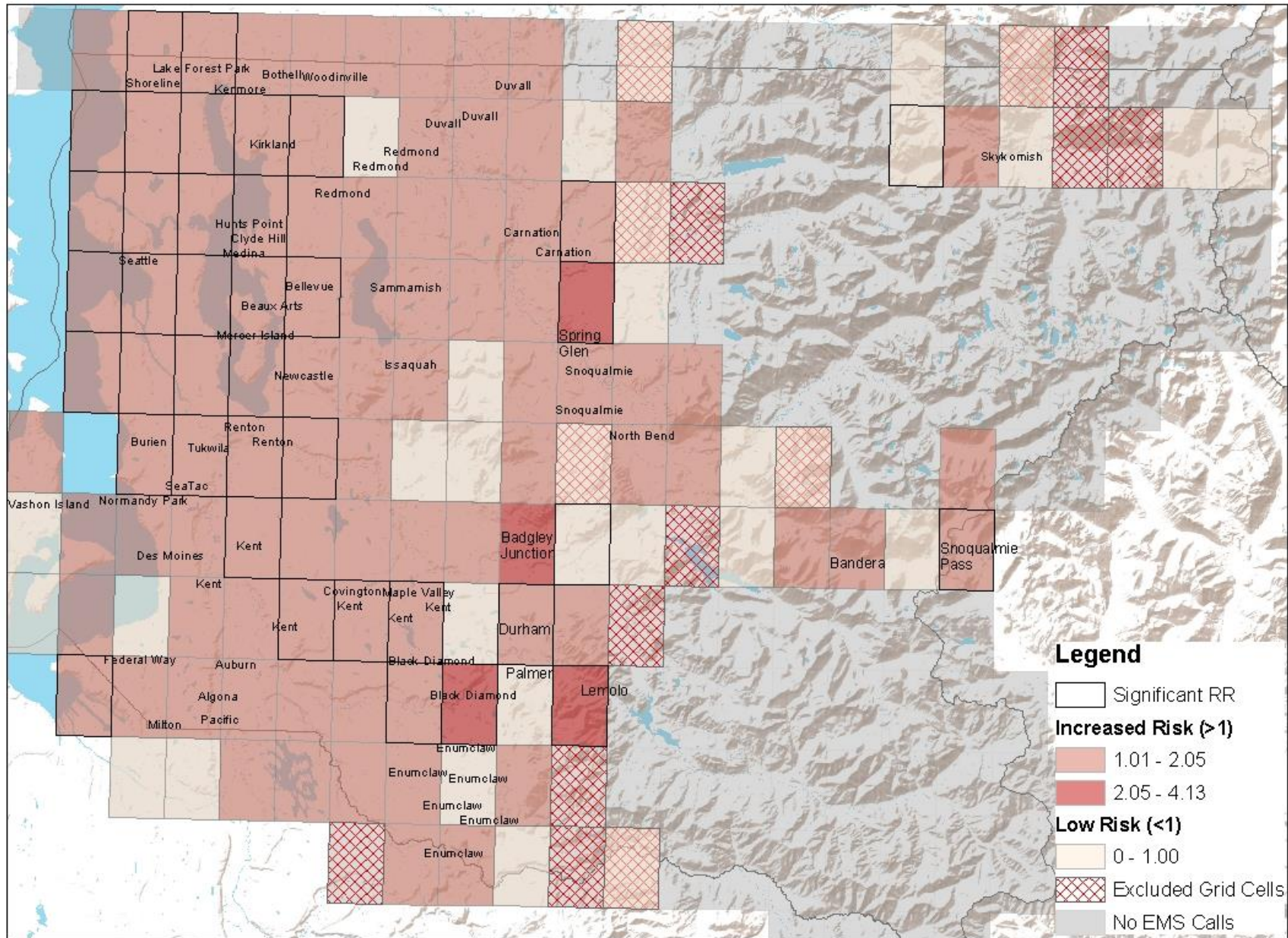
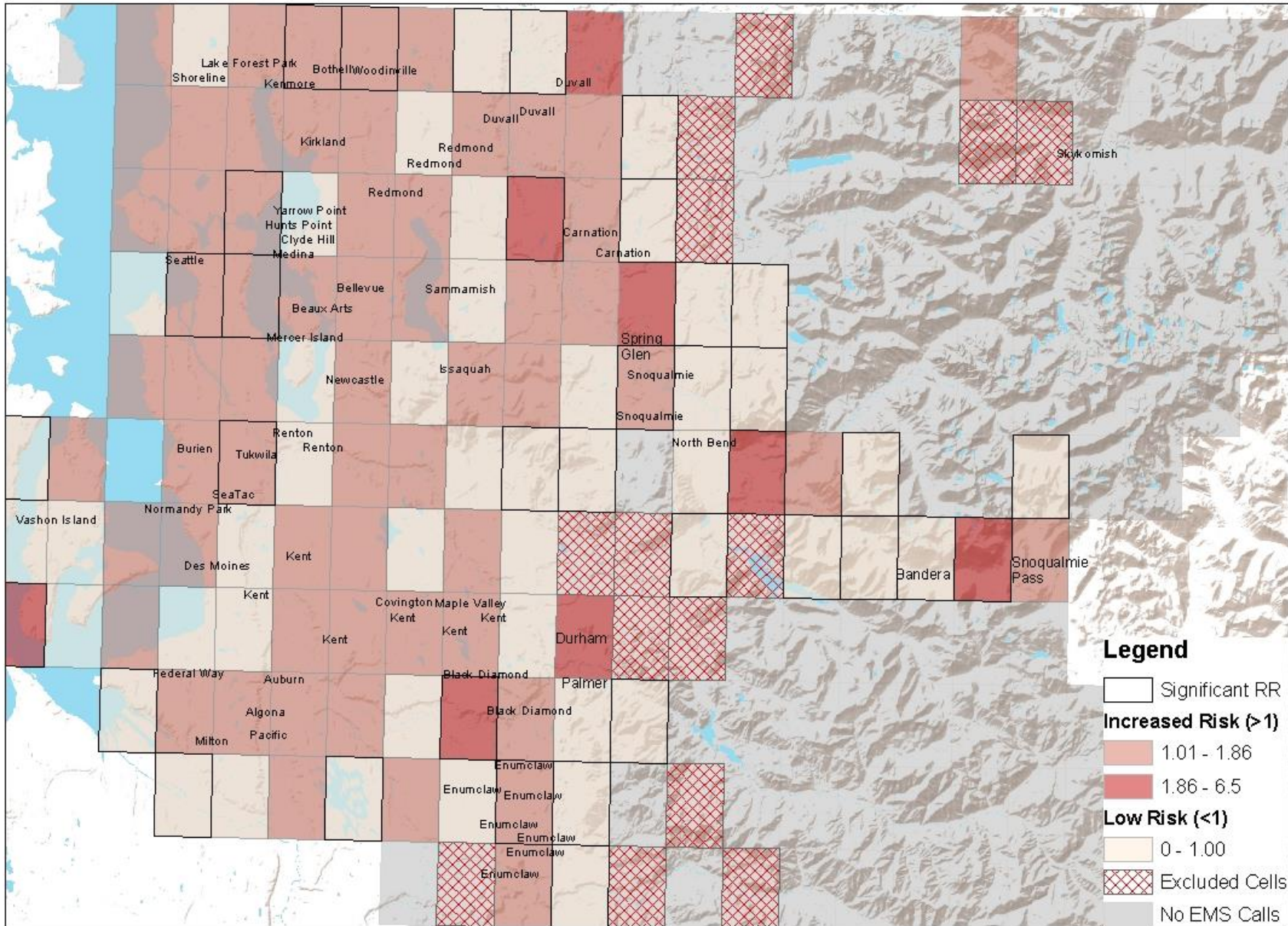


Figure 25: ALS Crude RR with City Labels



Exploratory graphs and maps, showed strong collinearity between population, impervious surface, and tree canopy. As population increased, so did the percent impervious surface. Similarly, tree canopy decreased as population and impervious surface increased. These relationships can be seen in the maps for quartiles of log population, impervious surface, and tree canopy. The highest population and highest impervious surface grid cells are also the grid cells with the lowest tree canopy; these grids are located along the I-5 corridor where the city of Seattle, Renton, Kent and Federal Way are located. In addition, the highest quartiles of percent poverty and lowest quartiles of median household income were more or less located in areas with the highest impervious surface quartile and highest log population quartile.

For individual linear regression models with quartiles of percent impervious surface, the BLS dataset showed a clear trend of decreasing mean relative risk as quartile of impervious surface increase. Since percent impervious surface and percent canopy have a strong inverse relationship, BLS quartiles of percent canopy also had a clear trend of increasing mean relative risk as quartiles of percent canopy increase. In summary, quartile four grid cells of percent canopy, which match up well with quartile one grid cells of percent impervious surface, had the highest risk of a BLS call, while quartile one of percent canopy and quartile four of percent impervious surface had the lowest risk of a BLS call on an extreme heat day compared to a non-heat day. When looking at the quartile maps (Figure 15 and 16), this means the lowest risk of a BLS calls are along the I-5 corridor where the larger cities are located, while risk of a BLS calls

increases as one moves outside of the city, particularly into the forested, mountainous regions of central and eastern King County. Previous research found that increased canopy and decreased impervious surface were protective/cooling factors during extreme heat events; the BLS results were opposite of our original hypothesis. The high mean relative risks in the lowest quartile for percent impervious surface and highest quartile for percent canopy may indicate that BLS calls could be more related to activities of the patient. On nice days, people in King County are avid hikers who enjoy the natural beauty in the Cascade Mountains. We speculate that the increased physical activity on extreme heat days in the high percent canopy grid cells of the Cascade Mountains may have led to the increased risk in BLS calls.

The ALS results for percent impervious surface and percent canopy have a similar trend with one major difference: quartile four of percent canopy and quartile one of percent impervious surface (those quartiles in the most forested region, generally furthest east) have the lowest risk of an ALS call on an extreme heat day compared to a non-heat day. Because ALS calls are more severe, they may correspond in large part to patients with previous health conditions. These patients with underlying health conditions will probably not go out hiking on extreme heat days in the mountainous regions of quartile four grid cells for percent canopy and quartile one grid cells for percent impervious surface. When looking at the map of percent canopy, the large cities or smaller towns are not located in the quartile four grid cells. The quartile four grid cells border the towns, but are not areas with high populations. Therefore, we hypothesize these eastern grid cells are grid cells people may be traveling to for recreational

activities, but those with health conditions may be less inclined to be participate in recreational activities. In conclusion, we hypothesize that the BLS calls may be more related to physical activity on extreme heat days, while ALS calls might be caused from a combination of activity as well as underlying disease.

Individual linear regression model results for the BLS and ALS dataset showed similar results for the quartiles of median household income. Out of the quartiles of median income, the lowest quartile of median income had the lowest mean relative risk of a BLS and an ALS call on an extreme heat day compared to a non-heat day. Conversely, quartile two of median income had the highest mean relative risk for both BLS and ALS calls. This quartile had a statistically significant increase in relative risk for the BLS dataset by 0.26 compared to the lowest quartile; on average, there were 1.3 times the number of BLS calls on an extreme heat day compared to a non-heat day in quartile two grid cells of median household income. Overall, the lowest quartile of median income grid cells were located in high impervious surface areas along the I-5 corridor. Because lower income populations were known to have more underlying health effects, it was not necessarily surprising that quartile two of median income had a high mean relative risk of BLS and ALS calls on an extreme heat day. However, it was somewhat surprising that the lowest quartile of median income was related to the lowest risks for both BLS and ALS datasets. It is possible this could be due to the high costs of medical attention. One hypothesis may be that people in low income areas may be much less willing to seek medical attention due to the steep costs of this process. These

results could also be correlated to the location of quartile two grid cells. When looking at the spatial distribution of these grid cells, they are dispersed throughout the county, often in the smaller cities/towns. These areas could be high recreational areas where people hike from or areas where there are hazardous industrial activities occurring. Since median income measured the income level of the population who lived in the grid cell, it did not necessarily portray the income level of the person who made the BLS or ALS call. Therefore, we cannot say whether these results are driven directly from household income or from other factors which are related to the location of the income quartiles.

There were no trends in quartiles of percent poverty for the BLS or ALS datasets, nor any statistically significant results. This may indicate that poverty does not have a strong correlation to risk of an EMS call on extreme heat day compared to a non-heat day.

BLS and ALS data had different results when relative risk was modeled with log population of the grid cells. BLS relative risk decreased for each one unit increase in log population, while ALS relative risk increased for each one unit increase in log population. These BLS result may support the activity hypothesis for BLS calls because population decreases as one travels outside of the city into more recreational areas. Furthermore, the ALS results may be different due to the hypothesis that ALS calls are more related to chronic health conditions which can be present in more populated areas.

Moreover, the BLS and ALS results for the grid cell age group populations also varied. These trends could be due to a combination of differences in activities, risk mindsets, and/or

underlying health conditions in each age group. The only statistically significant results were an increase in ALS relative risk with each one percent increase in percent of the population younger than 5 and a decreases in ALS relative risk with each one percent increase in percent of the population age 45-64. These results could be due to a more cautious mindset or financial stability those aged 45-64, and a higher risk of underlying health conditions in children younger than 5. However, it is difficult to accurately predict reasons for these age group trends without further research. It is important to remember that these age groups were characteristics of the grid cell populations, not ages for the actual ALS and BLS patients.

Model 1 of the BLS formal model selection process supported the activity-based hypothesis with strong trends of decreased relative risk in higher quartiles of percent impervious surface after adjusting for log population and quartiles of median income. In addition, when comparing grid cells with similar log populations and quartiles of impervious surface, quartiles of median income had the same trend as its individual model: quartile one of median income had the lowest risk and quartile two had the highest risk of BLS call on an extreme heat day compared to a non-heat day. In order to confirm the BLS physical activity hypothesis, further research needs to be done to collect patient specific information on activity during the call and details about the incident environment. The first ALS formal model selection process continue to highlight the differences in BLS and ALS call trends. For ALS model 1, the best fit model includes only a positive relationship with log population. This model indicated that no environmental or socioeconomic variable stand out as a strong

predictor for ALS calls. This could be due to a lack of statistical power to detect these effects, or because ALS calls could be more related to underlying health problems in the patients rather than activity. When the population age group variables were included in both the BLS and ALS formal model selection process, only age group populations were included in the models. However, as previously stated, the age groups were characteristics of those living in the grid cell, not of the specific patients, so it is difficult to heavily rely on these factors as causal factors for BLS and ALS relative risks.

LIMITATIONS AND FURTHER RESEARCH

There were a number of limitations to this research. To start, grid cell data was collected from only one of the six years in the study time frame, so because this data was cross-sectional, it did not account for natural population, environmental, or socioeconomic changes over time. It also assumed that the average canopy, income, poverty, and impervious surface for the grid cell represented every area of the cell, but half of the grid could be covered in trees while the other half was fully industrialized. Even more uncertainty stemmed from the extrapolation of population, income, and poverty information from the census tract level to the grid cell level. This assignment assumed population, income and poverty were evenly distributed throughout census tracts and calculated grid cell averages based on weighted percentages of the census tract inside each grid cell. Extrapolation from the census tract to the grid cell level was particularly a problem on the eastern side of the county where census tracts were large and encompassed multiple grid cells with sparse populations. Ideally, all grid cell variables would be collected on the grid cell level, instead of extrapolated, for each year in the study period.

These data also limited our evaluation of health related heat effects to only the people who call for EMS help. There may be many other people who seek care for heat related health effects, but found their own transportation to a hospital, emergency care facilities, or used private ambulance services. Calkins et al. (2016) suspected that many elderly facilities used private ambulance services which could have greatly reduced the count and relative risk of EMS

calls on local heat and non-heat days. In the future, a dataset should include calls from all ambulance sources.

We adjusted for some time trend variables such as weekday/weekend, but there may be others that were not accounted for due to a lack of data. For example, traffic counts and flows or air pollution data would be potential time trend variables affecting call counts over the six year period. Additionally, there could be monthly trends which were not included. Furthermore, the time trends were based on county-wide averages instead of the grid cell level.

An important limitation to note in this analysis was the use of an *a priori* threshold to define a heat day and non-heat day. This threshold was determined by Calkins et al. (2016) based on county-wide humidex averages and EMS calls. However, because this analysis was done on a more precise grid cell level and county wide averages were not used, the threshold for BLS and ALS calls could be significantly different than the county-wide threshold. It should also be noted that the extended 2009 extreme heat event did increase the extreme heat threshold over the 5 year study period and therefore affected the number of heat and non-heat days. We helped adjust for this factor by including multiple years before and after 2009. However, even a small difference in humidex threshold would affect all of the results in the analysis. A relative risk was calculated through differences in EMS call volumes from a heat day and non-heat defined through the humidex threshold. If the relative risk results changed from a change in the extreme heat threshold, this has potential to alter the results of all of the regression models. A future analysis of the BLS and ALS dataset should re-examine the heat day

and non-heat day threshold or look at a more detailed time series analysis where call volumes in each grid cell increased by X amount for each one unit increase in daily humidex.

Additionally, limitations occurred through assumptions of patient and grid cell data. There was no information the patient's health history, activities before/during the EMS call, environment the patient was located in, or the patient's specific socioeconomic status. It is likely these factors are major contributors to the person's susceptibility to heat related health effects and should be accounted for. In an attempt to consider some of these factors, this analysis found grid cell averages for percent canopy, percent impervious surfaces, percent water, percent development, median household income, percent of the population in designated age groups, and percent below poverty. However, these characteristics were averages for the population living in the local grid cells in which the EMS call was made, but it is very possible that the patient did not live in the same grid cell they called for an ambulance in. People frequently travel throughout King County for work or other activities on a daily basis. Particularly, the areas of highest BLS relative risk are also popular destinations people travel to for recreational activities. Therefore, it was a large assumption to accept that the characteristics of the grid cell where the call was made were relevant to the risk of an EMS call on a local extreme heat day.

Specific information on the environment of the call location such as whether the patient was indoors, with or without AC, or outdoors, in the urban core or under shaded tree canopy. Furthermore, physical activity in the sun would cause a much higher heat burden than

working at a desk in an air conditioned building. In addition to these extrinsic factors of heat burden, there were also intrinsic factors for heat burden related to age, gender, and previous health conditions, particularly respiratory disease, cardiovascular disease, or diabetes conditions (U.S. Global Change Research Program, 2016). Based on the lack of a consistent trend for the ALS dataset, we hypothesize that ALS calls were more correlated to these intrinsic factors, and a future study could better assess the relationship between advanced life support calls and previous health conditions, age, gender, or diagnosis of call. Due to statistical power of the refined spatial scale, we were unable to account for this information in our analysis. In addition, household income and poverty status can be determinants of regular access to protective heat factors such as AC and water. These are all key predictors that should be collected for each patient instead of for average grid cell characteristics in a future study analyzing the health effects of extreme heat.

CONCLUSION

This study re-defines the spatial scale of Emergency service medical calls in King County WA from the research done by Calkins et al. (2016). Calkins et al. (2016) used a county-wide daily humidex value to define an extreme heat day and non-heat day, but it did not account for the wide variation in humidex values across the county on any given day. This more spatial sensitive analysis highlighted the areas that were particularly vulnerable to an EMS call in the event of extreme heat. Although low impervious surface and high tree canopy effect modifiers are proven to decrease local air temperatures, our results indicated a reverse relationship with relative risk and BLS call volumes, which raises the question whether physical activity may be a better predictor for a BLS call on an extreme heat day compared to non-heat day. In order to better assess predictor variables of ALS calls, data needs to be collected on underlying health conditions of the patient. Further research should be done to analyze the relationship between patient-specific activity, environment, and health conditions with the risk of an EMS call in King County, WA.

REFERENCES

- Akbari H. Energy Saving Potentials and Air Quality Benefits of Urban Heat Island Mitigation. Lawrence Berkeley National Laboratory. 2005.
- Alessandrini E, Sajani S, Scotto F, Miglio R, Marchesi S, Lauriola P. Emergency ambulance dispatches and apparent temperature: a time series analysis in Emilia-Romagna, Italy. *Environmental Research*. 2011; 111:1192-1200.
- Bassil KL, Cole DC, Moineddin R, Lou W, Craig AM, Schwartz B, Rea E. The relationship between temperature and ambulance response calls for heat-related illness in Toronto, Ontario, 2005. *Journal of Epidemiology Community Health*. 2011; 65:829-831.
- Busch Isaksen T, Fenske R, Hom E, Ren Y, Lyons H, Yost, M. Increased mortality associated with extreme-heat exposure in King County, Washington, 1980-2010. *International Journal of Biometeorology*. 2016; 85-98.
- Busch Isaksen T, Yost M, Hom E, Ren Y, Lyons H, Fenske R. Increased hospital admissions associated with extreme-heat exposure in King County, Washington 1990-2010. *Reviews on Environmental Health*. 2014; 51-64.
- Buyantuyev A, Wu J. Urban heat islands and landscape heterogeneity: linking spatiotemporal variations in surface temperatures to land-cover and socioeconomic patterns. *Landscape Ecology*. 2010; 17-33.
- Calkins MM, Isaksen TB, Stubbs BA, Yost MG, Fenske RA. Impacts of extreme heat on emergency medical service calls in King County, Washington, 2007–2012: relative risk and time series analyses of basic and advanced life support. *Environ. Heal*. 2016; 15:13.
- Carrega P. A method for the reconstruction of mountain air temperatures with automatic cartographic applications. *Theoretical Applied Climatology*. 1995; 69-84.
- Center for Disease Control (CDC). Climate and Health Program. 2016. Retrieved from <https://health2016.globalchange.gov/temperature-related-death-and-illness>.
- Center for Disease Control (CDC). About Extreme Heat. 2004. Retrieved from <http://www.bt.cdc.gov/disasters/extremeheat/about.asp>
- Congressional Black Caucus Foundation (CBCF). African Americans and climate change: an unequal burden. Washington, D.C: Redefining Progress. 2004.
- Curriero FC, Heiner KS, Samet JM, Zeger SL, Strug L, & Patz JA. Temperature and mortality in 11

- cities of the eastern United States. *Am J Epidemiol.* 2002; 155(1): 80-87.
- Davis RE, Knappenberger PC, Michaels PJ, Novicoff WM. Changing heat-related mortality in the United States. *Environmental Health Perspectives.* 2003; 1712-1718.
- Department of Ecology and NOAA. Western Washington Land Cover Change. 2016. Retrieved from Washington State Department of Ecology: <http://www.ecy.wa.gov/services/gis/data/imageryBaseMapsEarthCover/landcover/landcover.htm>.
- Dolney TJ, Sheridan SC. The relationship between extreme heat and ambulance response calls for the city of Toronto, Ontario, Canada. *Environmental Research.* 2006; 101: 94-103.
- Eliasson I, Svensson MK. Spatial air temperature variations and urban land use - a statistical approach. *Meteorological Applications.* 2003; 135-143.
- Ghumman U, Horney J. Characterizing the Impact of Extreme Heat on Mortality, Karachi, Pakistan. *Prehospital Disaster Medicine.* 2016; 263-266.
- Golden JS, Hartz D, Brazel A, Luber G, Phelan P. A biometeorology study of climate and heat-related morbidity in Phoenix from 2001 to 2006. *International Journal of Biometeorology.* 2008; 52:471-480.
- Harlan SL, Brazel AJ, Prashad L, Stefanov WL, Larsen L. Neighborhood microclimates and vulnerability to heat stress. *Social Science & Medicine.* 2006; 2847-2863.
- Harlan SL, Deplet-Barreto JH, Stefanov WL, Petitti DB. Neighborhood Effects on Heat Deaths: Social and Environmental Predictors of Vulnerability in Maricopa County, Arizona. *Environmental Health Perspectives.* 2013; 197-204.
- Hoppe P. The physiological equivalent temperature - a universal index for the biometeorological assessment of the thermal environment. *International Journal of Biometeorology.* 1999; 71-5.
- Huang G, Zhou W, Cadenasso ML. Is everyone hot in the city? Spatial pattern of land surface temperatures, land cover, and neighborhood socioeconomic characteristics in Baltimore, MD. *Journal of Environmental Management.* 2011; 1753-1759.
- International Federation of Red Cross (IFRC). India: Heat wave. *Information Bulletin 1/2003.* 2003. Available at www.ifrc.org.
- James G, Witten D, Hastie T, Tibshirani R. *An Introduction to Statistical Learning with Applications in R.* New York: Springer. 2013

- Jenerette GD, Harlan SL, Stefanov WL, Martin CA. Ecosystem services and urban heat riskscape moderation: water, green spaces and social inequality in Phoenix, USA. *Ecological Applications*. 2011; 2637-2651.
- Johnson DP, Wilson JS. The socio-spatial dynamics of extreme urban heat events: the case of heat-related deaths in Philadelphia. *Applied Geography*. 2009; 419-434.
- Johnson DP, Stanforth A, Lulla V, Lubert G. Developing an applied extreme heat vulnerability index utilizing socioeconomic and environmental data. *Applied Geography*. 2012; 23-31.
- Kestens Y, Brand A, Fournier M, Goudreau S, Kosatsky T, Maloley M, Smargiassi A. Modelling the variation of land surface temperature as determinant of risk of heat-related health events. *International Journal of Health Geographics*. 2011; 1-9.
- Kilbourne EM. Heat-related illness: Current status of prevention efforts. *American Journal of Preventive Medicine*. 2002; 328-329.
- Klinenberg E. *Heat wave: A social autopsy of disaster in Chicago*. University of Chicago Press. 2002.
- Knutti R, Hegerl GC. The equilibrium sensitivity of the earth's temperature to radiation changes. *Nature Geoscience*. 2008; 735-742.
- Kolpak P, Wang L. Exploring the social and neighborhood predictors of diabetes: A comparison between Toronto and Chicago. *Primary Health Care Research Development*. 2017; 1-9.
- Kue RC, Dyer K. The impact of heat waves on transport volumes in an urban emergency medical services system: a retrospective review. *Prehospital and Disaster Medicine*. 2013; 28:610-615.
- Laing B, Weng Q. Multiscale analysis of Census-based land surface temperature variations and determinants in Indianapolis, United States. *Journal of Urban Planning and Development*. 2008; 129-139.
- Lindqvist S. *Bebyggelseklimatologiska studier* PhD thesis, Lund University. CWK Gleerup. 1970.
- Long JS, Ervin LH. Using Heteroscedasticity Consistent Standard Errors in the Linear Regression Model. *The American Statistician*. 2000; 54:217-224.
- Maurer EP, Wood AW, Adam JC, Lettenmaier DP, Nijssen B. A long-term hydrologically based data set of land surface fluxes and states for the conterminous United States. *Journal of Climate*. 2002; 15:3237-3325.

- Medina-Ramon M, Zanobetti A, Cavanagh DP, Schwartz J. Extreme temperature and mortality: assessing effect modification by personal characteristics and specific cause of death in a multi-city case-only analysis. *Environmental Health Perspectives*. 2006; 114:1331-1336.
- Meinshausen ME. Greenhouse-gas emission targets for limiting global warming to 2 degrees C. *Nature*. 2009; 1158-1162.
- Montenegro A, Brovkin V, Eby M, Archer D, Weaver AJ. Long term fate of anthropogenic carbon. *Geophysical Research Letter*. 2007; 34:L19707.
- Naughton MP, Henderson A, Mirabelli MC, Kaiser R, Wilhelm JL, Kieszak SM, McGeehin MA. Heat-related mortality during a 1999 heat wave in Chicago. *American Journal of Preventive Medicine*, 2002; 221-227.
- Naughton GA, Carlson JS. Reducing the risk of heat-related decrements to physical activity in young people. *Journal of Science and Medicine in Sport*. 2008; 11:58-65.
- Reid CE, O'Neil MS, Gronlund CJ, Brines SJ, Brown DG, Diez-Roux AV, et al. Mapping community determinants of heat vulnerability. *Environmental Health Perspectives*. 2009; 117:1730-1736.
- Roe GH, Baker MB. Why is climate sensitivity so unpredictable? *Science* 2007; 629-632.
- Rogot E, Sorlie PD, Backlund E. Air conditioning and mortality in hot weather. *American Journal of Epidemiology*. 1992; 106-116.
- Santee WR, Wallace RF. Use of Humidex to set Thermal Work Limits for Emergency Workers in Protective Clothing. *Industrial Health*. 2011; 49: 95-106.
- Semenza JC, Rubin CH, Falter KH, Selanikio JD, Flanders WD, Howe HL, et al. Heat-related deaths during the July 1995 heat wave in Chicago. *New England Journal of Medicine*. 1996; 84-90.
- Sherwood SC, Huber M. An adaptability limit to climate change due to heat stress. *PNAS*. 2010; 9552-9555.
- Smoyer KE. Putting risk in its place: methodological considerations for investigating extreme event health risk. *Social Science Medicine*. 1998; 1809-1824.
- Svensson M, Eliasson I, Holmer B. A GIS-based empirical model to simulate air temperature variations in the Göteborg urban area during the night. *Climate Research*. 2002; 215-226.

- Tveito OE, Førland EJ. Mapping temperatures in Norway: applying terrain information, geostatistics and GIS. *Norwegian Journal of Geography*. 1999; 202-212.
- U.S. Census Bureau. Age Groups and Sex: 2010. 2010. Retrieved from https://factfinder.census.gov/faces/tableservices/jsf/pages/productview.xhtml?pid=DEC_10_SF1_QTP1&prodType=table
- U.S. Census Bureau. 2010 Poverty Status in the Past 12 Months by Sex and Age. 2010. Retrieved from https://factfinder.census.gov/faces/tableservices/jsf/pages/productview.xhtml?pid=ACS_10_5YR_B17001&prodType=table
- U.S. Census Bureau. 2010 Income in the Past 12 Months (In 2010 Inflation-Adjusted Dollars). 2010. Retrieved from https://factfinder.census.gov/faces/tableservices/jsf/pages/productview.xhtml?pid=ACS_10_5YR_S1901&prodType=table
- U.S. Global Change Research Program. *Climate and Health Assessment*. 2016. Retrieved from GlobalChange.gov: <https://health2016.globalchange.gov/>
- Watkins R, Palmer J, Kolokotroni M. Increased temperature and intensification of the urban heat island: implications for the human comfort and urban design. *Built Environ*. 2007; 33:85–96.
- Weather Underground. Historical Weather. The Weather Company, LLC. Retrieved from: <https://www.wunderground.com/history/?MR=1>.
- Weng Q, Yang S. Managing the adverse thermal effects of urban development in a densely populated Chinese city. *Journal of Environmental Management*. 2004; 145-156.
- Weng Q, Lu D, Liang B. Urban surface biophysical descriptors and land surface temperature variations. *Photogrammetric Engineering and Remote Sensing*. 2006; 1275-1286.
- White H. A Heteroskedasticity-Consistent Covariance Matrix and a Direct Test for Heteroskedasticity. *Econometrica* 1980; 48: 817–838.
- Wong MS, Peng F, Zou B, Shi WZ, Wilson GJ. Spatially Analyzing the Inequity of the Hong Kong Urban Heat Island by Socio-Demographic Characteristics. *International Journal of Environmental Research and Public Health*. 2016; 1-17.
- Yuan F, Bauer ME. Comparison of impervious surface area and normalized difference vegetation index as indicators of surface urban heat island effects in Landsat imagery. *Remote Sensing of Environment*. 2007; 375-386.

Zhang K, Oxwald EM, Brown DG, Brines SJ, Gronlund CJ, White-Newsome JL, et al. Geospatial exploration of spatial variation of summertime temperatures in the Detroit metropolitan region. *Environmental Resources*. 2011; 1046-1053.

APPENDIX

List of Appendices

Appendix.....	102
1. Data Cleaning and Preparation.....	105
2. Data Cleaning and Preparation ArcGIS Instructions.....	110
3. Data Cleaning and Preparation R Markdown.....	113
4. Methods Temporal Analysis.....	134
5. Methods + Results Temporal Analysis R Markdown.....	136
6. Methods Relative Risk Analysis.....	137
7. Methods + Results Relative Risk R Markdown.....	139
8. Methods Analysis of Community-Level Predictors.....	148
9. Methods + Results Analysis of Community-Level Predictors R Markdown.....	151

List of Tables

Table 3.1: BLS Call Counts per Hour.....	116
Table 6.1: BLS Call Counts by Time Block.....	136
Table 6.2: BLS Call Counts by Time Block and Heat/Non-Heat Day.....	136
Table 8.1: BLS RR and Predictor Variables by Grid Cell.....	141
Table 8.2: ALS RR and Predictor Variables by Grid Cell.....	144

List of Figures

Figure 3.1: BLS Quadratic Relationship.....	121
Figure 3.2: Histogram of BLS Call Count Frequency.....	121
Figure 3.3: Histogram of BLS RR without Grid Cell Exclusion.....	123
Figure 3.4: Histogram of BLS RR with Grid Cell Exclusion.....	124
Figure 3.5: Correlation Coefficients.....	126
Figure 3.6: BLS RR and Log Population.....	127
Figure 3.7: BLS RR and Percent Age Younger than 5.....	127
Figure 3.8: BLS RR and Percent Age 5-14.....	128
Figure 3.9: BLS RR and Percent Age 15-44.....	128
Figure 3.10: BLS RR and Percent Age 45-64.....	129
Figure 3.11: BLS RR and Percent Age 65-84.....	129
Figure 3.12: BLS RR and Percent Age Older than 85.....	130
Figure 3.13: BLS RR and Percent Water Quartiles.....	130
Figure 3.14: BLS RR and Percent Development Quartiles.....	131
Figure 3.15: BLS RR and Percent Canopy Quartiles.....	131
Figure 3.16: BLS RR and Percent Impervious Surface Quartiles.....	132
Figure 3.17: BLS RR and Median Income Quartiles.....	132
Table 3.18: BLS RR and Percent Poverty Quartiles.....	133
Figure 8.1: King County Grid Cell ID Labels.....	147

APPENDIX 1: DATA CLEANING AND PREPARATION

The following appendix will provide detailed instructions for ArcGIS data preparation as well as R code used for the completion of this research. To begin, ArcGIS was used to map call locations; find center point of the EMS location variable, geogrid; match the geogrid center point to a 4km by 7.5km grid cell; match each grid cell to its center point latitude and longitude where the meteorological data is interpolated from; perform zonal statistics as table to find average percentages for each environmental raster data file; and use the intersect tool to extrapolate population densities from the census tract level to the grid cell level, in addition to finding poverty populations and median household incomes. The ArcGIS instructions can be found in Appendix 2. Next, the ArcGIS files were all uploaded on R, where missing data was excluded (missing geocode, grid cell, and time variables), calls were matched to a grid cell and to a grid cell center point so that each call could be assigned a daily maximum humidex value based on the grid cell center point and the date of the call. A time block variable as well as a heat day variable were also created in R for data preparation. In addition, time trends, plots, and correlation coefficients were explored during the R data cleaning and preparation phase. R code for this process can be found in Appendix 3.

EMS Data Preparation

The EMT personnel of Seattle and King County Division of the Department of Public Health prepared, de-identified, and supplied the University of Washington researchers with

Emergency Medical Service call data. These data included information on EMS calls from the mid-1990s until 2012, but this research focused on six recent years: 2007-2012. These years contained the most accurate and well documented information due to King County EMS' transition to electronic data collection. These EMS data included two datasets depending on the severity of the call, one for basic life support (BLS) calls and another for advanced life support (ALS) calls. However, despite whether an ALS unit responded, all calls in King County received a BLS response, so this was the main dataset of the analysis.

For the temporal analysis, data preparation excluded calls with missing location variable and missing notified call times. The calls were grouped into four time blocks: low humidex (4-7am), before peak humidex (7am-3pm), peak humidex (3-6pm), and after peak humidex (6-10pm) based on hourly Weather Underground data. Overnight hours were excluded from this analysis; extreme heat was not an important factor during overnight hours and including calls overnight would only increase the potential for bias from non-heat related calls, such as late night exhaustion or alcohol induced accidents. Data exclusion decreased the number of BLS calls from 441,119 to 351,208 and ALS calls from 121,794 to 97,052.

Before the spatial analysis, all EMS calls were mapped based on their geocode (Figure 1), and all geocodes were assigned to a 4km by 7.5km grid cell. The grid cells were the spatial unit for this analysis. Nearly all grid cells had a center point, where daily temperature, humidity, and vapor pressure data were interpolated in order to calculate a daily humidex value for the grid cell. However, a handful of grids in King County were missing land surface stations

because they were located over water. The few with missing center points were matched to the meteorological data from the nearest bordering center point. Based on this gridded model, each of the 221 grid cells in King County had a maximum humidex value for every day in the study time frame, and each day in every grid cell was classified as a local heat day or non-heat day based on if the humidex value was above or below the extreme heat threshold determined *a priori* from Calkins et al. (2016). Data preparation excluded calls with a missing geocode (location) variable, calls located on the outer border of the grid cell map, and calls in grid cells with 5 or less total calls for the entire study period. BLS call counts decreased from 441,119 to 434,853 and ALS call counts decreased from 121,794 to 120,638.

Population and Socioeconomic Data

Population data by age (U.S. Census Bureau, *Age Groups and Sex: 2010, 2010*), median household income (U.S. Census Bureau, *2010 Income in the Past 12 Months, 2010*), and population below poverty (U.S. Census Bureau, *2010 Poverty Status in the Past 12 Months by Sex and Age, 2010*) were downloaded from the US Census Bureau American Fact Finder database. These data were downloaded on the census tract level in Washington State for 2010. In order to extrapolate estimates to the grid cell scale, the intersect tool in ArcGIS found the percent of each census tract inside a given grid cell. These percentages were then used as weights to find approximated population (total and by age groups) and poverty population for each grid cell. The estimated total population in each intersected area between census tracts and grid cells aided in finding a weighted median income for each grid cell. The authors did not

think it was necessary to collect data for more than one year; there was already some uncertainty with the data due to extrapolation from census tract level to the grid cell scale, and the study frame was a short six year time period where population changes likely would not affect the results. 2010 was the most accurate census year in the study period 2007-2012. Lastly, poverty and median income data were categorized into four quartiles in order to compare the risk of an EMS call on an extreme heat day compared to a non-heat day between grid cells with the lowest and highest economic status.

Environmental Data

The environmental factors, tree canopy, impervious surfaces, and land cover were all downloaded from the Washington State Department of Ecology as shapefiles in the form of raster data from remote sensing imagery techniques (Department of Ecology and NOAA, 2016). The tree canopy and impervious surface data was from 2006, and included a percentage value for each pixel in the county. After the data was uploaded into ArcGIS, the zonal statistics as table tool estimated the average percent tree canopy and percent impervious surfaces for each grid cell. While the land cover data was collected in a more recent year (2011), this data classified each pixel as a certain land type instead of a percentage. These land types included High Intensity Development, Medium Intensity Development, Low Intensity Development, and Open Water. The high, medium, and low development pixels were based on vegetation and percent impervious surface. In order to find percent water and percent developed areas, raster values for water and developed land were separately reclassified from the land cover raster

dataset as 0 (not water or not developed land) and 1 (water or developed land) using the reclassify tool in spatial analyst tools of ArcCatalog. Then, zonal statistics was utilized with the newly reclassified data in order to find the percent of the grid cell that was water and the percent that was developed land. Because percent development was based off of the percent impervious surface data, these two datasets were highly correlated. In addition, percent impervious surface and percent canopy were more accurate data sets because they use a percentage scale per pixel instead of classifying the pixel as developed or not developed. As a result, we made the decision not to use the percent development or percent water datasets in this analysis. Finally, grid cells were categorized into four equal quartiles for each environmental trait in order to compare grids with the lowest percent environmental trait to the grid cells with highest percentages.

APPENDIX 2:

DATA CLEANING AND PREPARATION – ARCGIS INSTRUCTIONS

Map Call Densities:

1. Right click on excel file with calls you wish to map → Open Attribute Table
2. Right click on GeocodeAux (or other spatial reference column)
3. Summarize
4. Name and Save table
5. Add table to map (note: geogrids with zero calls will not be included in this file)
6. Add new geogrid shapefile
7. Right click on Geogrid shapefile → Joins and relates → Join
8. Join attributes from a table
9. Choose the field in this layer: GeocodeAux
10. Choose the table to join to this layer: new table summary table with counts per geocode
11. Choose the field in the table to base the join on: GeocodeAux
12. Keep only matching records
13. Click Yes
14. Right click on geogrid layer → Properties
15. Click on Symbology tab
16. Click on Quantities
17. Value: Count_GeocodeAux
18. Choose Classification

Find Geogrid (EMS Geocode Location Variable) Center Point

1. Right click on geogrid shapefile → Open Attribute Table
2. Click on top left Table Options drop down menu
3. Make two new columns by clicking Add Field in Table Options menu
4. Name one CentX and the other CentY
5. Right click on CentX
6. Click Calculate geometry
7. Click Yes
8. Property: X Coordinate of Centroid
NOTE: make sure that the coordinate system is the same as the data source (otherwise the points will not map in the correct location)
9. Click OK and Yes.
10. Repeat steps 5-9 for the Y coordinate of centroid
11. Click Table Options from the Attribute Table drop down menu → Export

12. Name and save file in appropriate folder
13. Click Add Data and add the new excel file to your map
14. Right click on the new excel file in Table of Contents → Display XY Data
15. Match the X Field with CentX and the Y Field With Cent Y
NOTE: Again, make sure the coordinate system is correct (click edit if changes are needed)

Match Geogrid Center Point to a Grid Cell (VIC 4km x 7.5km Grid Cells):

1. Right click on Geogrid Center Points layer → Join and Relate → Join
2. Under what do you want to join this layer?: 'Join data from another layer based on spatial location'
3. Choose the layer to join to this layer, or load spatial data from disk: Grid Cell
4. Select: It falls inside
5. Name and save in appropriate folder

Match Geogrid with Nearest Grid Cell Center Point

1. Right click on new geogrid/grid cell join layer → Join and Relate → Join
2. Under what do you want to join this layer?: 'Join data from another layer based on spatial location'
3. Choose the layer to join to this layer, or load spatial data from disk: VIC Grid CenterPoints
4. Click 'Each polygon will be given all the attributes of the point that is closest to its boundary, and a distance field showing how close the point is (in the units of the target layer)'
5. Name and save in appropriate folder

Zonal Statistics and Mapping Environmental Layers by Grid Cell

1. Load WA, King Co, and Grid Cell shapefiles in addition to raster environmental characteristics (impervious surface, canopy, and landcover data)
NOTE: For water and developed land raster data in the king co Landuse file, you must first reclassify Value field as 0 (non-water or not-developed) and 1 (water or developed) using the reclassify tool in Arc Catalog (Spatial Analyst Tools → Reclass → Reclassify).
Then start at step 2 with the zonal statistics as table tool.
2. Find Zonal Statistics As Table in ArcToolbox (Spatial Analyst Tools → Zonal → Zonal Statistics As Table) and double click
3. Raster or feature zone data: Grid Cells
4. Input value raster: Environmental Shapefile (impervious surfaces, canopy, development, or water)
5. Name and save in appropriate folder

6. Choose statistics desired (mean for our case)
7. Repeat steps 2-7 for all raster files
8. Add additional Grid Cell shapefiles to the map, one for each environmental variable
9. Right click on new Grid Cell layer → Click Join and Relate → Click Join
10. Join attributes from a table
11. Choose the field in this layer: Grid Cell
12. Choose the table to join to this layer: Environmental Zonal Statistics Table
13. Choose the field in the table to base the join on: Grid Cell
14. Keep only matching records
15. Click Yes
16. Right click on Grid Cell/Env Zonal Statistics layer join → Click Properties
17. Click on Symbology tab
18. Click on Quantities → Click Graduated colors
19. Value: mean
20. Decide how you would like the values grouped
21. Repeat 11-22 for all Environmental Zonal Statistics Table and each added Grid Cell layer

Extrapolating Population Data from census tract to grid cells

1. Right click on grid cell layer → Open Attribute Table
2. Table Options menu → Add Field
3. Name field Old Area and use Double as Field Type
4. Right click on new field → Calculate geometry → Yes
5. Property: Area (Make sure Projection is correct) and choose units
6. Geoprocessing → Intersect
7. Input Features: Add census tract layer then grid cell layer
8. Name and save in appropriate folder
9. In the new intersect layer, add field and calculate geometry (New Area) again
10. Add another field for population of each intersected area (Intersect_Pop)
11. Right click on new population field → Field calculator → Yes
12. In Total = box, use the following formula: $(\text{new area}/\text{old area}) \times \text{census tract population}$
13. Right click grid cell column in intersect table → summarize
14. Choose one or more summary field statistics to be included in the output table: Under Intersect_Pop field, click sum box
15. Name and save to appropriate folder

APPENDIX 3:

DATA CLEANING AND PREPARATION – R MARKDOWN

```
#####
```

##Load All Datasets

```
#####
```

###EMS BLS Data

```
emsBLS <- sqlQuery(channel, "select StudyID, IncidentDate, AgencyTypeKCEMS, AgencyNumberKCEMS,
  PatientAgeYears, PatientGenderID, PatientNumber, GeocodeAux, Latitude, Longitude,
  PropertyUse, LocationTypeID, ActionTaken, HighestLevelCareReceived, IncidentType,
  InitialDispatchCode, PatientTypeCode, TransportLevel, TransportDestinationCategory, agecat
  from ems_ExtremeHeatBLS order by IncidentDate")
```

###EMS BLS Time

```
emsBLS_RT <- sqlQuery(channel, "select StudyID, DTNotifiedDate, DTNotifiedTime from
  ems_ExtremeHeatBLS_RT order by StudyID")
```

###ArcGIS Geocode and VIC Grid Data

```
Geocode_VICgrid_Join <- readOGR("Geocode_VICgrid_Join")
Geocode_VICgrid_Join <- as(Geocode_VICgrid_Join, "data.frame")
Geocode_VICgrid_Join <- Geocode_VICgrid_Join[order(Geocode_VICgrid_Join$GRIDCODE),]
names(Geocode_VICgrid_Join)[names(Geocode_VICgrid_Join)=="GEOCODE"]<-"GeocodeAux"
```

###ArcGIS VIC Grid and VIC Centerpoint Data

```
VICgrid_VICcenter_Join <- readOGR("VICgrid_VICcenter_Join")
VICgrid_VICcenter_Join <- as(VICgrid_VICcenter_Join, "data.frame")
names(VICgrid_VICcenter_Join)[names(VICgrid_VICcenter_Join)=="Longitude"]<-"VICPointLongitude"
names(VICgrid_VICcenter_Join)[names(VICgrid_VICcenter_Join)=="Latitude"]<-"VICPointLatitude"
```

Met Data

```
WAmet2012EMS <- sqlQuery(channel, "select id, lat, lng, metdate, rh, tmax, hmdxmax, tavg, hmdxavg, tmin,
  hmdxmin, prec from WAmet2012EMS order by metdate")
WAmet2012EMS$Year = format(WAmet2012EMS$metdate, "%Y")
WAmet2012EMS$month = months(WAmet2012EMS$metdate)
WAmet2012EMS$Date = WAmet2012EMS$metdate
WAmet2012EMSSummer = WAmet2012EMS[WAmet2012EMS$month %in%
  c("May", "June", "July", "August", "September"),]
names(WAmet2012EMSSummer)[names(WAmet2012EMSSummer)=="lat"]<-"VICPointLatitude"
names(WAmet2012EMSSummer)[names(WAmet2012EMSSummer)=="lng"]<-"VICPointLongitude"
names(WAmet2012EMSSummer)[names(WAmet2012EMSSummer)=="metdate"]<-"IncidentDate"
```

###Environmental Data

```
PercentWater <- readOGR("VICGrid_Water")
PercentWater <- as(PercentWater, "data.frame")
names(PercentWater)[names(PercentWater)=="WATER_MEAN"]<-"PercentWater"
PercentWater <- subset(PercentWater, select = -c(1,3))
```

```
PercentImpervious <- readOGR(",layer="VICGrid_Impervious")
PercentImpervious <- as(PercentImpervious, "data.frame")
names(PercentImpervious)[names(PercentImpervious)=="IMPERVIOUS"]<-"PercentImpervious"
PercentImpervious <- subset(PercentImpervious, select = -c(1))
```

```
PercentDevelopment <- readOGR("VICGrid_Development")
PercentDevelopment <- as(PercentDevelopment, "data.frame")
names(PercentDevelopment)[names(PercentDevelopment)=="DEVELOPMEN"]<-"PercentDevelopment"
PercentDevelopment <- subset(PercentDevelopment, select = -c(1,3))
```

```
PercentCanopy <- readOGR("VICGrid_Canopy")
PercentCanopy <- as(PercentCanopy, "data.frame")
names(PercentCanopy)[names(PercentCanopy)=="CANOPY_MEA"]<-"PercentCanopy"
PercentCanopy <- subset(PercentCanopy, select = -c(1))
```

###population, poverty, and income data

```
VIC2010PopPovInc <- read.csv("VIC_CorrectedPopPovInc.csv")
names(VIC2010PopPovInc)[names(VIC2010PopPovInc)=="Gridcode"]<-"GRIDCODE"
```

###VIC Grid Shapefile for Moran's I test

```
vicgrid <- readShapePoly(fn="vic_polygon_EMS_clip", proj4string = CRS("+proj=longlat"), repair=T)
```

remove population variables as these were estimated based on 2000 data

```
vicgrid@data[, c("popL5", "pop5_14", "pop14_44", "pop45_64", "pop65_84", "popG85")] <- list(NULL)
```

```
#####
```

###Data Prep for Temporal and Spatial Analysis

```
#####
```

###Exclude Missing Geocode Cases

```
A.emsBLS.CompleteGeocode <- emsBLS[complete.cases(emsBLS[,c(8)]),]
```

###Match Geocode with VIC Grid

```
B.emsBLS.Spatial <- left_join(A.emsBLS.CompleteGeocode, Geocode_VICgrid_Join, c("GeocodeAux"))
```

###Exclude Missing Grid Cell Cases

```
C.emsBLS.CompleteSpatial<-subset(B.emsBLS.Spatial, !is.na(GRIDCODE))
```

###Format Date

```
C.emsBLS.CompleteSpatial$Year = format(C.emsBLS.CompleteSpatial$IncidentDate,"%Y")
```

```
C.emsBLS.CompleteSpatial$month = months(C.emsBLS.CompleteSpatial$IncidentDate)
```

```
C.emsBLS.CompleteSpatial$Date = C.emsBLS.CompleteSpatial$IncidentDate
```

###Add Count Variable

```
C.emsBLS.CompleteSpatial$count = 1
```

###Merge Calls and Time Data

```
D.emsBLS.Spatial.Time <- left_join(C.emsBLS.CompleteSpatial, emsBLS_RT, by="StudyID")
```

###Exclude Missing Time Cases

```
D.emsBLS.Spatial.Time <- subset(D.emsBLS.Spatial.Time, !is.na(DTNotifiedTime))
```

###Match Grid Cell to Grid Cell Centerpoint

```
E.emsBLS.Time.Spatial.Humidex <- left_join(D.emsBLS.Spatial.Time, VICgrid_VICcenter_Join, c("GRIDCODE"))
```

###Mactch Grid Cell Centerpoint to Daily Humidex Data

```
intersect(names(WAmet2012EMSSummer), names(E.emsBLS.Time.Spatial.Humidex))
```

```
## [1] "VICPointLatitude" "VICPointLongitude" "IncidentDate" "Year" "month" "Date"
```

```
E.emsBLS.Time.Spatial.Humidex <- left_join(E.emsBLS.Time.Spatial.Humidex, WAmet2012EMSSummer,  
c("VICPointLongitude", "VICPointLatitude", "IncidentDate", "Year", "month", "Date"))
```

###Define a Heat vs Non-Heat Event

```
E.emsBLS.Time.Spatial.Humidex$HeatEvents <-
```

```
ifelse(E.emsBLS.Time.Spatial.Humidex$hmdxmax>=29.71602,c("Heat"),c("Nonheat"))
```

###Define Time Blocks

```
gsub("(\\d+):.*", "\\1",
```

```
E.emsBLS.Time.Spatial.Humidex$DTNotifiedTime)E.emsBLS.Time.Spatial.Humidex$Hours <-
```

```
as.numeric(gsub("(^\\d+):.*", "\\1", E.emsBLS.Time.Spatial.Humidex$DTNotifiedTime))
```

```
E.emsBLS.Time.Spatial.Humidex$Minutes <- as.numeric(gsub("(^\\d+:(\\d+):.*", "\\1",
```

```
E.emsBLS.Time.Spatial.Humidex$DTNotifiedTime))
```

```
E.emsBLS.Time.Spatial.Humidex[, c('Hours', 'Minutes', 'DTNotifiedTime')]
```

```
table(E.emsBLS.Time.Spatial.Humidex$Hours)
```

Table 3.1: BLS Call Counts per Hour

0	1	2	3	4	5	6	7	8	9	10	11	12	13	14	15	16	17	18	19	20	21	22	23
13,473	12,699	11,234	8,976	8,083	8,352	10,320	13,481	17,347	19,911	21,844	23,078	23,755	23,751	23,903	24,140	24,495	24,906	23,966	22,158	21,641	19,798	18,232	15,343

```
TimeBlockFunction <- function(x){
  if(4<=x & x<7)
    return("LowHumidexHeat")
  if(7<=x & x<15)
    return("BeforePeakHeat")
  if(15<=x & x<18)
    return("PeakHeat")
  if(18<=x & x<22)
    return("AfterPeakHeat")
  else
    return(NA)
}
```

```
E.emsBLS.Time.Spatial.Humidex$TimeBlock<- sapply(E.emsBLS.Time.Spatial.Humidex$Hours,
TimeBlockFunction)
```

```
E.emsBLS.Time.Spatial.Humidex$TimeBlock<-as.factor(E.emsBLS.Time.Spatial.Humidex$TimeBlock)
```

```
E.emsBLS.Time.Spatial.Humidex$HeatEvents<-as.factor(E.emsBLS.Time.Spatial.Humidex$HeatEvents)
```

###Aggregate Calls per Grid Cell per Day

```
BLSCallsperVICGridperDay <- aggregate(count~Date+GRIDCODE, data=C.emsBLS.CompleteSpatial, FUN=sum,
drop=FALSE)
```

###Match Grid Cell to Grid Cell Center Point

```
BLSCallsperVICGridperDay<- left_join(BLSCallsperVICGridperDay, VICgrid_VICcenter_Join, c("GRIDCODE"))
```

###Mactch VIC Centerpoint to Daily Humidex Data (Join by Lat, Lng, and Date)

```
names(BLSCallsperVICGridperDay)[names(BLSCallsperVICGridperDay)=="Date"]<-"IncidentDate"
```

```
BLSCallsperVICGridperDay <- left_join(BLSCallsperVICGridperDay, WAmet2012EMSSummer,
c("VICPointLongitude","VICPointLatitude","IncidentDate"))
```

###Create an HD Column

```
BLSopt.RR = 29.71602
```

```
BLSCallsperVICGridperDay$HD <- (BLSCallsperVICGridperDay$hmdxmax>BLSopt.RR)*1
```

```
#####
###Time Trend Models
#####

##### Create new time variables
BLSCallsperVICGridperDay$DayofWeek <- weekdays(as.Date(BLSCallsperVICGridperDay$Date))
BLSCallsperVICGridperDay$weekend <- (as.character(BLSCallsperVICGridperDay$DayofWeek) == "Saturday") |
(as.character(BLSCallsperVICGridperDay$DayofWeek) == "Sunday")

###Create time variable
BLSdatelist <- as.Date(as.character(BLSCallsperVICGridperDay$IncidentDate), "%Y-%m-%d")
BLSstartdate <- BLSdatelist[1]-1
BLSCallsperVICGridperDay$time <- as.numeric(BLSdatelist-BLSstartdate)

###Create list of Grid cells
BLSviclist <- unique(BLSCallsperVICGridperDay$GRIDCODE)

###Time Trend Regressions
mod1 <- glm(count ~ time, data=BLSCallsperVICGridperDay, family = quasipoisson(link = "log"))
summary(mod1)
## Call:
## glm(formula = count ~ time, family = quasipoisson(link = "log"),
## data = BLSCallsperVICGridperDay)
##
## Deviance Residuals:
##   Min       1Q   Median       3Q      Max
## -2.6531  -2.6165  -2.5715   0.3222  22.9548
##
## Coefficients:
##              Estimate Std. Error t value Pr(>|t|)
## (Intercept)  1.258e+00  1.052e-02  119.648 < 2e-16 ***
## time        -3.243e-05  9.061e-06  -3.579  0.000344 ***
## ---
## Signif. codes:  0 '***' 0.001 '**' 0.01 '*' 0.05 '.' 0.1 ' ' 1
##
## (Dispersion parameter for quasipoisson family taken to be 13.96598)
##
## Null deviance: 1077218 on 127601 degrees of freedom
## Residual deviance: 1077039 on 127600 degrees of freedom
## AIC: NA
## Number of Fisher Scoring iterations: 6
```

```

mod2 <- glm(count ~ DayofWeek, data=BLSCallsperVICGridperDay, family = quasipoisson(link = "log"))
summary(mod2)
## Call:
## glm(formula = count ~ DayofWeek, family = quasipoisson(link = "log"),
## data = BLSCallsperVICGridperDay)
##
## Deviance Residuals:
##   Min       1Q   Median       3Q      Max
## -2.6520  -2.6076  -2.5573   0.3165  22.8902
##
## Coefficients:
##              Estimate Std. Error t value Pr(>|t|)
## (Intercept)    1.2574982  0.0147767   85.100 < 2e-16 ***
## DayofWeekMonday -0.0335438  0.0211161  -1.589  0.112166
## DayofWeekSaturday -0.0002343  0.0208986  -0.011  0.991056
## DayofWeekSunday -0.0727409  0.0212461  -3.424  0.000618 ***
## DayofWeekThursday -0.0337486  0.0210760  -1.601  0.109316
## DayofWeekTuesday -0.0441192  0.0210908  -2.092  0.036452 *
## DayofWeekWednesday -0.0346536  0.0210808  -1.644  0.100211
## ---
## Signif. codes:  0 '***' 0.001 '**' 0.01 '*' 0.05 '.' 0.1 ' ' 1
##
## (Dispersion parameter for quasipoisson family taken to be 13.98201)
##
## Null deviance: 1077218 on 127601 degrees of freedom
## Residual deviance: 1076979 on 127595 degrees of freedom
## AIC: NA
##
## Number of Fisher Scoring iterations: 6

```

```

mod3 <- glm(count ~ weekend, data=BLSCallsperVICGridperDay, family = quasipoisson(link = "log"))
summary(mod3)
## Call:
## glm(formula = count ~ weekend, family = quasipoisson(link = "log"),
## data = BLSCallsperVICGridperDay)
##
## Deviance Residuals:
##   Min       1Q   Median       3Q      Max
## -2.6137  -2.6137  -2.6048   0.3077  23.0513
##

```

```

## Coefficients:
##           Estimate Std. Error  t value    Pr(>|t|)
## (Intercept)  1.228384  0.006708  183.109  <2e-16 ***
## weekendTRUE  -0.006855  0.012564  -0.546   0.585
## ---
## Signif. codes:  0 '***' 0.001 '**' 0.01 '*' 0.05 '.' 0.1 ' ' 1
##
## (Dispersion parameter for quasipoisson family taken to be 13.99554)
##
## Null deviance: 1077218 on 127601 degrees of freedom
## Residual deviance: 1077214 on 127600 degrees of freedom
## AIC: NA
##
## Number of Fisher Scoring iterations: 6

mod4 <- glm(count ~ time + DayofWeek, data=BLSCallsperVICGridperDay, family = quasipoisson(link = "log"))
summary(mod4)
## Call:
## glm(formula = count ~ time + DayofWeek, family = quasipoisson(link = "log"),
## data = BLSCallsperVICGridperDay)
##
## Deviance Residuals:
##   Min       1Q   Median       3Q      Max
## -2.6943 -2.6146 -2.5488  0.3237  22.8162
##
## Coefficients:
##           Estimate Std. Error  t value    Pr(>|t|)
## (Intercept)  1.289e+00  1.721e-02  74.930  < 2e-16 ***
## time        -3.236e-05  9.057e-06  -3.573  0.000354 ***
## DayofWeekMonday  -3.349e-02  2.109e-02  -1.588  0.112362
## DayofWeekSaturday -3.283e-04  2.088e-02  -0.016  0.987452
## DayofWeekSunday  -7.269e-02  2.122e-02  -3.425  0.000616 ***
## DayofWeekThursday -3.365e-02  2.105e-02  -1.598  0.109950
## DayofWeekTuesday  -4.407e-02  2.107e-02  -2.092  0.036445 *
## DayofWeekWednesday -3.446e-02  2.106e-02  -1.636  0.101754
##
## Signif. codes:  0 '***' 0.001 '**' 0.01 '*' 0.05 '.' 0.1 ' ' 1
##
## (Dispersion parameter for quasipoisson family taken to be 13.95261)
##
## Null deviance: 1077218 on 127601 degrees of freedom

```

```

## Residual deviance: 1076801 on 127594 degrees of freedom
## AIC: NA
##
## Number of Fisher Scoring iterations: 6

mod5 <- glm(count ~ time + weekend, data=BLSCallsperVICGridperDay, family = quasipoisson(link = "log"))
summary(mod5)
## Call:
## glm(formula = count ~ time + weekend, family = quasipoisson(link = "log"),
## data = BLSCallsperVICGridperDay)
##
## Deviance Residuals:
##   Min       1Q   Median       3Q      Max
## -2.6558  -2.6132  -2.5723   0.3204  22.9771
##
## Coefficients:
##              Estimate Std. Error t value Pr(>|t|)
## (Intercept)  1.260e+00  1.112e-02  113.389 < 2e-16 ***
## time        -3.244e-05  9.061e-06  -3.581  0.000343 ***
## weekendTRUE  -6.951e-03  1.255e-02  -0.554  0.579694
##
## Signif. codes:  0 '***' 0.001 '**' 0.01 '*' 0.05 '.' 0.1 ' ' 1
##
## (Dispersion parameter for quasipoisson family taken to be 13.96606)
##
## Null deviance: 1077218 on 127601 degrees of freedom
## Residual deviance: 1077035 on 127599 degrees of freedom
## AIC: NA
##
## Number of Fisher Scoring iterations: 6

```

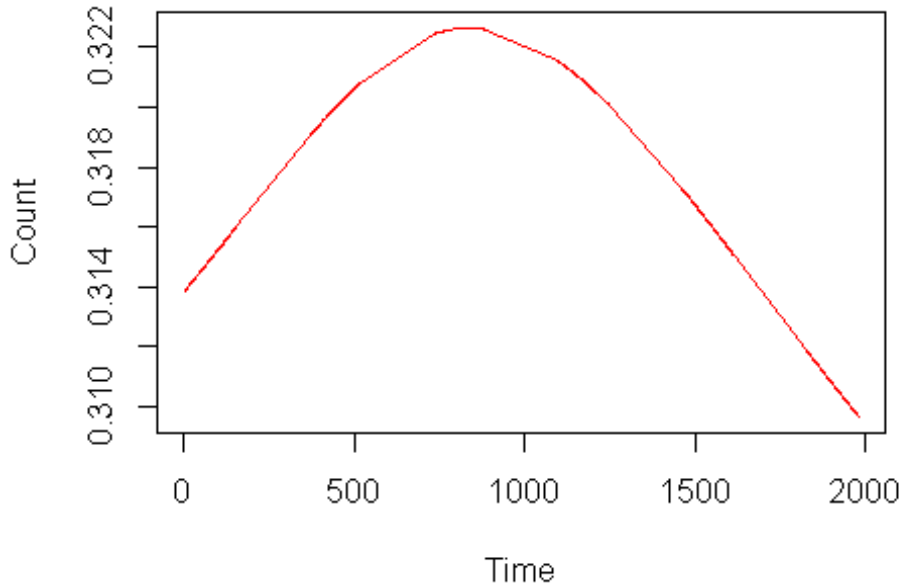
###Must decide which time trends to include based on the results of these models
###BLS data shows noise from saturday and sunday --> included a weekend variable
###ALS data shows noise from sunday and tuesday --> included day of week variable

```

BLSCallsperVICGridperDay$count2 <- BLSCallsperVICGridperDay$count
BLSCallsperVICGridperDay$count2[BLSCallsperVICGridperDay$count == 0] <- 0.5
BLSCallsperVICGridperDay$logcount2 <- log(BLSCallsperVICGridperDay$count2)
plot(smooth.spline(BLSCallsperVICGridperDay$time, BLSCallsperVICGridperDay$logcount2, df=3), type="l",
ylab="Count", xlab="Time")
lines(smooth.spline(BLSCallsperVICGridperDay$time, BLSCallsperVICGridperDay$logcount2, df=3), col="red")

```

Figure 3.1: BLS Quadratic Relationship

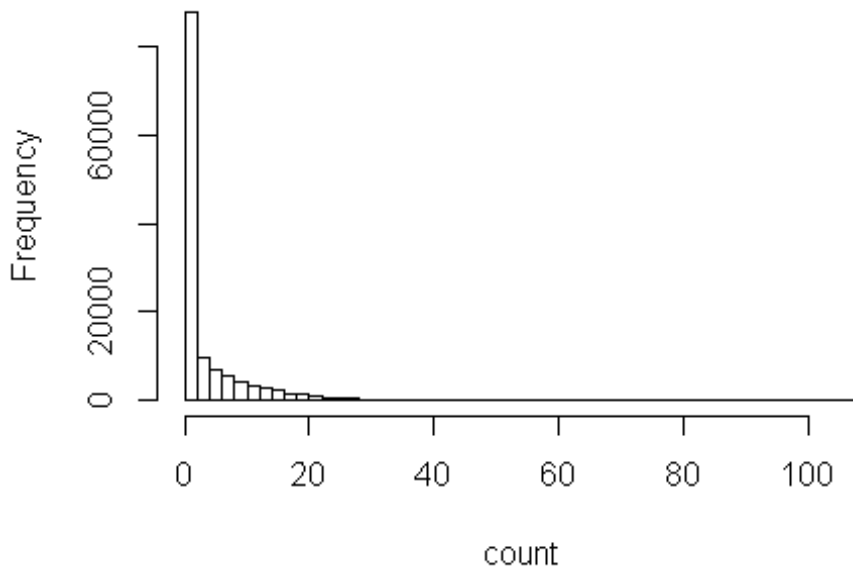


###BLS data shows strong quadratic relationship, so include time^2 in the model
###ALS data does not show this relationship

```
hist(BLSCallsperVICGridperDay$count, xlab="count", breaks=50)
```

Figure 3.2: Histogram of BLS Call Count Frequency

Histogram of BLSCallsperVICGridperDay\$count



```
#####
```

```
###Data Prep for Model Analysis
```

```
#####
```

```
###Add new variables to demographic data
```

```
VIC2010PopPovInc$logPop <- log(VIC2010PopPovInc$Total.Population)
VIC2010PopPovInc$PctAgeL5 <- with(VIC2010PopPovInc, round(100*Pop.L5/Total.Population, 2))
VIC2010PopPovInc$PctAge5_14 <- with(VIC2010PopPovInc, round(100*Pop.5.14/Total.Population, 2))
VIC2010PopPovInc$PctAge15_44 <- with(VIC2010PopPovInc, round(100*Pop.15.44/Total.Population, 2))
VIC2010PopPovInc$PctAge45_64 <- with(VIC2010PopPovInc, round(100*Pop.45.64/Total.Population, 2))
VIC2010PopPovInc$PctAge65_84 <- with(VIC2010PopPovInc, round(100*Pop.65.84/Total.Population, 2))
VIC2010PopPovInc$PctAgeG85 <- with(VIC2010PopPovInc, round(100*Pop.G85/Total.Population, 2))
VIC2010PopPovInc$PctPoverty <- with(VIC2010PopPovInc, round(100*Pop.Poverty/Total.Population, 2))
VIC2010PopPovInc$logIncome <- log(VIC2010PopPovInc$Median.Income)
```

```
###Match Grid Cells and Environmental Data
```

```
BLSRR_Env_dat <- left_join(BLSRR_dat, PercentWater, c("GRIDCODE"))
BLSRR_Env_dat <- left_join(BLSRR_Env_dat, PercentImpervious, c("GRIDCODE"))
BLSRR_Env_dat <- left_join(BLSRR_Env_dat, PercentDevelopment, c("GRIDCODE"))
BLSRR_Env_dat <- left_join(BLSRR_Env_dat, PercentCanopy, c("GRIDCODE"))
```

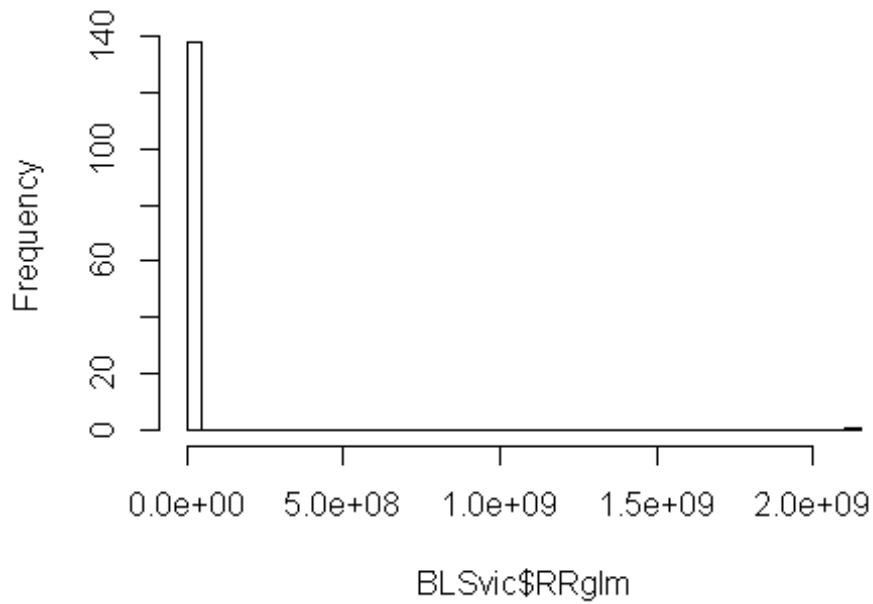
```
###Add population, poverty, and income in new data frame
```

```
BLSvic <- merge(BLSRR_Env_dat, VIC2010PopPovInc, by = "GRIDCODE", all.x = TRUE)
BLSvic$TotalCallCount <- BLSvic$count_call_HD + BLSvic$count_call_nonHD
Edited_BLSvic <- subset(BLSvic, select = -c(8,9,11,14,20,21,22,23,24,25,26,28,37))
View(Edited_BLSvic)
```

```
hist(BLSvic$RRglm, breaks=50)
```

Figure 3.3: Histogram of BLS RR without Grid Cell Exclusion

Histogram of BLSvic\$RRglm



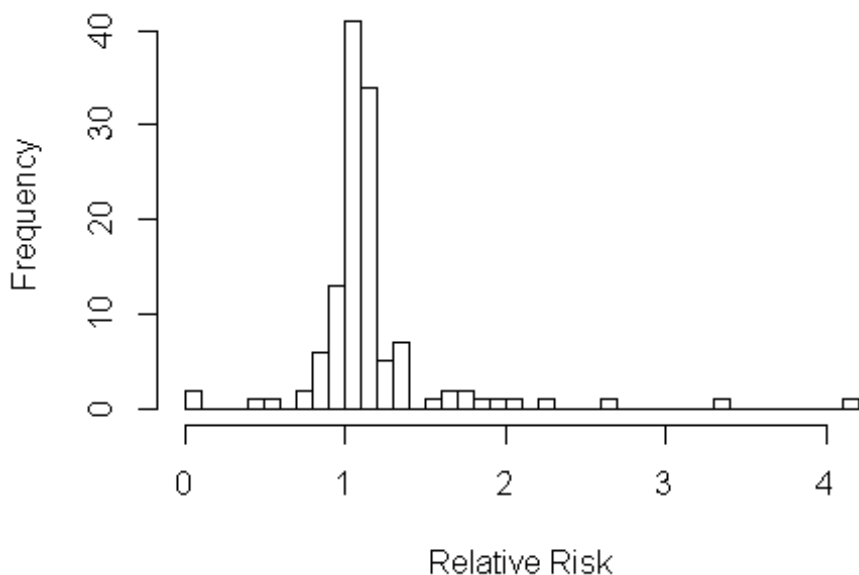
Exclude Grids with 5 or less calls

```
BLSvic2 <- subset(BLSvic, TotalCallCount > 5)
```

```
hist(BLSvic2$RRglm, breaks=50, xlab="Relative Risk", main="BLS RR Histogram")
```

Figure 3.4: Histogram of BLS RR with Grid Cell Exclusion

BLS RR Histogram



Predictor variables as vectors

```
PctWater <- as.vector(by(BLSvic2$PercentWater, INDICES=BLSvic2$GRIDCODE, FUN=mean))
PctImpervious <- as.vector(by(BLSvic2$PercentImpervious, INDICES=BLSvic2$GRIDCODE, FUN=mean))
PctDevelopment <- as.vector(by(BLSvic2$PercentDevelopment, INDICES=BLSvic2$GRIDCODE, FUN=mean))
PctCanopy <- as.vector(by(BLSvic2$PercentCanopy, INDICES=BLSvic2$GRIDCODE, FUN=mean))
```

```
PctPoverty <- as.vector(by(BLSvic2$Percent.Poverty, INDICES=BLSvic2$GRIDCODE, FUN=mean))
MedlogIncome <- as.vector(by(BLSvic2$logIncome, INDICES=BLSvic2$GRIDCODE, FUN=mean))
MedIncome <- as.vector(by(BLSvic2$Median.Income, INDICES=BLSvic2$GRIDCODE, FUN=mean))
GRIDCODE <- as.vector(by(BLSvic2$GRIDCODE, INDICES=BLSvic2$GRIDCODE, FUN=mean))
```

categorize factors

```
PctWater_cat <- cut(PctWater, quantile(PctWater, c(0, 0.25, 0.5, 0.75, 1)), include.lowest = TRUE)
summary(PctWater_cat)
## [0,0.514] (0.514,1.4] (1.4,5.55] (5.55,83.6]
## 31 31 31 31
levels(PctWater_cat) <- c("[0, 25th]", "(25th, 50th]", "(50th, 75th]", "(75th, 100th]")
PctImpervious_cat <- cut(PctImpervious, quantile(PctImpervious, c(0, 0.25, 0.5, 0.75, 1)), include.lowest = TRUE)
summary(PctImpervious_cat)
## [0.229,1.66] (1.66,7.62] (7.62,24.2] (24.2,56.7]
## 31 31 31 31
levels(PctImpervious_cat) <- c("[0, 25th]", "(25th, 50th]", "(50th, 75th]", "(75th, 100th]")
```

```

PctDevelopment_cat <- cut(PctDevelopment, quantile(PctDevelopment, c(0, 0.25, 0.5, 0.75, 1)), include.lowest
= TRUE)
summary(PctDevelopment_cat)
## [0.406,4.41] (4.41,19.9] (19.9,55.2] (55.2,87.7]
##      31      31      31      31
levels(PctDevelopment_cat) <- c("[0, 25th]", "(25th, 50th]", "(50th, 75th]", "(75th, 100th]")
PctCanopy_cat <- cut(PctCanopy, quantile(PctCanopy, c(0, 0.25, 0.5, 0.75, 1)), include.lowest = TRUE)
summary(PctCanopy_cat)
## [3.97,23.3] (23.3,42.1] (42.1,62.6] (62.6,86.2]
##      31      31      31      31
levels(PctCanopy_cat) <- c("[0, 25th]", "(25th, 50th]", "(50th, 75th]", "(75th, 100th]")
PctPoverty_cat <- cut(PctPoverty, quantile(PctPoverty, c(0, 0.25, 0.5, 0.75, 1)), include.lowest = TRUE)
summary(PctPoverty_cat)
## [1.95,4.12] (4.12,5.78] (5.78,7.87] (7.87,18.5]
##      31      31      31      31
levels(PctPoverty_cat) <- c("[0, 25th]", "(25th, 50th]", "(50th, 75th]", "(75th, 100th]")
MedlogIncome_cat <- cut(MedlogIncome, quantile(MedlogIncome, c(0, 0.25, 0.5, 0.75, 1)), include.lowest =
TRUE)
summary(MedlogIncome_cat)
## [10.6,11.2] (11.2,11.3] (11.3,11.5] (11.5,11.8]
##      31      31      31      31
levels(MedlogIncome_cat) <- c("[0, 25th]", "(25th, 50th]", "(50th, 75th]", "(75th, 100th]")
MedIncome_cat <- cut(MedIncome, quantile(MedIncome, c(0, 0.25, 0.5, 0.75, 1)), include.lowest=TRUE)
summary(MedIncome_cat)
## [4.2e+04,7.01e+04] (7.01e+04,8.11e+04] (8.11e+04,9.7e+04] (9.7e+04,1.36e+05]
##      31      31      31      31
levels(MedIncome_cat) <- c("[0, 25th]", "(25th, 50th]", "(50th, 75th]", "(75th, 100th]")

BLS_Env_dat <- data.frame(GRIDCODE,PctWater_cat, PctImpervious_cat, PctDevelopment_cat,
PctCanopy_cat,PctPoverty_cat, MedlogIncome_cat, MedIncome_cat)
BLSvic2 <- merge(BLS_Env_dat, BLSvic2, by = "GRIDCODE", all.x = TRUE)

#####
###Plots and Descriptives
#####

## correlation between continuous predictor variables
subgroup <- BLSvic2[, c("PercentWater", "PercentImpervious", "PercentDevelopment", "PercentCanopy",
"Total.Population", "logPop", "PctAgeL5", "PctAge5_14", "PctAge15_44", "PctAge45_64",
"PctAge65_84", "PctAgeG85",
"Median.Income", "logIncome", "PctPoverty")]

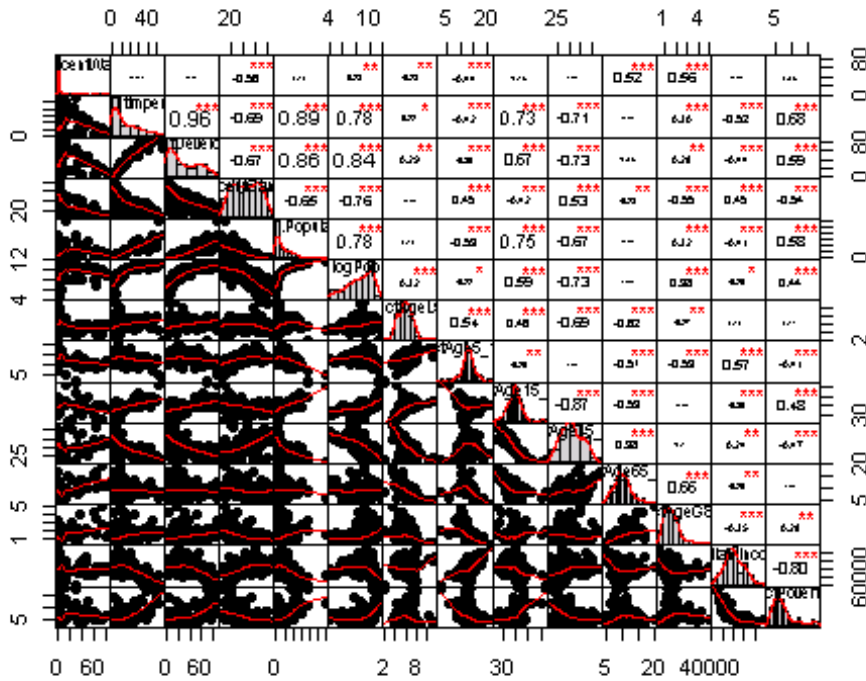
```

```

correlations <- cor(subgroup, use="complete.obs", method="spearman")
View(correlations)
correlation_data <- BLSvic2[,c("PercentWater", "PercentImpervious", "PercentDevelopment",
    "PercentCanopy", "Total.Population", "logPop", "Median.Income", "PctPoverty"
    "PctAgeL5", "PctAge5_14", "PctAge15_44", "PctAge45_64", "PctAge65_84", "PctAgeG85"),]
chart.Correlation(correlation_data, histogram=TRUE, pch=19)

```

Figure 3.5: Correlation Coefficients



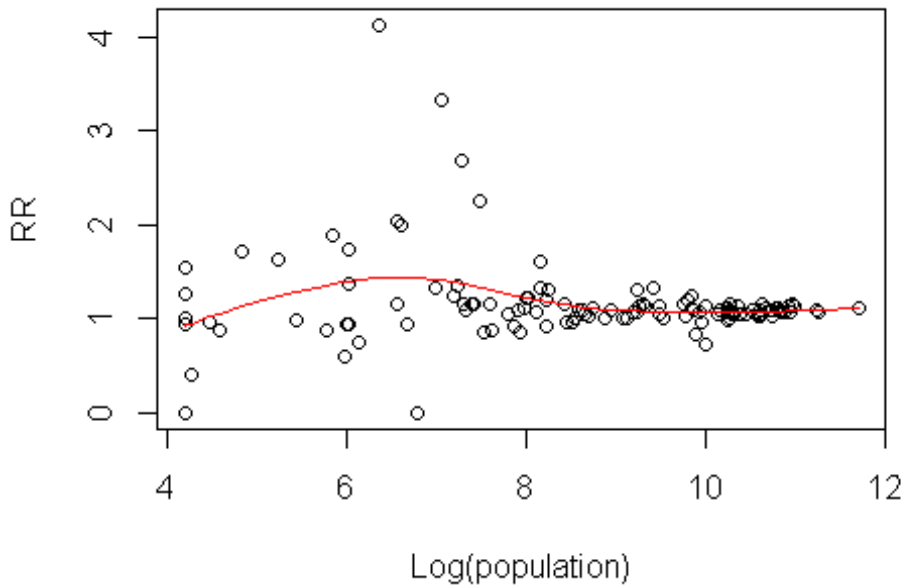
Total Log Population Graph

```

plot(BLSvic2$logPop, BLSvic2$RRgIm, ylab="RR", xlab="Log(population)")
lines(smooth.spline(BLSvic2$logPop, BLSvic2$RRgIm, df=5), col="red")

```

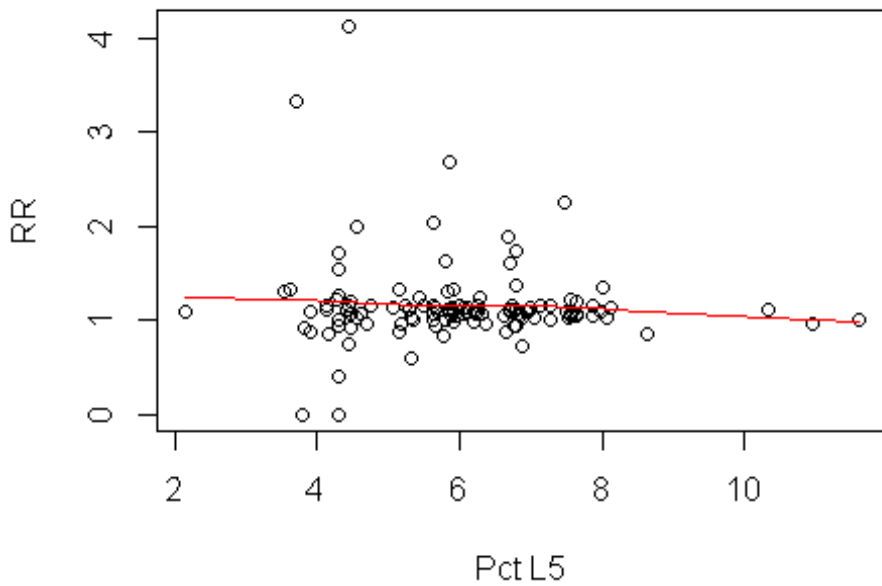
Figure 3.6: BLS RR and Log Population



###Percent Population Graphs

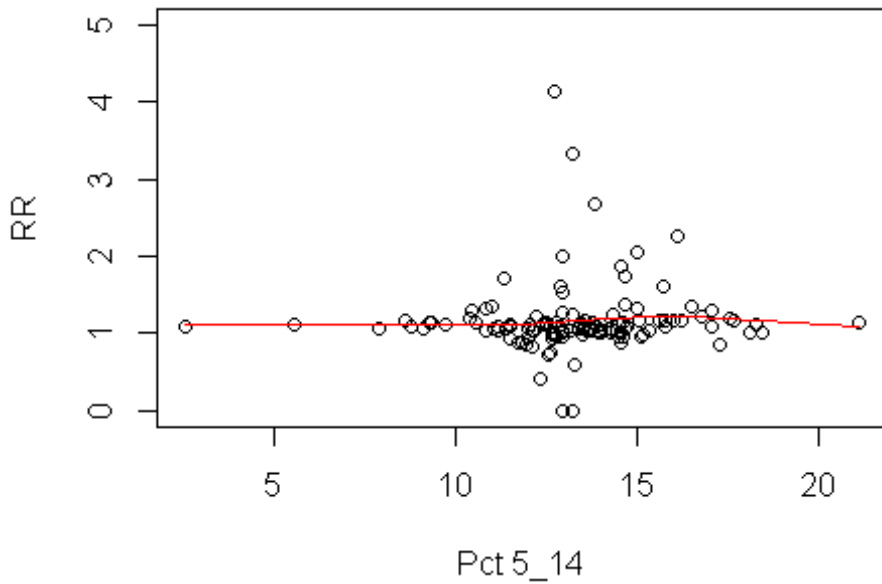
```
plot(BLSvic2$PctAgeL5, BLSvic2$RRglm, ylab="RR", xlab="Pct L5")  
lines(smooth.spline(BLSvic2$PctAgeL5, BLSvic2$RRglm, df=5), col="red")
```

Figure 3.7: BLS RR and Percent Age Younger than 5



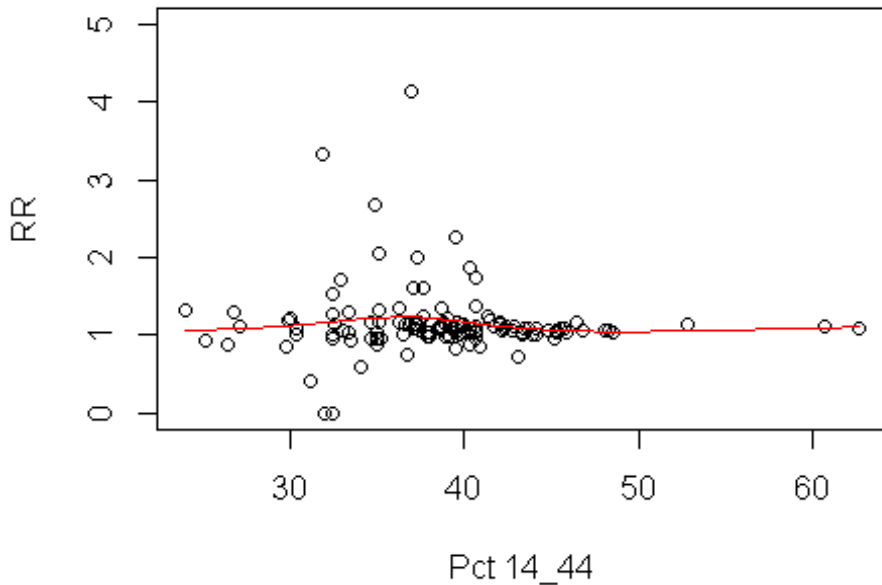
```
plot(BLSvic2$PctAge5_14, BLSvic2$RRglm, ylab="RR", xlab="Pct 5_14", ylim=c(0, 5))  
lines(smooth.spline(BLSvic2$PctAge5_14, BLSvic2$RRglm, df=5), col="red")
```

Figure 3.8: BLS RR and Percent Age 5-14



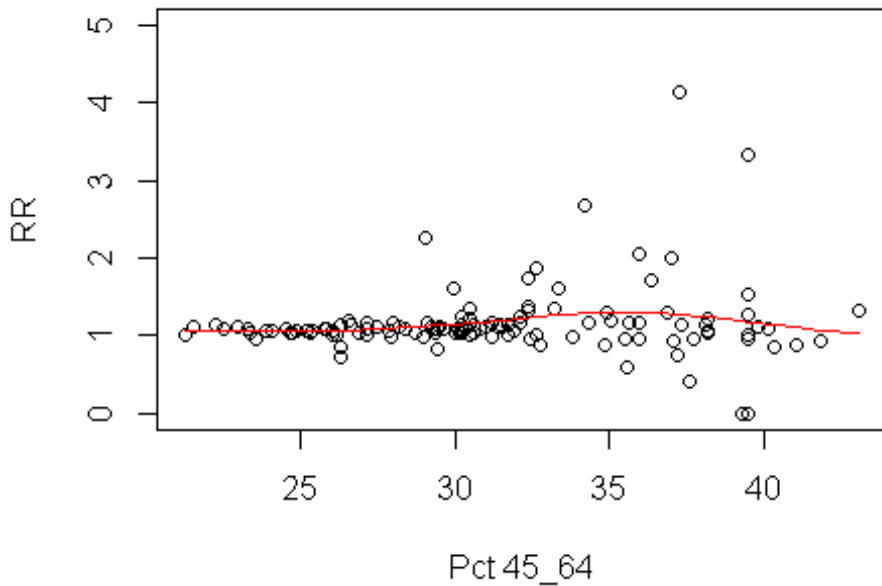
```
plot(BLSvic2$PctAge15_44, BLSvic2$RRglm, ylab="RR", xlab="Pct 14_44", ylim=c(0, 5))  
lines(smooth.spline(BLSvic2$PctAge15_44, BLSvic2$RRglm, df=5), col="red")
```

Figure 3.9: BLS RR and Percent Age 15-44



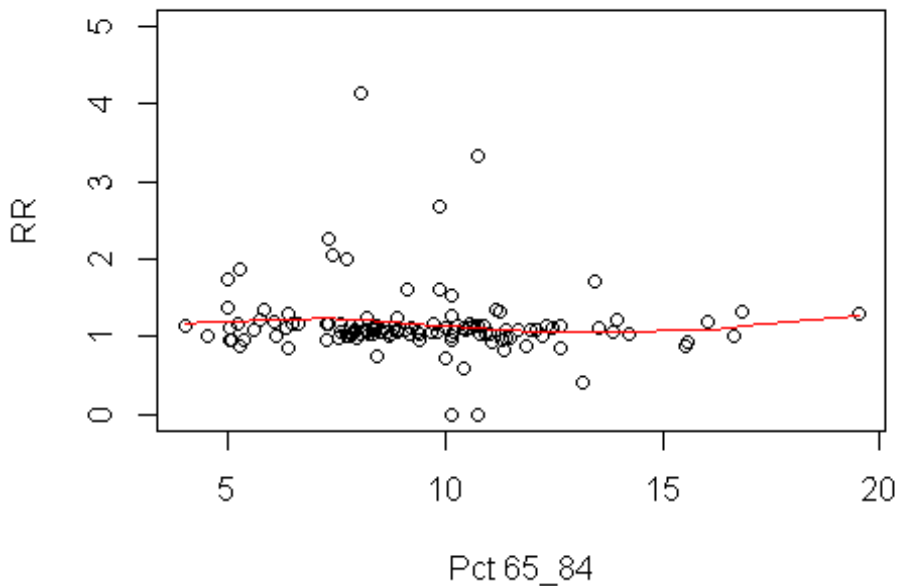
```
plot(BLSvic2$PctAge45_64, BLSvic2$RRglm, ylab="RR", xlab="Pct 45_64", ylim=c(0, 5))  
lines(smooth.spline(BLSvic2$PctAge45_64, BLSvic2$RRglm, df=5), col="red")
```

Figure 3.10: BLS RR and Percent Age 45-64



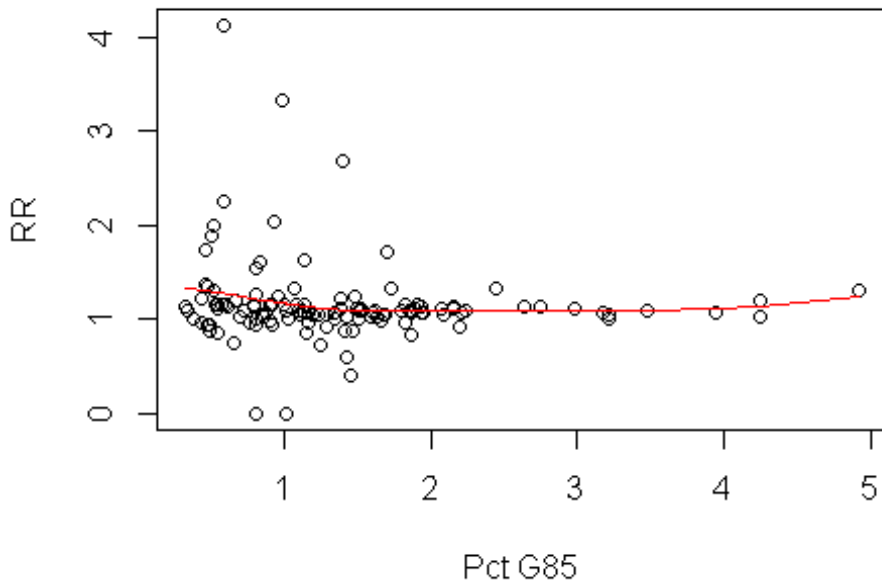
```
plot(BLSvic2$PctAge65_84, BLSvic2$RRglm, ylab="RR", xlab="Pct 65_84", ylim=c(0, 5))  
lines(smooth.spline(BLSvic2$PctAge65_84, BLSvic2$RRglm, df=5), col="red")
```

Figure 3.11: BLS RR and Percent Age 65-84



```
plot(BLSvic2$PctAgeG85, BLSvic2$RRglm, ylab="RR", xlab="Pct G85")  
lines(smooth.spline(BLSvic2$PctAgeG85, BLSvic2$RRglm, df=5), col="red")
```

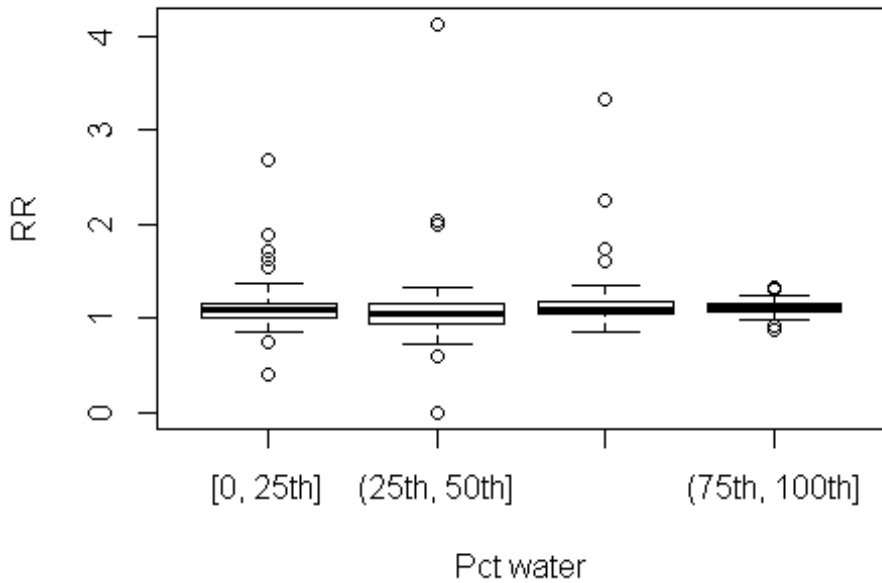
Figure 3.12: BLS RR and Percent Age Older than 85



Categorical Variable Graphs

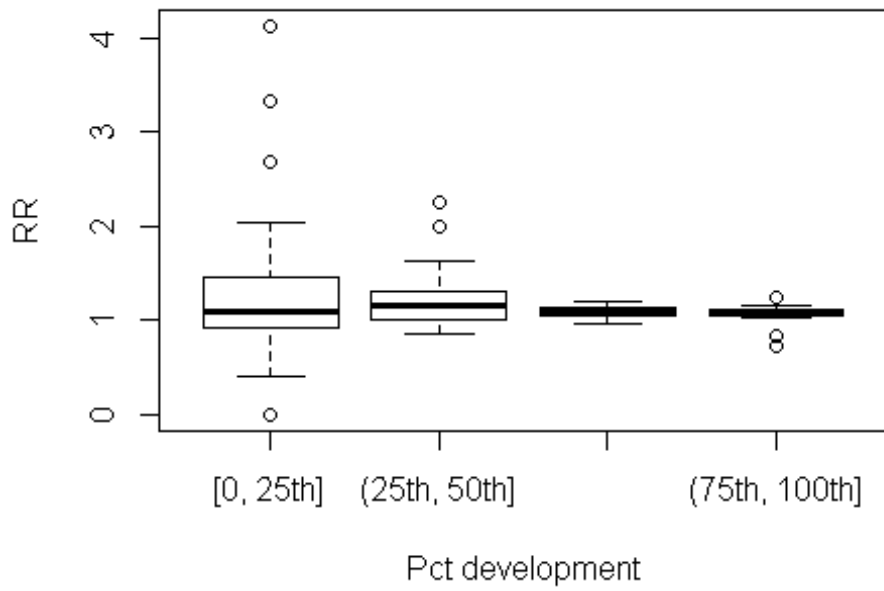
```
boxplot(RRglm ~ PctWater_cat, data=BLSvic2, ylab="RR", xlab="Pct water")
```

Figure 3.13: BLS RR and Percent Water Quartiles



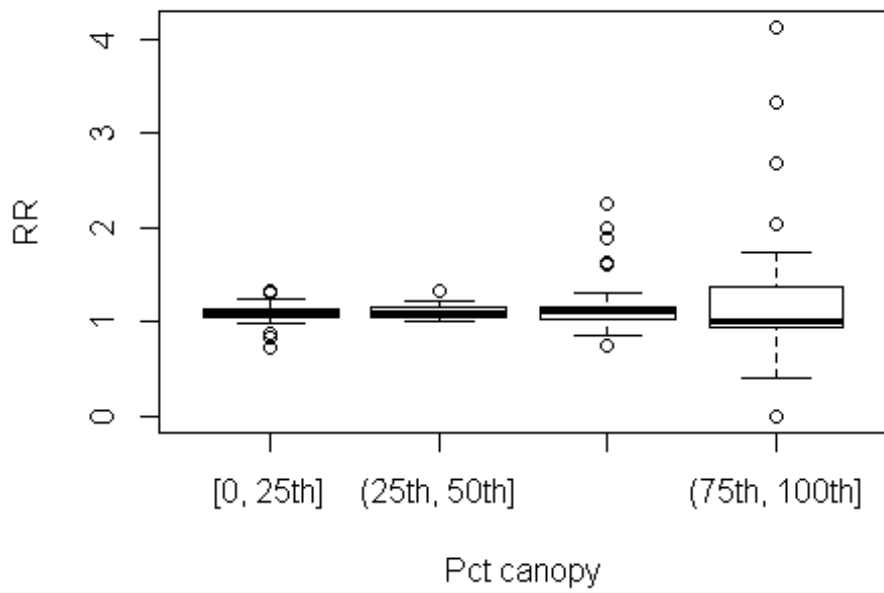
```
boxplot(RRglm ~ PctDevelopment_cat, data=BLSvic2, ylab="RR", xlab="Pct development")
```

Figure 3.14: BLS RR and Percent Development Quartiles



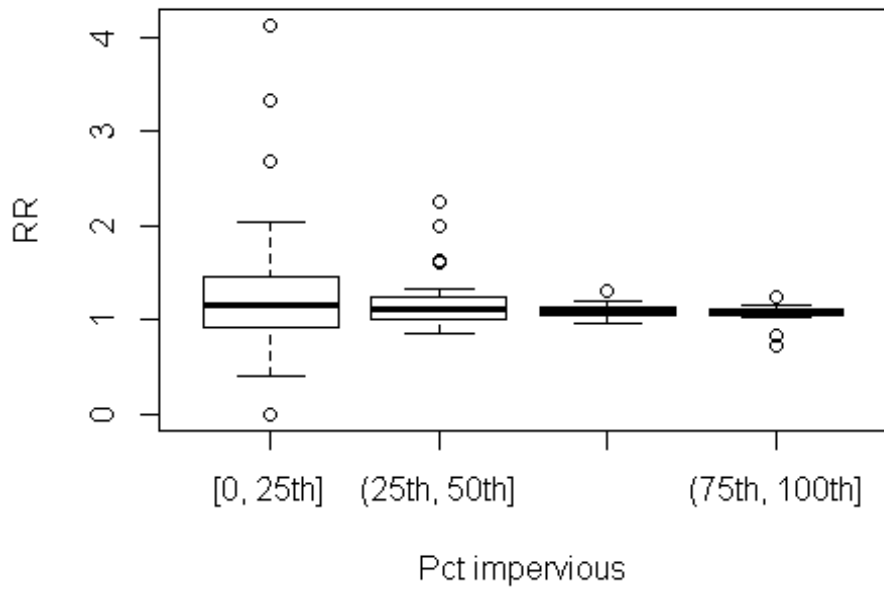
```
boxplot(RRglm ~ PctCanopy_cat, data=BLSvic2, ylab="RR", xlab="Pct canopy")
```

Figure 3.15: BLS RR and Percent Canopy Quartiles



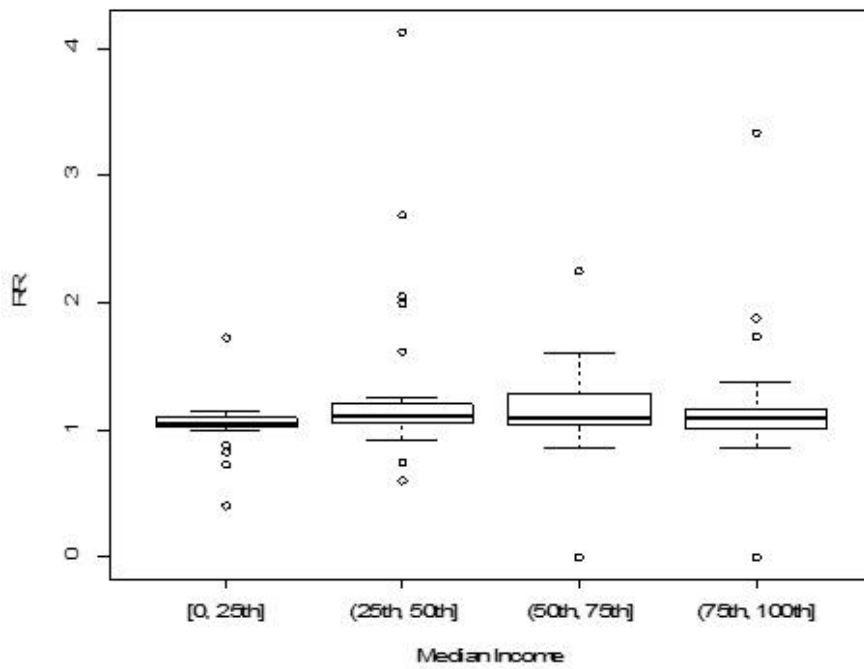
```
boxplot(RRglm ~ PctImpervious_cat, data=BLSvic2, ylab="RR", xlab="Pct impervious")
```

Figure 3.16: BLS RR and Percent Impervious Surface Quartiles



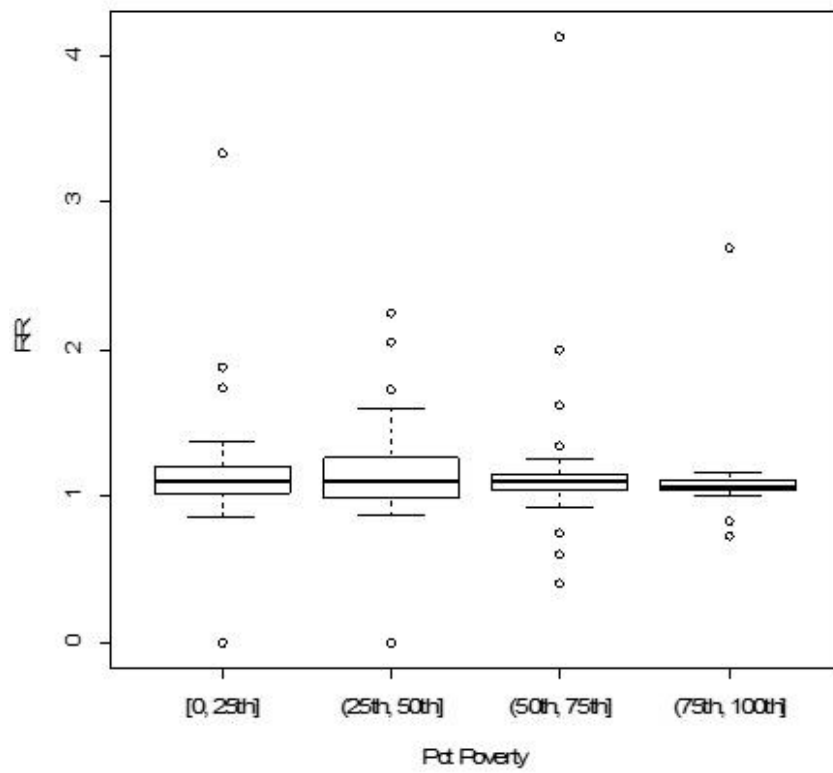
```
boxplot(RRglm ~ MedIncome_cat, data=BLSvic2, ylab="RR", xlab="Median Income")
```

Figure 3.17: BLS RR and Median Income Quartiles



```
boxplot(RRglm ~ PctPoverty_cat, data=BLSvic2, ylab="RR", xlab="Pct Poverty")
```

Table 3.18: BLS RR and Percent Poverty Quartiles



APPENDIX 4:

METHODS + RESULTS – TEMPORAL ANALYSIS

The first specific aim was to describe the temporal variations in BLS and ALS calls throughout King County. Due to limitations in statistical power for the grid cell spatial scale, this aim simply looked at county-wide temporal variations.

After the 3-6pm time block was identified as the peak extreme heat time block based on hourly Weather Underground data, three other time blocks were set to compare call volumes on an extreme heat day compared to a non-heat day: Low Humidex (4-7am), Before Peak Heat (7am-3pm), and After Peak Heat (6-10pm). Again, overnight hours were excluded to reduce bias from non-heat related EMS calls, such as those from exhaustion or alcohol. First, call counts for each time block were determined on all days, county-wide. Next, we distinguished BLS and ALS call counts in each time block on a heat day and non-heat day. These call counts were location specific because each call was classified as a heat day call or a non-heat day call based on its local, grid cell daily humidex value. Then, the number of extreme heat days and non-heat days in each grid cell with EMS calls were averaged to get a county-wide average number of extreme heat days and non-heat days: 149 extreme heat days and 769 non-heat days for the BLS threshold; 28 extreme heat days and 890 non-heat days for the ALS threshold. First, the total heat day call counts for each time block were divided by the average number of heat days, and the total non-heat day call counts for each time block were divided by the average number of non-heat days. Then, the average number of calls per heat day was divided

by the average number of calls per non-heat day for each time block to find a simple relative risk estimate.

For the Low Humidex and Before Peak Heat time blocks, there were slightly reduced or equal call volumes on a heat day compared to a non-heat day. However, call volumes were 1.06 and 1.05 times higher on extreme heat days compared to non-heat days in the Peak Heat time block for BLS and ALS calls, respectively. Interestingly, the After Peak Heat hours had greater estimated relative risks than the Peak Heat time block of 1.10 and 1.08 for BLS and ALS calls, respectively.

APPENDIX 5:

METHODS + RESULTS – TEMPORAL ANALYSIS R MARKDOWN

table(E.emsBLS.Time.Spatial.Humidex\$TimeBlock)

Table 6.1: BLS Call Counts by Time Block

	Low Humidex	Before Peak Heat	Peak Heat	After Peak Heat
All Days	26,755	167,070	73,541	87,563

table(E.emsBLS.Time.Spatial.Humidex\$HeatEvents, E.emsBLS.Time.Spatial.Humidex\$TimeBlock)

Table 6.2: BLS Call Counts by Time Block and Heat/Non-Heat Day

	Low Humidex	Before Peak Heat	Peak Heat	After Peak Heat
Non-Heat Day	22,515	139,997	60,984	72,210
Heat Day	4,240	27,073	12,557	15,353

APPENDIX 6:

METHODS – RELATIVE RISK ANALYSIS

A crude relative risk (RR) using poisson regression estimated the relationship between extreme heat and EMS call counts. It estimated the difference of expected EMS call counts on heat days compared to non-heat days. It was calculated for both BLS and ALS calls in each grid cell, and included calls of all causes and ages. The RR equation was as follows:

$$\log(\mu_j) = \beta_0 + \beta_1 I_j\{\text{humidex} > \text{threshold}\} + \beta_2(\text{time}) + \beta_3(\text{weekend/day of week})$$

Where j indexes the day, μ_j is the expected call count on day j , $I_j\{\text{humidex} > \text{threshold}\}$ is the indicator of a heat day, defined as whether its humidex exceeds a threshold, time is an overall time trend variable for all days in the study period, and $\text{weekend/day of the week}$ is a time trend variable adjusting for differences in call volumes on the weekend or on every day of the week.

In order to classify days as extreme heat days or non-heat days, this research used an *a priori* threshold based on the research of Calkins et al. (2016). Calkins et al. (2016), used the same meteorological dataset and the Akaike Information Criterion (AIC) to determine the maximum likelihood best fit in the model between the 90th, 95th, and 99th percentile full year humidex values. For the BLS data, the AIC best fit threshold was the 95th percentile humidex value or 29.7 °C, and for the ALS data, the best fit threshold was the 99th percentile humidex value or 36.7 °C. For both BLS and ALS datasets, days with a daily maximum humidex above their respective thresholds were considered extreme heat days.

A generalized linear regression for each grid cell fit the daily call counts by the predictor of interest, heat or non-heat day. The quasi-poisson model with a log link function allowed for flexibility in the mean-variance relationship, accepting over or under dispersion. Because this dataset had many grid cells with 0 calls per day, it was not realistic to assume the variance was always equal to the mean. For statistical power purposes, any grid cell with 5 or fewer total calls during the six year study period was eliminated from the analysis. This excluded 15 grid cells for the BLS dataset and 14 grid cells for the ALS dataset. For each grid cell relative risk, the 95% confidence interval was calculated using the Huber-White sandwich estimate of the standard error. This approach helped correct for heteroscedasticity that could occur from a wide range of variability across the predictor variable (Long and Ervin 2000; White 1980).

Furthermore, this dataset was collected over a period of six years, meaning temporal correlations in the observations were likely. In order to account for this, the model included some functions of time based on trends in the aggregated data. An overall time trend variable was adjusted for in addition to adjusting for certain days of the week. They were determined from full year trends, and on time trends in each individual grid cell because of the inefficiency and difficulty to compare relative risks across grid cells if each included different mean models.

APPENDIX 7:

METHODS + RESULTS – RELATIVE RISK ANALYSIS R MARKDOWN

```
#####
```

###RR Analysis

```
#####
```

Calculate RRs, adjusted for time and weekend/non-weekend

```
RR <- logRR <- lowerbound <- upperbound <- se_RR <- rep(NA, length(BLSviclist))
out1 <- data.frame(id = BLSviclist, RR, logRR, lowerbound, upperbound, se_RR)
q = qnorm(0.975)
for(i in 1:length(BLSviclist)){
  dat <- subset(BLSCallsperVICGridperDay, GRIDCODE == BLSviclist[i])
  if(length(table(dat$HD))==2){
    mod <- glm(count ~ HD + time + time^2 + DayofWeek, data=dat, family = quasipoisson(link = "log"))
    beta <- mod$coefficients[2]
    se <- sqrt(diag(vcovHC(mod, type = "HCO")))[2]
    out1$RR[i] <- exp(beta)
    out1$logRR[i] <- beta
    out1$lowerbound[i] <- exp(beta - q*se)
    out1$upperbound[i] <- exp(beta + q*se)
    out1$se_RR[i] <- se
  }
}
```

```
#####
```

Construct the final dataset

```
#####
```

RRs

```
GRIDCODE <- BLSviclist
count_HD <- as.vector(by(BLSCallsperVICGridperDay$HD, INDICES=BLSCallsperVICGridperDay$GRIDCODE,
FUN=sum))
count_nonHD <- as.vector(by(BLSCallsperVICGridperDay$HD, INDICES=BLSCallsperVICGridperDay$GRIDCODE,
FUN=function(x){ length(x)-sum(x) }))
count_call_HD <- as.vector(by(BLSCallsperVICGridperDay, INDICES=BLSCallsperVICGridperDay$GRIDCODE,
FUN=function(x){ sum(x$count[x$HD==1]) }))
count_call_nonHD <- as.vector(by(BLSCallsperVICGridperDay, INDICES=BLSCallsperVICGridperDay$GRIDCODE,
```

```
FUN=function(x){ sum(x$count[x$HD==0]) })
average_call_HD <- count_call_HD/count_HD
average_call_nonHD <- count_call_nonHD/count_nonHD
RRsimple <- average_call_HD/average_call_nonHD
logRRsimple <- log(RRsimple)
RRglm <- out1$RR
logRRglm <- out1$logRR
RRglm_lower <- out1$lowerbound
RRglm_upper <- out1$upperbound
RRglm_se <- out1$se
```

##Final RRs

```
BLSRR_dat <- data.frame(GRIDCODE, count_HD, count_nonHD, count_call_HD, count_call_nonHD,
  average_call_HD, average_call_nonHD, RRsimple, logRRsimple, RRglm, logRRglm, RRglm_lower,
  RRglm_upper, RRglm_se)
```

Table 8.1: BLS RR and Predictor Variables by Grid Cell

Grid Cell	#Heat Days	#Non-Heat Days	Heat Day Call Count	Non-Heat Day Call Count	Total Call Count	Avg Calls/Day	Avg Calls/Heat Day	Avg Calls/Non-Heat Day	RR	Lower 95% CI	Upper 95% CI	Pct Water	Pct Impervious	Pct Development	Pct Canopy	Median Income	Pct Poverty	logPop	Pct AgeL5	Pct Age5-14	Pct Age15-44	Pct Age45-64	Pct Age65-84	Pct AgeG85
1	130	788	7796	42213	50009	54.48	59.97	53.57	1.10*	1.07	1.14	29.21	56.72	67.63	3.97	42025	17.83	11.24	2.14	2.5	62.69	22.51	8.31	1.85
2	113	805	502	3171	3673	4.00	4.44	3.94	1.13*	1.03	1.24	74.01	11.34	20.28	4.58	76949	5.87	9.99	5.89	9.27	39.99	31.47	10.64	2.75
3	132	786	603	3236	3839	4.18	4.57	4.12	1.10*	1.01	1.20	64.20	15.22	28.99	7.00	76308	6.92	10.26	6.19	8.79	40.26	30.82	10.47	3.48
4	172	746	799	3332	4131	4.50	4.65	4.47	1.04	0.95	1.13	58.65	14.34	30.17	12.21	67915	8.40	9.78	5.32	11.17	34.92	30.11	14.24	4.25
5	171	747	852	3788	4640	5.05	4.98	5.07	0.99	0.93	1.07	45.46	17.31	37.59	18.70	64431	10.18	10.24	6.21	12.65	39.15	28.96	11.38	1.66
6	147	771	91	471	562	0.61	0.62	0.61	1.02	0.82	1.27	78.61	3.30	8.77	9.41	75020	6.64	8.87	5.64	12.66	36.43	31.7	12.23	1.34
7	113	805	154	810	964	1.05	1.36	1.01	1.34*	1.14	1.58	83.61	5.01	9.58	4.51	84975	6.15	9.41	5.92	11.01	36.23	33.22	11.17	2.45
8	100	818	68	422	490	0.53	0.68	0.52	1.31	0.99	1.72	73.58	8.05	15.58	8.59	87352	5.09	9.23	3.54	10.45	26.69	34.88	19.52	4.92
9	124	794	15	75	90	0.10	0.12	0.09	1.22	0.67	2.23	39.00	2.05	5.79	40.58	75130	6.79	8.00	4.27	12.21	30.01	38.18	13.96	1.39
10	129	789	14	70	84	0.09	0.11	0.09	1.20	0.68	2.12	60.86	1.48	4.03	29.25	77462	4.23	8.22	4.47	10.4	29.83	35.01	16.04	4.25
11	131	787	22	157	179	0.19	0.17	0.20	0.88	0.56	1.38	64.16	1.05	3.56	22.94	86348	4.32	7.62	3.9	11.71	26.36	41.04	15.51	1.47
12	128	790	215	1201	1416	1.54	1.68	1.52	1.11	0.96	1.30	23.37	3.42	12.54	46.50	75402	8.26	7.98	4.12	12.5	27.06	39.81	13.52	2.98
13	128	790	103	679	782	0.85	0.80	0.86	0.93	0.76	1.15	16.78	3.57	12.10	46.83	79639	6.23	7.87	3.81	11.47	25.07	41.85	15.6	2.2
14	148	770	27	109	136	0.15	0.18	0.14	1.33	0.85	2.10	64.12	1.31	4.51	18.06	82192	5.01	6.99	3.62	10.85	23.87	43.07	16.85	1.73
2291	102	816	0	1	1	0.00	0.00	0.00	0.00	0.00	0.00	0.76	1.02	1.97	50.01	67240	5.10	4.36	6.05	12.43	37.11	33.17	10.16	1.09
2292	139	779	1	3	4	0.00	0.01	0.00	1.68	0.23	12.11	1.31	0.79	1.58	53.13	66182	5.44	4.58	5.12	11.84	34.85	34.86	11.91	1.42
2293	165	753	5	25	30	0.03	0.03	0.03	0.88	0.34	2.29	0.92	1.10	1.81	68.20	66209	5.43	4.57	5.14	11.85	34.91	34.82	11.86	1.41
2294	188	730	12	45	57	0.06	0.06	0.06	1.04	0.53	2.05	1.10	1.71	3.94	53.11	64198	14.63	7.78	5.96	13.16	37.95	30.2	11.03	1.69
2295	201	717	15	50	65	0.07	0.07	0.07	1.05	0.50	2.17	1.27	7.16	18.47	37.50	65179	13.00	8.65	5.88	13.59	37.91	30.01	10.94	1.67
2296	197	721	0	1	1	0.00	0.00	0.00	0.00	0.00	0.00	0.25	7.70	23.45	34.41	67546	9.14	8.94	5.5	15.38	39.71	30.65	7.99	0.76
2406	93	825	0	2	2	0.00	0.00	0.00	0.00	0.00	0.00	0.00	0.93	1.64	60.53	65255	5.73	4.81	4.31	11.33	32.87	36.35	13.44	1.7
2407	148	770	5	18	23	0.03	0.03	0.02	1.45	0.54	3.90	0.04	0.77	1.86	69.74	65255	5.73	4.81	4.31	11.33	32.87	36.35	13.44	1.7
2408	197	721	501	1852	2353	2.56	2.54	2.57	1.00	0.90	1.11	0.09	11.32	28.88	21.16	59910	9.80	8.53	5.79	12.7	38.91	27.9	11.5	3.21
2409	197	721	199	679	878	0.96	1.01	0.94	1.08	0.88	1.32	0.01	8.17	22.77	9.84	69990	7.09	8.57	5.69	13.53	37.15	29.29	12.1	2.24
2410	199	719	112	312	424	0.46	0.56	0.43	1.32	0.95	1.85	0.87	3.26	8.32	27.48	91050	4.01	8.14	5.15	15.03	35.1	32.38	11.28	1.07
2411	186	732	4	13	17	0.02	0.02	0.02	1.16	0.32	4.27	31.12	11.79	31.17	27.15	87318	4.00	9.29	6	15.63	38.79	31.2	7.6	0.79
2412	198	720	73	244	317	0.35	0.37	0.34	1.13	0.84	1.50	3.24	27.94	57.98	22.84	69631	5.62	9.84	6.79	13.46	41.71	27.43	9.23	1.38
2413	178	740	5	24	29	0.03	0.03	0.03	0.83	0.26	2.66	0.94	29.48	76.40	20.32	60844	8.52	9.88	5.77	12.11	39.5	29.39	11.35	1.87
2414	171	747	1	7	8	0.01	0.01	0.01	0.73	0.09	6.09	0.56	28.48	62.27	14.08	57418	8.10	10.00	6.87	12.54	43.03	26.31	9.99	1.25
2520	133	785	9	13	22	0.02	0.07	0.02	4.13*	1.65	10.32	0.52	0.56	0.90	72.18	74958	6.07	6.36	4.44	12.73	36.91	37.26	8.07	0.59
2521	169	749	10	58	68	0.07	0.06	0.08	0.75	0.36	1.57	0.19	1.15	3.27	60.59	74302	6.04	6.14	4.44	12.63	36.64	37.19	8.43	0.66
2522	191	727	74	126	200	0.22	0.39	0.17	2.25	1.31	3.87	2.13	2.32	7.44	54.25	87293	4.18	7.48	7.47	16.09	39.5	29.03	7.31	0.59
2523	195	723	166	384	550	0.60	0.85	0.53	1.60*	1.27	2.02	1.90	4.00	12.89	54.16	89430	5.13	8.16	6.72	15.73	37.67	29.94	9.1	0.84
2524	186	732	155	522	677	0.74	0.83	0.71	1.17	0.95	1.43	0.89	5.78	19.06	40.49	86390	5.06	8.41	4.75	13.55	34.6	35.6	10.58	0.91
2525	175	743	242	943	1185	1.29	1.38	1.27	1.08	0.91	1.27	2.16	7.23	23.99	41.33	69782	10.52	9.22	6.05	13.66	39.55	30.24	9.35	1.14
2526	174	744	2016	8245	10261	11.18	11.59	11.08	1.04	0.99	1.10	1.41	38.57	68.94	18.54	49488	18.46	10.38	7.88	14.09	43.31	25.29	8.25	1.19
2527	162	756	966	4351	5317	5.79	5.96	5.76	1.04	0.97	1.13	2.12	25.76	64.49	35.34	66569	9.28	10.12	6.63	13.73	40.67	28.69	9.17	1.11
2528	162	756	1327	6110	7437	8.10	8.19	8.08	1.02	0.95	1.09	0.81	32.72	70.30	29.10	60427	12.23	10.58	6.87	14.28	43.3	26.14	7.79	1.63
2529	147	771	115	504	619	0.67	0.78	0.65	1.25*	1.01	1.56	24.46	40.81	63.03	11.18	78244	6.55	9.84	5.43	13.23	41.31	30.19	8.88	0.96
2634	97	821	0	3	3	0.00	0.00	0.00	0.00	0.00	0.00	0.00	0.63	0.50	80.98	70017	5.89	5.30	4.38	12.01	34.85	36.8	10.81	1.16
2635	135	783	4	17	21	0.02	0.03	0.02	1.16	0.40	3.33	0.12	0.58	0.93	70.51	75427	6.08	6.55	4.45	12.79	37.11	37.3	7.81	0.53
2636	164	754	45	106	151	0.16	0.27	0.14	1.95*	1.27	3.01	1.09	2.67	8.81	50.13	75875	6.01	6.61	4.56	12.92	37.24	37.02	7.73	0.52
2637	185	733	38	174	212	0.23	0.21	0.24	0.86	0.58	1.26	2.16	2.54	7.43	62.51	89715	3.16	7.93	8.62	17.29	40.89	26.29	6.37	0.54
2638	190	728	441	1417	1858	2.02	2.32	1.95	1.19*	1.06	1.34	4.54	15.26	42.66	39.85	92676	2.22	9.80	7.65	17.58	41.51	26.53	6.07	0.67
2639	188	730	636	2232	2868	3.12	3.38	3.06	1.10*	1.01	1.21	1.39	18.09	53.14	38.62	85251	4.72	9.86	6.09	14.73	40.5	30.05	7.91	0.72
2640	182	736	1070	3729	4799	5.23	5.88	5.07	1.16*	1.08	1.25	1.69	22.86	61.75	26.69	77512	8.09	10.26	6.73	15.78	42.06	27.15	7.28	1
2641	190	728	1834	6693	8527	9.29	9.65	9.19	1.05	0.99	1.12	0.22	35.75	68.33	18.36	49744	18.48	10.30	7.55	13.64	42.68	23.83	10.21	2.09
2642	171	747	1752	7468	9220	10.04	10.25	10.00	1.02	0.97	1.08	1.62	29.15	64.02	29.33	61493	11.45	10.74	7.53	13.93	43.91	26.04	7.74	0.86
2740	97	821	40	207	247	0.27	0.41	0.25	1.62*	1.09	2.41	0.48	3.74	7.37	59.65	76033	7.39	5.23	5.79	12.87	37.02	33.32	9.86	1.14
2741	82	836	7	74	81	0.09	0.09	0.09	0.95	0.31	2.91	1.07	1.51	3.02	64.46	102581	3.32	6.01	6.79	14.64	40.68	32.4	5.01	0.48

Grid Cell	#Heat Days	#Non-Heat Days	Heat Day Call Count	Non-Heat Day Call Count	Total Call Count	Avg Calls/Day	Avg Calls/Heat Day	Avg Calls/Non-Heat Day	RR	Lower 95% CI	Upper 95% CI	Pct Water	Pct Impervious	Pct Development	Pct Canopy	Median Income	Pct Poverty	logPop	Pct Age15-	Pct Age5-14	Pct Age15-44	Pct Age45-64	Pct Age65-84	Pct AgeG85
2742	78	840	5	31	36	0.04	0.06	0.04	1.74	0.57	5.28	2.38	1.18	2.55	68.07	102729	3.30	6.02	6.8	14.65	40.7	32.39	4.98	0.47
2743	77	841	8	60	68	0.07	0.10	0.07	1.38	0.45	4.23	0.06	1.49	2.60	67.58	102729	3.30	6.02	6.8	14.65	40.7	32.39	4.98	0.47
2744	75	843	2	25	27	0.03	0.03	0.03	0.95	0.21	4.23	5.42	1.27	2.34	57.56	102247	3.33	5.99	6.77	14.61	40.6	32.44	5.09	0.49
2745	104	814	0	1	1	0.00	0.00	0.00	0.00	0.00	0.00	15.04	0.51	0.46	67.73	96555	3.70	5.69	6.39	14.1	39.41	33.04	6.37	0.68
2746	118	800	3	18	21	0.02	0.03	0.02	0.99	0.32	3.06	1.59	1.36	2.16	81.20	89794	4.13	5.43	5.91	13.49	37.92	33.82	7.96	0.9
2747	137	781	0	10	10	0.01	0.00	0.01	0.00*	0.00	0.00	0.68	0.64	0.62	86.22	103876	1.99	6.77	3.79	13.22	31.96	39.26	10.76	1.01
2748	156	762	3	4	7	0.01	0.02	0.01	3.34	0.72	15.50	1.72	0.49	0.41	84.95	104440	1.95	7.06	3.71	13.23	31.84	39.5	10.74	0.98
2749	188	730	72	244	316	0.34	0.38	0.33	1.16	0.87	1.53	0.62	4.59	14.99	61.41	102420	2.06	7.30	4.12	13.45	32.48	38.11	10.75	1.08
2750	191	727	420	1438	1858	2.02	2.20	1.98	1.10	0.97	1.24	0.54	12.70	39.72	47.66	90783	3.59	8.93	6.72	15.77	38.57	29.44	8.37	1.13
2751	176	742	178	669	847	0.92	1.01	0.90	1.13	0.95	1.35	5.92	8.86	31.74	46.61	86959	6.48	9.26	6.11	14.49	39.19	31	8.59	0.61
2752	170	748	643	2724	3367	3.67	3.78	3.64	1.04	0.95	1.15	4.55	18.91	54.83	31.44	83526	5.83	10.29	5.9	14.34	39.98	30.6	8.34	0.85
2753	185	733	3013	10981	13994	15.24	16.29	14.98	1.09*	1.04	1.14	0.03	50.07	86.18	16.94	51341	17.10	10.74	7.99	13.55	45.53	23.26	8.16	1.51
2754	172	746	2250	9375	11625	12.66	13.08	12.57	1.04	0.98	1.09	2.13	38.16	74.30	18.80	51362	17.40	10.60	8.08	12.11	45.89	24.62	7.86	1.43
2852	77	841	4	20	24	0.03	0.05	0.02	1.88	0.48	7.37	0.13	0.23	0.47	62.49	101399	3.44	5.83	6.69	14.55	40.34	32.65	5.26	0.5
2855	64	854	0	2	2	0.00	0.00	0.00	0.00	0.00	0.00	1.14	0.08	0.06	70.96	102729	3.30	6.01	6.8	14.65	40.7	32.39	4.98	0.47
2856	127	791	12	82	94	0.10	0.09	0.10	0.89	0.35	2.28	1.29	0.76	1.39	77.02	101551	3.37	5.76	6.66	14.56	40.25	32.78	5.26	0.49
2857	160	758	107	403	510	0.56	0.67	0.53	1.25	0.96	1.63	1.62	4.48	11.54	69.07	74921	5.54	7.18	6.28	14.31	37.67	32.1	8.17	1.48
2858	164	754	373	1600	1973	2.15	2.27	2.12	1.07	0.94	1.21	1.11	8.56	25.40	57.85	71622	5.85	8.11	6.24	14.29	37.42	31.93	8.51	1.6
2859	123	795	0	4	4	0.00	0.00	0.01	0.00	0.00	0.00	0.00	0.37	0.54	64.72	105538	2.39	6.68	4.63	13.7	34.38	37.23	9.18	0.88
2860	140	778	13	67	80	0.09	0.09	0.09	1.09	0.50	2.40	0.00	0.72	1.39	73.24	105388	3.17	7.31	3.9	12.61	30.31	40.11	11.96	1.1
2861	144	774	32	198	230	0.25	0.22	0.26	0.87	0.58	1.29	0.00	1.67	4.78	76.78	101198	4.81	7.53	4.15	11.92	29.78	40.33	12.66	1.15
2862	170	748	68	314	382	0.42	0.40	0.42	0.96	0.71	1.30	0.19	3.86	12.32	59.95	89456	2.81	8.44	4.69	12.75	34.57	35.5	11.32	1.17
2863	168	750	259	1009	1268	1.38	1.54	1.35	1.13	0.97	1.32	1.79	12.16	38.97	49.57	89471	2.68	9.49	6.06	13.79	36.76	31.71	10.88	0.8
2864	154	764	1434	6509	7943	8.65	9.31	8.52	1.10*	1.03	1.18	0.02	31.34	73.70	30.41	71325	7.73	10.83	7.6	13.24	43.44	25.83	8.87	1.02
2865	159	759	2849	12767	15616	17.01	17.92	16.82	1.06*	1.02	1.11	0.58	49.43	85.30	17.65	54285	12.98	10.58	7.57	11.39	44.85	25.35	8.88	1.95
2866	154	764	3731	17582	21313	23.22	24.23	23.01	1.05*	1.01	1.09	1.35	49.18	87.69	15.57	45683	18.00	10.46	7.65	12.93	45.33	24.73	8.07	1.29
2867	148	770	2206	10244	12450	13.56	14.91	13.30	1.12*	1.07	1.18	11.45	32.07	67.72	24.22	52830	13.89	10.67	6.7	12.07	40.61	28.15	10.56	1.9
2868	128	790	4	26	30	0.03	0.03	0.03	0.93	0.34	2.59	31.17	2.59	8.94	45.78	80919	5.96	8.22	4.46	12.68	33.42	37.08	11.07	1.29
2971	117	801	7	31	38	0.04	0.06	0.04	1.54	0.62	3.85	0.30	0.65	1.23	74.77	81204	4.67	4.19	4.31	12.94	32.34	39.46	10.14	0.81
2972	183	735	70	253	323	0.35	0.38	0.34	1.10	0.77	1.59	1.48	2.60	10.90	62.81	70022	8.07	7.91	6.08	13.98	38.64	31.39	8.39	1.52
2973	183	735	388	1414	1802	1.96	2.12	1.92	1.11	0.95	1.28	1.84	8.00	25.64	53.96	108169	6.77	8.75	10.34	18.29	42.86	22.92	5.05	0.54
2974	185	733	191	748	939	1.02	1.03	1.02	1.02	0.84	1.24	0.74	4.20	13.41	65.94	112720	4.11	9.06	11.6	18.14	44.15	21.22	4.51	0.38
2975	148	770	38	206	244	0.27	0.26	0.27	0.96	0.67	1.37	0.01	3.09	7.31	76.90	101575	2.34	8.51	10.96	14.52	45.21	23.52	5.36	0.43
2976	166	752	754	3261	4015	4.37	4.54	4.34	1.05	0.96	1.15	0.22	15.95	37.43	52.62	79984	4.53	9.48	6.84	12.14	40.13	26.86	10.81	3.22
2977	146	772	166	864	1030	1.12	1.14	1.12	1.02	0.85	1.22	2.05	8.71	21.71	62.70	112368	3.40	9.52	5.79	14.56	38.99	30.47	8.68	1.51
2978	146	772	743	3772	4515	4.92	5.09	4.89	1.05	0.96	1.14	0.18	24.20	62.33	41.32	92705	5.92	10.60	6.61	13.92	39.45	29.38	9.42	1.23
2979	146	772	481	2205	2686	2.93	3.29	2.86	1.13*	1.02	1.26	47.73	15.86	35.37	21.28	98506	6.40	10.35	5.65	12.77	36.54	30.57	12.31	2.15
2980	132	786	2252	11770	14022	15.27	17.06	14.97	1.13*	1.07	1.19	12.12	43.72	77.65	13.31	52839	18.39	10.93	6.98	12.51	42.01	26.25	10.3	1.94
2981	132	786	2188	12137	14325	15.60	16.58	15.44	1.07*	1.02	1.13	2.06	49.95	84.48	16.39	53055	15.61	10.88	7.65	11.99	46.8	24.81	7.57	1.17
3084	175	743	3	22	25	0.03	0.02	0.03	0.60	0.18	2.01	1.18	0.50	0.65	76.16	76154	7.86	5.98	5.31	13.27	34.04	35.54	10.41	1.42
3085	168	750	39	64	103	0.11	0.23	0.09	2.68*	1.42	5.05	0.18	0.51	1.15	77.76	78354	7.90	7.27	5.85	13.83	34.88	34.17	9.88	1.4
3086	191	727	165	541	706	0.77	0.86	0.74	1.15	0.91	1.46	2.31	3.25	10.59	43.00	84661	6.65	7.39	7.12	14.6	37.26	31.44	8.44	1.14
3087	164	754	157	626	783	0.85	0.96	0.83	1.14	0.91	1.43	0.69	6.88	19.52	58.05	135607	4.33	9.32	8.12	21.12	39.82	26.63	3.99	0.32
3088	163	755	637	2905	3542	3.86	3.91	3.85	1.02	0.93	1.11	2.40	19.66	54.90	41.67	120578	4.13	10.27	7.28	18.44	39.69	27.15	6.09	1.35
3089	154	764	427	1951	2378	2.59	2.77	2.55	1.09	0.98	1.21	44.40	13.67	35.36	25.24	705789	3.93	10.15	5.91	13.87	37.1	29.59	11.66	1.87
3090	143	775	1795	9012	10807	11.77	12.55	11.63	1.08*	1.02	1.14	0.49	38.51	77.70	32.63	103466	8.25	10.82	6.3	11.49	44.08	24.52	11.41	2.21
3091	138	780	1550	8112	9662	10.53	11.23	10.40	1.07	1.00	1.15	37.62	24.17	50.59	21.80	95526	4.21	10.28	4.48	11.07	40.59	26.05	13.87	3.94
3092	130	788	2096	11865	13961	15.21	16.12	15.06	1.06*	1.01	1.12	48.63	24.90	47.59	9.02	66686	12.46	10.95	5.85	9.11	48.1	25.18	9.83	1.93
3195	138	780	1	0	1	0.00	0.01	0.00	21.04e ²	28.43e ²	15.57e ³	0.52	1.24	2.48	59.24	81204	4.67	4.18	4.31	12.94	32.34	39.46	10.14	0.81
3196	150	768	0	1	1	0.00	0.00	0.00	0.00	0.00	0.00	0.01	0.38	0.39	66.86	81041	4.67	4.42	4.62	13.44	32.98	38.65	9.48	0.83
3197	185	733	21	41	62	0.07	0.11	0.06	2.05*	1.19	3.55	1.08	0.47	0.52	72.22	80347	4.81	6.54	5.63	15.02	35.07	35.95	7.39	0.93
3198	187	731	171	576	747	0.81	0.91	0.79	1.16	0.94	1.43	2.41	4.05	12.23	47.94	98871	3.56	7.40	6.25	16.21	36.18	34.3	6.47	0.6

Grid Cell	#Heat Days	#Non-Heat Days	Heat Day Call Count	Non-Heat Day Call Count	Total Call Count	Avg Calls/Day	Avg Calls/Heat Day	Avg Calls/Non-Heat Day	RR	Lower 95% CI	Upper 95% CI	Pct Water	Pct Impervious	Pct Development	Pct Canopy	Median Income	Pct Poverty	logPop	Pct Age15	Pct Age5-14	Pct Age15-44	Pct Age45-64	Pct Age65-84	Pct AgeG85
3199	167	751	103	352	455	0.50	0.62	0.47	1.30	1.00	1.69	1.57	4.13	13.39	54.50	120629	2.35	8.25	5.83	17.04	33.36	36.86	6.38	0.52
3200	153	765	206	887	1093	1.19	1.35	1.16	1.16	0.99	1.36	0.12	11.52	35.13	55.27	122961	2.31	9.76	7.87	17.66	39.63	29.09	5.21	0.55
3201	155	763	907	4155	5062	5.51	5.85	5.45	1.07	1.00	1.16	12.17	22.48	49.76	28.91	100437	4.91	10.24	7.63	13.51	45.25	24.06	8.2	1.34
3202	134	784	1601	9068	10669	11.62	11.95	11.57	1.03	0.98	1.09	0.20	38.86	77.33	36.08	86101	5.05	10.59	7.04	10.8	48.49	23.32	8.76	1.59
3203	127	791	813	4525	5338	5.81	6.40	5.72	1.12*	1.04	1.22	46.30	19.99	43.99	16.73	112701	4.93	10.24	5.29	12.37	38.57	29.23	12.48	2.07
3204	119	799	1118	6469	7587	8.26	9.39	8.10	1.15*	1.06	1.24	30.71	28.48	60.82	16.27	78014	12.03	10.96	5.24	9.33	52.87	22.22	8.44	1.91
3205	111	807	2237	14322	16559	18.04	20.15	17.75	1.12*	1.07	1.17	11.81	52.56	84.91	10.48	67399	11.37	11.70	4.42	5.51	60.72	21.52	6.34	1.49
3206	113	805	778	4738	5516	6.01	6.88	5.89	1.16*	1.08	1.25	38.71	29.17	48.45	8.62	78645	5.86	10.62	5.5	8.58	46.41	27.99	9.71	1.82
3299	54	864	1	36	37	0.04	0.02	0.04	0.41	0.05	3.15	0.13	1.04	2.42	68.71	68404	7.32	4.25	4.3	12.35	31.14	37.59	13.17	1.45
3300	91	827	2	17	19	0.02	0.02	0.02	1.00	0.23	4.39	0.14	1.26	2.91	72.85	81204	4.67	4.18	4.31	12.94	32.34	39.46	10.14	0.81
3301	92	826	3	2	5	0.01	0.03	0.00	12.33	1.29	117.83	0.26	1.22	2.92	76.71	81204	4.67	4.18	4.31	12.94	32.34	39.46	10.14	0.81
3302	114	804	1	3	4	0.00	0.01	0.00	2.16	0.23	20.27	0.85	0.95	1.67	78.16	81204	4.67	4.18	4.31	12.94	32.34	39.46	10.14	0.81
3303	153	765	30	156	186	0.20	0.20	0.20	0.95	0.63	1.43	0.97	1.95	4.42	75.06	81204	4.67	4.18	4.31	12.94	32.34	39.46	10.14	0.81
3304	145	773	7	28	35	0.04	0.05	0.04	1.27	0.50	3.21	1.09	1.16	2.26	74.29	81204	4.67	4.18	4.31	12.94	32.34	39.46	10.14	0.81
3305	105	813	0	14	14	0.02	0.00	0.02	0.00*	0.00	0.00	0.54	0.39	0.57	68.67	81204	4.67	4.18	4.31	12.94	32.34	39.46	10.14	0.81
3310	150	768	2	9	11	0.01	0.01	0.01	1.17	0.26	5.32	0.48	0.65	1.03	58.43	80502	4.70	6.55	5.64	15.08	35.1	35.98	7.29	0.92
3311	165	753	9	46	55	0.06	0.05	0.06	0.95	0.44	2.09	1.72	0.66	1.55	67.42	80494	4.70	6.66	5.65	15.1	35.13	35.94	7.26	0.92
3312	166	752	103	382	485	0.53	0.62	0.51	1.22	0.95	1.57	0.41	4.31	14.68	64.90	98639	2.85	8.01	7.57	16.77	38.99	30.49	5.75	0.43
3313	177	741	270	1032	1302	1.42	1.53	1.39	1.09	0.92	1.29	2.36	6.03	17.92	42.50	102903	2.91	8.63	7.51	17.04	39.43	30.1	5.59	0.34
3314	157	761	240	1157	1397	1.52	1.53	1.52	1.01	0.87	1.18	1.03	8.59	27.33	54.60	112664	2.72	9.11	5.34	13.99	30.35	32.63	16.66	1.03
3315	143	775	309	1730	2039	2.22	2.16	2.23	0.98	0.86	1.10	0.09	15.53	50.83	47.73	110443	4.19	9.95	6.37	15.19	37.88	31.18	7.56	1.82
3316	134	784	876	4696	5572	6.07	6.54	5.99	1.10*	1.02	1.19	0.16	26.52	61.44	29.07	85807	6.29	10.51	6.97	11.49	45.72	25.78	8.19	1.85
3317	120	798	926	5668	6594	7.18	7.72	7.10	1.09*	1.01	1.18	11.94	23.27	56.00	38.42	82643	6.01	10.71	6.26	11.18	43.66	28.39	8.89	1.62
3318	113	805	1159	7429	8588	9.36	10.26	9.23	1.11*	1.04	1.19	32.44	23.30	52.50	24.05	70125	9.60	10.77	5.83	9.73	42.37	29.47	10.44	2.16
3319	100	818	2363	18087	20450	22.28	23.63	22.11	1.07*	1.02	1.12	0.44	44.22	85.51	23.45	59184	11.19	11.24	5.63	7.89	48.29	25.36	9.66	3.17
3414	119	799	0	2	2	0.00	0.00	0.00	0.00	0.00	0.00	0.00	1.24	3.36	76.32	71691	7.04	4.45	5.16	12	34.87	37.78	9.44	0.77
3415	75	843	0	1	1	0.00	0.00	0.00	0.05	0.00	139.76	0.03	0.57	1.42	66.71	71764	7.02	4.45	5.15	12	34.85	37.79	9.44	0.77
3417	142	776	11	61	72	0.08	0.08	0.08	0.96	0.49	1.89	1.05	0.89	1.93	71.47	71507	7.08	4.46	5.17	11.98	34.92	37.74	9.42	0.76
3422	116	802	0	1	1	0.00	0.00	0.00	0.00	0.00	0.00	0.30	0.40	0.25	70.61	78392	5.24	5.98	5.65	14.56	35.31	36.07	7.52	0.89
3424	131	787	15	65	80	0.09	0.11	0.08	1.35	0.66	2.78	1.94	1.21	3.08	69.03	96543	2.40	7.24	8.01	16.53	38.72	30.45	5.82	0.48
3425	177	741	15	54	69	0.08	0.08	0.07	1.17	0.60	2.27	1.19	1.61	4.37	37.63	100150	2.17	7.60	7.28	16.03	37.42	32.09	6.62	0.57
3426	149	769	42	208	250	0.27	0.28	0.27	1.03	0.72	1.48	0.75	5.62	17.64	62.12	116054	3.79	8.68	4.56	15.36	33.37	38.2	7.81	0.7
3427	133	785	113	626	739	0.81	0.85	0.80	1.07	0.87	1.32	1.59	11.08	33.84	59.65	111774	4.00	9.19	4.61	14.67	33.02	38.19	8.64	0.87
3428	123	795	540	3263	3803	4.14	4.39	4.10	1.07	0.98	1.17	0.12	26.16	59.51	41.26	84375	4.57	9.92	6.81	13.38	42.17	27.86	7.91	1.87
3429	114	804	1048	6765	7813	8.51	9.19	8.41	1.09	1.00	1.18	0.32	28.93	66.63	37.10	72342	6.57	10.61	6.94	12.81	42.26	27.13	9.06	1.8
3430	102	816	590	4311	4901	5.34	5.78	5.28	1.11*	1.01	1.23	3.03	30.45	72.78	36.33	75552	7.32	10.81	5.85	11.52	39.62	31.5	9.98	1.52
3431	100	818	946	6797	7743	8.43	9.46	8.31	1.14*	1.06	1.22	1.31	42.20	86.61	26.51	64827	7.23	10.99	5.07	10.55	38.91	30.18	12.65	2.64

*Grid Cells with statistically significant results

Grid Cells excluded ≤ 5 total calls

Table 8.2: ALS RR and Predictor Variables by Grid Cell

Grid Cell	#Heat Days	#Non-Heat Days	Heat Day Call Count	Non-Heat Day Call Count	Total Call Count	Avg Calls/Day	Avg Calls/Heat Day	Avg Calls/Non-Heat Day	RR	Lower 95% CI	Upper 95% CI	Pct Water	Pct Impervious	Pct Development	Pct Canopy	Median Income	Pct Poverty	logPop	Pct Age15	Pct Age5-14	Pct Age15-44	Pct Age45-64	Pct Age65-84	Pct Age685
1	22	896	423	14365	14788	16.11	19.23	16.03	1.21*	1.11	1.32	29.21	56.72	67.63	3.97	42025	17.83	11.24	2.14	2.5	62.69	22.51	8.31	1.85
2	18	900	25	1366	1391	1.52	1.39	1.52	0.91	0.65	1.28	74.01	11.34	20.28	4.58	76949	5.87	9.99	5.89	9.27	39.99	31.47	10.64	2.75
3	24	894	46	1324	1370	1.49	1.92	1.48	1.29	0.97	1.73	64.20	15.22	28.99	7.00	76308	6.92	10.26	6.19	9.29	40.26	30.82	10.47	3.48
4	33	885	41	866	907	0.99	1.24	0.98	1.27	0.88	1.83	58.65	14.34	30.17	12.21	67915	8.40	9.78	5.32	11.17	34.92	30.11	14.24	4.25
5	30	888	30	1010	1040	1.13	1.00	1.14	0.88	0.58	1.34	45.46	17.31	37.59	18.70	64431	10.18	10.24	6.21	12.65	39.15	28.96	11.38	1.66
6	23	895	7	161	168	0.18	0.30	0.18	1.68	0.72	3.90	78.61	3.30	8.77	9.41	75020	6.64	8.87	5.64	12.66	36.43	31.7	12.23	1.34
7	18	900	8	358	366	0.40	0.44	0.40	1.13	0.66	1.93	83.61	5.01	9.58	4.51	84975	6.15	9.41	5.92	11.01	36.23	33.22	11.17	2.45
8	14	904	3	189	192	0.21	0.21	0.21	1.09	0.40	2.96	73.58	8.05	15.58	8.59	87352	5.09	9.23	3.54	10.45	26.69	34.88	19.52	4.92
9	22	896	1	44	45	0.05	0.05	0.05	0.96	0.14	6.67	39.00	2.05	5.79	40.58	75130	6.79	8.00	4.27	12.21	30.01	38.18	13.96	1.39
10	20	898	3	46	49	0.05	0.15	0.05	2.99*	1.02	8.81	60.86	1.48	4.03	29.25	77462	4.23	8.22	4.47	10.4	29.83	35.01	16.04	4.25
11	20	898	2	94	96	0.10	0.10	0.10	0.96	0.26	3.62	64.16	1.05	3.56	22.94	86348	4.32	7.62	3.9	11.71	26.36	41.04	15.51	1.47
12	25	893	23	633	656	0.71	0.92	0.71	1.27	0.79	2.06	23.37	3.42	12.54	46.50	75402	8.26	7.98	4.12	12.5	27.06	39.81	13.52	2.98
13	25	893	10	376	386	0.42	0.40	0.42	0.94	0.53	1.67	16.78	3.57	12.10	46.83	79639	6.23	7.87	3.81	11.47	25.07	41.85	15.6	2.2
14	25	893	3	60	63	0.07	0.12	0.07	1.75	0.56	5.40	64.12	1.31	4.51	18.06	82192	5.01	6.99	3.62	10.85	23.87	43.07	16.85	1.73
2290	15	903	0	4	4	0.00	0.00	0.00	0.00	0.00	0.00	0.62	0.85	1.18	59.58	66434	5.36	4.52	5.34	11.98	35.39	34.46	11.49	1.34
2292	28	890	0	1	1	0.00	0.00	0.00	0.00	0.00	0.00	1.31	0.79	1.58	53.13	66182	5.44	4.58	5.12	11.84	34.85	34.86	11.91	1.42
2293	33	885	0	16	16	0.02	0.00	0.02	0.00*	0.00	0.00	0.92	1.10	11.81	68.20	66209	5.43	4.57	5.14	11.85	34.91	34.82	11.86	1.41
2294	41	877	1	16	17	0.02	0.02	0.02	1.26	0.16	9.67	1.10	1.71	3.94	53.11	64198	14.63	7.78	5.96	13.16	37.95	30.2	11.03	1.69
2295	44	874	0	4	4	0.00	0.00	0.00	0.00	0.00	0.00	1.27	7.16	18.47	37.50	65179	13.00	8.65	5.88	13.59	37.91	30.01	10.94	1.67
2405	17	901	0	1	1	0.00	0.00	0.00	0.00	0.00	0.00	0.09	0.56	0.80	68.78	65255	5.73	4.81	4.31	11.33	32.87	36.35	13.44	1.7
2407	31	887	0	17	17	0.02	0.00	0.02	0.00*	0.00	0.00	0.04	0.77	1.86	69.74	65255	5.73	4.81	4.31	11.33	32.87	36.35	13.44	1.7
2408	44	874	29	384	413	0.45	0.66	0.44	1.47*	1.01	2.13	0.09	11.32	28.88	21.16	59910	9.80	8.53	5.79	12.7	38.91	27.9	11.5	3.21
2409	44	874	8	181	189	0.21	0.18	0.21	0.87	0.41	1.81	0.01	8.17	22.77	9.84	69990	7.09	8.57	5.69	13.53	37.15	29.29	12.1	2.24
2410	42	876	8	97	105	0.11	0.19	0.11	1.65	0.78	3.50	0.87	3.26	8.32	27.48	91050	4.01	8.14	5.15	15.03	35.1	32.38	11.28	1.07
2411	37	881	0	19	19	0.02	0.00	0.02	0.00*	0.00	0.00	31.12	11.79	31.17	27.15	87318	4.00	9.29	6	15.63	38.79	31.2	7.6	0.79
2412	35	883	7	119	126	0.14	0.20	0.13	1.50	0.70	3.19	3.24	27.94	57.98	22.84	69631	5.62	9.84	6.79	13.46	41.71	27.43	9.23	1.38
2413	36	882	1	63	64	0.07	0.03	0.07	0.58	0.11	3.22	0.94	29.48	76.40	20.32	60844	8.52	9.88	5.77	12.11	39.5	29.39	11.35	1.87
2414	28	890	0	29	29	0.03	0.00	0.03	0.00*	0.00	0.00	0.56	28.48	62.27	14.08	57418	8.10	10.00	6.87	12.54	43.03	26.31	9.99	1.25
2520	24	894	0	9	9	0.01	0.00	0.01	0.00*	0.00	0.00	0.52	0.56	0.90	72.18	74958	6.07	6.36	4.44	12.73	36.91	37.26	8.07	0.59
2521	35	883	1	24	25	0.03	0.03	0.03	1.00	0.15	6.82	0.19	1.15	3.27	60.59	74302	6.04	6.14	4.44	12.63	36.64	37.19	8.43	0.66
2522	40	878	4	49	53	0.06	0.10	0.06	1.80	0.56	5.82	2.13	2.32	7.44	54.25	87293	4.18	7.48	7.47	16.09	39.5	29.03	7.31	0.59
2523	41	877	12	115	127	0.14	0.29	0.13	2.22*	1.16	4.26	1.90	4.00	12.89	54.16	89430	5.13	8.16	6.72	15.73	37.67	29.94	9.1	0.84
2524	36	882	3	165	168	0.18	0.08	0.19	0.44	0.15	1.31	0.89	5.78	19.06	40.49	86390	5.06	8.41	4.75	13.55	34.6	35.6	10.58	0.91
2525	33	885	11	282	293	0.32	0.33	0.32	1.03	0.56	1.88	2.16	7.23	23.99	41.33	69782	10.52	9.22	6.05	13.66	39.55	30.24	9.35	1.14
2526	28	890	83	2207	2290	2.49	2.96	2.48	1.20	1.00	1.43	1.41	38.57	68.94	18.54	49488	18.46	10.38	7.88	14.09	43.31	25.29	8.25	1.19
2527	24	894	30	1069	1099	1.20	1.25	1.20	1.05	0.80	1.37	2.12	25.76	64.49	35.34	66569	9.28	10.12	6.63	13.73	40.67	28.69	9.17	1.11
2528	22	896	50	1725	1775	1.93	2.27	1.93	1.17	0.84	1.64	0.81	32.72	70.30	29.10	60427	12.23	10.58	6.87	14.28	43.3	26.14	7.79	1.63
2529	23	895	0	179	179	0.19	0.00	0.20	0.00*	0.00	0.00	24.46	40.81	63.03	11.18	78244	6.55	9.84	5.43	13.23	41.31	30.19	8.88	0.96
2634	23	895	0	2	2	0.00	0.00	0.00	0.00	0.00	0.00	0.00	0.63	0.50	80.98	70017	5.89	5.30	4.38	12.01	34.85	36.8	10.81	1.16
2635	26	892	0	3	3	0.00	0.00	0.00	0.00	0.00	0.00	0.12	0.58	0.93	70.51	75427	6.08	6.55	4.45	12.79	37.11	37.3	7.81	0.53
2636	32	886	3	32	35	0.04	0.09	0.04	2.60	0.38	17.93	1.09	2.67	8.81	50.13	75875	6.01	6.61	4.56	12.92	37.24	37.02	7.73	0.52
2637	38	880	1	57	58	0.06	0.03	0.06	0.40	0.06	2.75	2.16	2.54	7.43	62.51	89715	3.16	7.93	8.62	17.29	40.89	26.29	6.37	0.54
2638	40	878	21	341	362	0.39	0.53	0.39	1.37	0.95	1.99	4.54	15.26	42.66	39.85	92676	2.22	9.80	7.65	17.58	41.51	26.53	6.07	0.67
2639	42	876	33	659	692	0.75	0.79	0.75	1.03	0.71	1.50	1.39	18.09	53.14	38.62	85251	4.72	9.86	6.09	14.73	40.5	30.05	7.91	0.72
2640	35	883	50	1026	1076	1.17	1.43	1.16	1.23	0.92	1.65	1.69	22.86	61.75	26.69	77512	8.09	10.26	6.73	15.78	42.06	27.15	7.28	1
2641	34	884	73	1602	1675	1.82	2.15	1.81	1.18	0.93	1.51	0.22	35.75	68.33	18.36	49744	18.48	10.30	7.55	13.64	42.68	23.83	10.21	2.09
2642	30	888	49	1772	1821	1.98	1.63	2.00	0.82	0.64	1.05	1.62	29.15	64.02	29.33	61493	11.45	10.74	7.53	13.93	43.91	26.04	7.74	0.86
2740	16	902	1	47	48	0.05	0.06	0.05	1.11	0.16	7.53	0.48	3.74	7.37	59.65	76033	7.39	5.23	5.79	12.87	37.02	33.32	9.86	1.14
2741	14	904	2	22	24	0.03	0.14	0.02	6.50*	1.06	40.03	1.07	1.51	3.02	64.46	102581	3.32	6.01	6.79	14.64	40.68	32.4	5.01	0.48
2742	14	904	0	12	12	0.01	0.00	0.01	0.00*	0.00	0.00	2.38	1.18	2.55	68.07	102729	3.30	6.02	6.8	14.65	40.7	32.39	4.98	0.47

Grid Cell	#Heat Days	#Non-Heat Days	Heat Day Call Count	Non-Heat Day Call Count	Total Call Count	Avg Calls/Day	Avg Calls/Heat Day	Avg Calls/Non-Heat Day	RR	Lower 95% CI	Upper 95% CI	Pct Water	Pct Impervious	Pct Development	Pct Canopy	Median Income	Pct Poverty	logPop	Pct Age15	Pct Age5-14	Pct Age15-44	Pct Age45-64	Pct Age65-84	Pct Age65-84
2743	14	904	0	13	13	0.01	0.00	0.01	0.00*	0.00	0.00	0.06	1.49	2.60	67.58	102729	3.30	6.02	6.8	14.65	40.7	32.39	4.98	0.47
2744	15	903	0	6	6	0.01	0.00	0.01	0.00*	0.00	0.00	5.42	1.27	2.34	57.56	102247	3.33	5.99	6.77	14.61	40.6	32.44	5.09	0.49
2745	21	897	0	3	3	0.00	0.00	0.00	0.00	0.00	0.00	15.04	0.51	0.46	67.73	96555	3.70	5.69	6.39	14.1	39.41	33.04	6.37	0.68
2746	24	894	0	19	19	0.02	0.00	0.02	0.00*	0.00	0.00	1.59	1.36	2.16	81.20	89794	4.13	5.43	5.91	13.49	37.92	33.82	7.96	0.9
2747	31	887	0	2	2	0.00	0.00	0.00	0.00	0.00	0.00	0.68	0.64	0.62	86.22	103876	1.99	6.77	3.79	13.22	31.96	39.26	10.76	1.01
2748	28	890	1	1	2	0.00	0.04	0.00	49.15	3.70	652.60	1.72	0.49	0.41	84.95	104440	1.95	7.06	3.71	13.23	31.84	39.5	10.74	0.98
2749	40	878	3	67	70	0.08	0.08	0.08	1.00	0.33	3.04	0.62	4.59	14.99	61.41	102420	2.06	7.30	4.12	13.45	32.48	38.11	10.75	1.08
2750	41	877	23	343	366	0.04	0.56	0.39	1.44	0.84	2.44	0.54	12.70	39.72	47.66	90783	3.59	8.93	6.72	15.77	38.57	29.44	8.37	1.13
2751	35	883	6	185	191	0.21	0.17	0.21	0.81	0.34	1.96	5.92	8.86	31.74	46.61	86959	6.48	9.26	6.11	14.49	39.19	31	8.59	0.61
2752	33	885	33	774	807	0.88	1.00	0.87	1.13	0.79	1.62	4.55	18.91	54.83	31.44	83526	5.83	10.29	5.9	14.34	39.98	30.6	8.34	0.85
2753	32	886	101	2610	2711	2.95	3.16	2.95	1.08	0.87	1.34	0.03	50.07	86.18	16.94	51341	17.10	10.74	7.99	13.55	45.53	23.26	8.16	1.51
2754	33	885	76	2101	2177	2.37	2.30	2.37	0.97	0.78	1.20	2.13	38.16	74.30	18.80	51362	17.40	10.60	8.08	12.11	45.89	24.62	7.86	1.43
2852	14	904	0	7	7	0.01	0.00	0.01	0.00*	0.00	0.00	0.13	0.23	0.47	62.49	101399	3.44	5.83	6.69	14.55	40.34	32.65	5.26	0.5
2855	12	906	0	13	13	0.01	0.00	0.01	0.00*	0.00	0.00	1.14	0.08	0.06	70.96	102729	3.30	6.01	6.8	14.65	40.7	32.39	4.98	0.47
2856	28	890	1	24	25	0.03	0.04	0.03	1.22	0.18	8.29	1.29	0.76	1.39	77.02	101551	3.37	5.76	6.66	14.56	40.25	32.78	5.26	0.49
2857	32	886	12	139	151	0.16	0.38	0.16	2.38*	1.33	4.27	1.62	4.48	11.54	69.07	74921	5.54	7.18	6.28	14.31	37.67	32.1	8.17	1.48
2858	33	885	20	585	605	0.66	0.61	0.66	0.89	0.57	1.38	1.11	8.56	25.40	57.85	71622	5.85	8.11	6.24	14.29	37.42	31.93	8.51	1.6
2860	26	892	0	37	37	0.04	0.00	0.04	0.00*	0.00	0.00	0.00	0.72	1.39	73.24	105388	3.17	7.31	3.9	12.61	30.31	40.11	11.96	1.1
2861	26	892	0	74	74	0.08	0.00	0.08	0.00*	0.00	0.00	0.00	1.67	4.78	76.78	101198	4.81	7.53	4.15	11.92	29.78	40.33	12.66	1.15
2862	32	886	3	118	121	0.13	0.09	0.13	0.69	0.23	2.07	0.19	3.86	12.32	59.95	89456	2.81	8.44	4.69	12.75	34.57	35.5	11.32	1.17
2863	33	885	14	298	312	0.34	0.42	0.34	1.27	0.80	2.03	1.79	12.16	38.97	49.57	89471	2.68	9.49	6.06	13.79	36.76	31.71	10.88	0.8
2864	30	888	66	1821	1887	2.06	2.20	2.05	1.09	0.84	1.42	0.02	31.34	73.70	30.41	71325	7.73	10.83	7.6	13.24	43.44	25.83	8.87	1.02
2865	32	886	95	3069	3164	3.45	2.97	3.46	0.88	0.72	1.07	0.58	49.43	85.30	17.65	54285	12.98	10.58	7.57	11.39	44.85	25.35	8.88	1.95
2866	27	891	117	2988	3105	3.38	4.33	3.35	1.31*	1.12	1.52	1.35	49.18	87.69	15.57	45683	18.00	10.46	7.65	12.93	45.33	24.73	8.07	1.29
2867	25	893	64	2281	2345	2.55	2.56	2.55	1.01	0.79	1.29	11.45	32.07	67.72	24.22	52830	13.89	10.67	6.7	12.07	40.61	28.15	10.56	1.9
2868	25	893	0	12	12	0.01	0.00	0.01	0.00*	0.00	0.00	31.17	2.59	8.94	45.78	80919	5.96	8.22	4.46	12.68	33.42	37.08	11.07	1.29
2971	23	895	0	36	36	0.04	0.00	0.04	0.00*	0.00	0.00	0.30	0.65	1.23	74.77	81204	4.67	4.19	4.31	12.94	32.34	39.46	10.14	0.81
2972	34	884	1	79	80	0.09	0.03	0.09	0.33	0.05	2.23	1.48	2.60	10.90	62.81	70022	8.07	7.91	6.08	13.98	38.64	31.39	8.39	1.52
2973	38	880	29	436	465	0.51	0.76	0.50	1.54*	1.03	2.28	1.84	8.00	25.64	53.96	108169	6.77	8.75	10.34	18.29	42.86	22.92	5.05	0.54
2974	35	883	8	226	234	0.25	0.23	0.26	0.91	0.48	1.70	0.74	4.20	13.41	65.94	112720	4.11	9.06	11.6	18.14	44.15	21.22	4.51	0.38
2975	29	889	5	84	89	0.10	0.17	0.09	1.86	0.81	4.26	0.01	3.09	7.31	76.90	101575	2.34	8.51	10.96	14.52	45.21	23.52	5.36	0.43
2976	30	888	48	1178	1226	1.34	1.60	1.33	1.22	0.85	1.74	0.22	15.95	37.43	52.62	79984	4.53	9.48	6.84	12.14	40.13	26.86	10.81	3.22
2977	27	891	10	354	364	0.40	0.37	0.40	0.93	0.49	1.75	2.05	8.71	21.71	62.70	112368	3.40	9.52	5.79	14.56	38.99	30.47	8.68	1.51
2978	28	890	43	1201	1244	1.36	1.54	1.35	1.14	0.84	1.55	0.18	24.20	62.33	41.32	92705	5.92	10.60	6.61	13.92	39.45	29.38	9.42	1.23
2979	29	889	23	734	757	0.82	0.79	0.83	0.95	0.64	1.41	47.73	15.86	35.37	21.28	98506	6.40	10.35	5.65	12.77	36.54	30.57	12.31	2.15
2980	23	895	140	4617	4757	5.18	6.09	5.16	1.18	0.95	1.47	12.12	43.72	77.65	13.31	52839	18.39	10.93	6.98	12.51	42.01	26.25	10.3	1.94
2981	24	894	114	3991	4105	4.47	4.75	4.46	1.06	0.89	1.27	2.06	49.95	84.48	16.39	53055	15.61	10.88	7.65	11.99	46.8	24.81	7.57	1.17
3083	27	891	0	13	13	0.01	0.00	0.01	0.00*	0.00	0.00	0.18	1.66	3.40	65.36	81204	4.67	4.18	4.31	12.94	32.34	39.46	10.14	0.81
3084	32	886	0	28	28	0.03	0.00	0.03	0.00*	0.00	0.00	1.18	0.50	0.65	76.16	76154	7.86	5.98	5.31	13.27	34.04	35.54	10.41	1.42
3085	30	888	2	24	26	0.03	0.07	0.03	2.47	0.61	10.03	0.18	0.51	1.15	77.76	78354	7.90	7.27	5.85	13.83	34.88	34.17	9.88	1.4
3086	41	877	8	128	136	0.15	0.20	0.15	1.31	0.62	2.74	2.31	3.25	10.59	43.00	84661	6.65	7.39	7.12	14.6	37.26	31.44	8.44	1.14
3087	31	887	11	205	216	0.24	0.35	0.23	1.53	0.88	2.64	0.69	6.88	19.52	58.05	135607	4.33	9.32	8.12	21.12	39.82	26.63	3.99	0.32
3088	28	890	30	1051	1081	1.18	1.07	1.18	0.90	0.67	1.22	2.40	19.66	54.90	41.67	120578	4.13	10.27	7.28	18.44	39.69	27.15	6.09	1.35
3089	30	888	31	699	730	0.80	1.03	0.79	1.30	0.92	1.83	44.40	13.67	35.36	25.24	105789	3.93	10.15	5.91	13.87	37.1	29.59	11.66	1.87
3090	27	891	102	2907	3009	3.28	3.78	3.26	1.16	0.96	1.40	0.49	38.51	77.70	32.63	73046	8.25	10.82	6.3	11.49	44.08	24.52	11.41	2.21
3091	25	893	72	2567	2639	2.87	2.88	2.87	1.01	0.76	1.33	37.62	24.17	50.59	21.80	95526	4.21	10.28	4.48	11.07	40.59	26.05	13.87	3.94
3092	22	896	154	5015	5169	5.63	7.00	5.60	1.26*	1.07	1.48	48.63	24.90	47.59	9.02	66686	12.46	10.95	5.85	9.11	48.1	25.18	9.83	1.93
3196	28	890	0	4	4	0.00	0.00	0.00	0.00	0.00	0.00	0.01	0.38	0.39	66.86	81041	4.67	4.42	4.62	13.44	32.98	38.65	9.48	0.83
3197	34	884	0	13	13	0.01	0.00	0.01	0.00*	0.00	0.00	1.08	0.47	0.52	72.22	80347	4.81	6.54	5.63	15.02	35.07	35.95	7.39	0.93
3198	32	886	6	161	167	0.18	0.19	0.18	1.02	0.49	2.11	2.41	4.05	12.23	47.94	98871	3.56	7.40	6.25	16.21	36.18	34.3	6.47	0.6
3199	29	889	12	163	175	0.19	0.41	0.18	2.24*	1.19	4.22	1.57	4.13	13.39	54.50	120629	2.35	8.25	5.83	17.04	33.36	36.86	6.38	0.52
3200	25	893	7	366	373	0.41	0.28	0.41	0.68	0.35	1.31	0.12	11.52	35.13	55.27	122961	2.31	9.76	7.87	17.66	39.63	29.09	5.21	0.55

Grid Cell	#Heat Days	#Non-Heat Days	Heat Day Call Count	Non-Heat Day Call Count	Total Call Count	Avg Calls/Day	Avg Calls/Heat Day	Avg Calls/Non-Heat Day	RR	Lower 95% CI	Upper 95% CI	Pct Water	Pct Impervious	Pct Development	Pct Canopy	Median Income	Pct Poverty	logPop	Pct AgeL5	Pct Age5-14	Pct Age15-44	Pct Age45-64	Pct Age65-84	Pct AgeG85
3201	25	893	58	1565	1623	1.77	2.32	1.75	1.32	0.99	1.78	12.17	22.48	49.76	28.91	100437	4.91	10.24	7.63	13.51	45.25	24.06	8.2	1.34
3202	24	894	88	2932	3020	3.29	3.67	3.28	1.14	0.96	1.37	0.20	38.86	77.33	36.08	86101	5.05	10.59	7.04	10.8	48.49	23.32	8.76	1.59
3203	23	895	34	1405	1439	1.57	1.48	1.57	0.95	0.70	1.31	46.30	19.99	43.99	16.73	112701	4.93	10.24	5.29	12.37	38.57	29.23	12.48	2.07
3204	19	899	66	2316	2382	2.59	3.47	2.58	1.35*	1.06	1.72	30.71	28.48	60.82	16.27	78014	12.03	10.96	5.24	9.33	52.87	22.22	8.44	1.91
3205	19	899	116	4997	5113	5.57	6.11	5.56	1.11	0.94	1.31	11.81	52.56	84.91	10.48	67399	11.37	11.70	4.42	5.51	60.72	21.52	6.34	1.49
3206	18	900	47	1792	1839	2.00	2.61	1.99	1.31	0.96	1.80	38.71	29.17	48.45	8.62	78645	5.86	10.62	5.5	8.58	46.41	27.99	9.71	1.82
3304	31	887	0	2	2	0.00	0.00	0.00	0.00	0.00	0.00	1.09	1.16	2.26	74.29	81204	4.67	4.18	4.31	12.94	32.34	39.46	10.14	0.81
3305	17	901	0	3	3	0.00	0.00	0.00	0.00	0.00	0.00	0.54	0.39	0.57	68.67	81204	4.67	4.18	4.31	12.94	32.34	39.46	10.14	0.81
3310	26	892	0	2	2	0.00	0.00	0.00	0.00	0.00	0.00	0.48	0.65	1.03	58.43	80502	4.70	6.55	5.64	15.08	35.1	35.98	7.29	0.92
3311	28	890	0	17	17	0.02	0.00	0.02	0.00*	0.00	0.00	1.72	0.66	1.55	67.42	80494	4.70	6.66	5.65	15.1	35.13	35.94	7.26	0.92
3312	28	890	7	138	145	0.16	0.25	0.16	1.61	0.50	5.24	0.41	4.31	14.68	64.90	98639	2.85	8.01	7.57	16.77	38.99	30.49	5.75	0.43
3313	29	889	15	392	407	0.44	0.52	0.44	1.18	0.68	2.06	2.36	6.03	17.92	42.50	102903	2.91	8.63	7.51	17.04	39.43	30.1	5.59	0.34
3314	25	893	18	466	484	0.53	0.72	0.52	1.37	0.81	2.30	1.03	8.59	27.33	54.60	112664	2.72	9.11	5.34	13.99	30.35	32.63	16.66	1.03
3315	25	893	17	615	632	0.69	0.68	0.69	0.99	0.60	1.66	0.09	15.53	50.83	47.73	110443	4.19	9.95	6.37	15.19	37.88	31.18	7.56	1.82
3316	23	895	56	1769	1825	1.99	2.43	1.98	1.25	1.00	1.57	0.16	26.52	61.44	29.07	85807	6.29	10.51	6.97	11.49	45.72	25.78	8.19	1.85
3317	20	898	53	2264	2317	2.52	2.65	2.52	1.05	0.73	1.52	11.94	23.27	56.00	38.42	82643	6.01	10.71	6.26	11.18	43.66	28.39	8.89	1.62
3318	18	900	61	2849	2910	3.17	3.39	3.17	1.08	0.83	1.40	32.44	23.30	52.50	24.05	70125	9.60	10.77	5.83	9.73	42.37	29.47	10.44	2.16
3319	16	902	126	6864	6990	7.61	7.88	7.61	1.05	0.89	1.25	0.44	44.22	85.51	23.45	59184	11.19	11.24	5.63	7.89	48.29	25.36	9.66	3.17
3417	31	887	1	18	19	0.02	0.03	0.02	1.41	0.21	9.49	1.05	0.89	1.93	71.47	71507	7.08	4.46	5.17	11.98	34.92	37.74	9.42	0.76
3421	14	904	0	3	3	0.00	0.00	0.00	0.00	0.00	0.00	0.09	0.56	0.72	72.69	78396	5.24	5.99	5.65	14.57	35.31	36.07	7.52	0.89
3424	23	895	2	31	33	0.04	0.09	0.03	2.42	0.64	9.08	1.94	1.21	3.08	69.03	96543	2.40	7.24	8.01	16.53	38.72	30.45	5.82	0.48
3425	26	892	0	14	14	0.02	0.00	0.02	0.00*	0.00	0.00	1.19	1.61	4.37	37.63	100150	2.17	7.60	7.28	16.03	37.42	32.09	6.62	0.57
3426	24	894	0	96	96	0.10	0.00	0.11	0.00*	0.00	0.00	0.75	5.62	17.64	62.12	116054	3.79	8.68	4.56	15.36	33.37	38.2	7.81	0.7
3427	21	897	8	257	265	0.29	0.38	0.29	1.35	0.58	3.10	1.59	11.08	33.84	59.65	111774	4.00	9.19	4.61	14.67	33.02	38.19	8.64	0.87
3428	18	900	34	1259	1293	1.41	1.89	1.40	1.35*	1.05	1.74	0.12	26.16	59.51	41.26	84375	4.57	9.92	6.81	13.38	42.17	27.86	7.91	1.87
3429	17	901	73	2975	3048	3.32	4.29	3.30	1.30*	1.05	1.62	0.32	28.93	66.63	37.10	72342	6.57	10.61	6.94	12.81	42.26	27.13	9.06	1.8
3430	14	904	38	1815	1853	2.02	2.71	2.01	1.37	0.98	1.91	3.03	30.45	72.78	36.33	75552	7.32	10.81	5.85	11.52	39.62	31.5	9.98	1.52
3431	14	904	40	3151	3191	3.48	2.86	3.49	0.83	0.62	1.11	1.31	42.20	86.61	26.51	64827	7.23	10.99	5.07	10.55	38.91	30.18	12.65	2.64

*Grid Cells with statistically significant results

Grid Cells excluded ≤ 5 total calls

APPENDIX 8:

METHODS – ANALYSIS OF COMMUNITY-LEVEL PREDICTORS

In order to evaluate the relationship between predictor variables and relative risk variations, each predictor variable was assessed individually in addition to performing a formal model selection process. The model selection process used a combination of best subset selection and cross-validation to identify a single best fit model for BLS and ALS grid cell relative risks. The potential predictors for model selection were grid cell log population, population younger than 5, 5 to 14, 15-44, 45-64, 65-84, and over 85; median household income; poverty; canopy; development; open water; and impervious surface. Models with each predictor variable gave a basic picture of their individual relationship with grid cell relative risk, while a formal model selection process helped assess the interaction between the grid cell predictors and relative risk. The formal model selection built a model that optimally described the data and was predictive for future data using cross-validation to help with the selection procedure.

The best subset selection procedure was a more thorough method than forward and backward stepwise selection, where a separate least square regression was fit for all combinations of the p predictors. Two R programs were considered for the model selection process: Bestglm and Leaps. Using a cross-validated selection process, the best model of all 2^p possibilities was chosen by the statistical program in two stages (James et al., 2013). First, the statistical program fit all $\binom{p}{k}$ models that contained exactly k predictors and identified the models among the $\binom{p}{k}$ models that have the lowest RSS or equivalently highest R^2 . Next, it used

the cross-validated prediction error, AIC criterion, to pick the single best fit model.

Again, the potential community-level predictors for this analysis were log population, percent younger than 5, percent age 5-14, percent age 14-44, percent age 45-64, percent age 65-84, percent older than 85, percent canopy, percent impervious surfaces, percent below poverty line, percent development, percent water, and median household income for each grid cell. Although, some information was lost when categorizing variables, percent canopy, percent impervious surfaces, percent development, percent water, percent poverty, and percent median income were all grouped into four equal quartiles. This categorization better compared and contrasted the differences in mean relative risks between grid cells with the lowest percentages of traits and grid cells with the highest percentages. In addition, plots, descriptive statistics, and correlation coefficients helped describe and explore the relationships between variables and their effect on relative risk. Due to the high correlation coefficient between development and impervious surface and to the less accurate data collection process, development and water were eliminated from the regression analysis.

Because the grid cell age group variables were a more detailed look at log population, the first model selection did not include the age group populations in order to analyze the overall effect of predictor variables. However, previous extreme heat research did show that age had a significant effect on health and one's vulnerability to extreme heat (Naughton, 2002; Naughton, 2008). Therefore, a second model selection analysis also included the age group variables to see if the age make-up of the community was an important predictive factor for

relative risk of an EMS call and how these variables changed the results of the previous model.

SPATIAL AUTOCORRELATION

After the final model selection process, the residuals from each regression were tested for spatial autocorrelation using the Moran's I test. Spatial autocorrelation measured how similar one object was to other nearby objects. It was important to test for because neighboring grids were more likely to have similar attributes than grid cells that were across the county. However, spatially correlated grid cells would violate the statistical assumption that observations were independent from one another. The Moran's I Index Value was calculated from the equation below and significance was assessed through its p-value.

$$I = \frac{N}{\sum_i \sum_i w_{ij}} \frac{\sum_i \sum_i w_{ij} (X_i - \bar{X})(X_j - \bar{X})}{\sum_i (X_i - \bar{X})^2}$$

Where N is the number of number of features indexed by i and j , X is the variable of interest, \bar{X} is the mean of X , and w_{ij} is the spatial weight between feature i and j .

The values of the Moran's index ranged from -1 to +1 and indicated different types of spatial patterns. A value of 0 indicated random dispersion, a value of negative 1 indicated a perfectly spaced checker board, and a value of positive 1 would have a clustered pattern.

APPENDIX 9:

METHODS + RESULTS – ANALYSIS OF COMMUNITY-LEVEL PREDICTORS R MARKDOWN

```
#####
```

##Individual Linear Regression on Predictor Variables

```
#####
```

##List of Variables

```
list_var1 <- c("PctImpervious_cat", "PctCanopy_cat", "logPop", "PctPoverty_cat", "MedIncome_cat", "RRglm")
list_var2 <- c("PctImpervious_cat", "PctCanopy_cat", "PctAgeL5", "PctAge5_14", "PctAge15_44",
              "PctAge45_64", "PctAge65_84", "PctAgeG85", "logPop", "PctPoverty_cat", "MedIncome_cat", "RRglm")
```

```
dat1 <- BLSvic2[, list_var1]
```

```
dat2 <- BLSvic2[, list_var2]
```

Individual Models

```
mod_inc <- lm(RRglm ~ MedIncome_cat, data = dat2)
```

```
summary(mod_inc)
```

```
## Call:
```

```
## lm(formula = RRglm ~ MedIncome_cat, data = dat2)
```

```
##
```

```
## Residuals:
```

```
##      Min       1Q   Median       3Q      Max
## -1.16503 -0.17326 -0.04676  0.03545  2.82796
```

```
##
```

```
## Coefficients:
```

```
##              Estimate Std. Error t value Pr(>|t|)
## Intercept           1.04268   0.08192  12.729 <2e-16 ***
## MedIncome_cat(25th, 50th] 0.25703   0.11585   2.219  0.0284 *
## MedIncome_cat(50th, 75th] 0.10398   0.11585   0.898  0.3712
## MedIncome_cat(75th, 100th] 0.12235   0.11585   1.056  0.2930
```

```
## ---
```

```
## Signif. codes:  0 '***' 0.001 '**' 0.01 '*' 0.05 '.' 0.1 ' ' 1
```

```
##
```

```
## Residual standard error: 0.4561 on 120 degrees of freedom
```

```
## Multiple R-squared:  0.03987, Adjusted R-squared:  0.01586
```

```
## F-statistic: 1.661 on 3 and 120 DF, p-value: 0.1791
```

```
beta_inc <- mod_inc$coefficient
```

```
beta_inc
```

```
##Intercept MedIncome_cat(25th, 50th] MedIncome_cat(50th, 75th] MedIncome_cat(75th, 100th]  
##1.0426796      0.2570286                0.1039831                0.1223531
```

```
se_inc <- sqrt(diag(vcovHC(mod_inc, type = "HCO")))
```

```
se_inc
```

```
##Intercept MedIncome_cat(25th, 50th]MedIncome_cat(50th, 75th] MedIncome_cat(75th, 100th]  
##0.03374560      0.12104669                0.06849178                0.09439122
```

```
cbind(beta_inc - q*se_inc, beta_inc + q*se_inc)
```

```
##                [,1]      [,2]  
## Intercept      0.97653942  1.1088197  
## MedIncome_cat(25th, 50th] 0.01978143  0.4942757  
## MedIncome_cat(50th, 75th] -0.03025829  0.2382246  
## MedIncome_cat(75th, 100th] -0.06265028  0.3073565
```

```
2*pnorm(abs(beta_inc/se_inc), lower.tail=FALSE)
```

```
##Intercept MedIncome_cat(25th, 50th] MedIncome_cat(50th, 75th] MedIncome_cat(75th, 100th]  
##1.261386e-209  3.372170e-02                1.289680e-01                1.948949e-01
```

```
mod_imp<-lm(RRglm~PctImpervious_cat,data=dat2)
```

```
summary(mod_imp)
```

```
## Call:
```

```
## lm(formula = RRglm ~ PctImpervious_cat, data = dat2)
```

```
##
```

```
## Residuals:
```

```
##      Min       1Q   Median       3Q      Max  
## -1.30326 -0.13679 -0.01779  0.04422  2.82441
```

```
##
```

```
## Coefficients:
```

```
##                Estimate Std. Error t value Pr(>|t|)  
## Intercept      1.30326  0.08187  15.920 <2e-16 ***  
## PctImpervious_cat(25th, 50th] -0.11264  0.11577  -0.973  0.3326  
## PctImpervious_cat(50th, 75th] -0.21153  0.11577  -1.827  0.0702 .  
## PctImpervious_cat(75th, 100th] -0.23480  0.11577  -2.028  0.0448 *
```

```
## ---
```

```
## Signif. codes:  0 '***' 0.001 '**' 0.01 '*' 0.05 '.' 0.1 ' ' 1
```

```
##
```

```

## Residual standard error: 0.4558 on 120 degrees of freedom
## Multiple R-squared: 0.04108, Adjusted R-squared: 0.0171
## F-statistic: 1.713 on 3 and 120 DF, p-value: 0.1679

beta_imp <- mod_imp$coefficient
beta_imp

##Intercept PctImpervious_cat(25th, 50th]PctImpervious_cat(50th, 75th]PctImpervious_cat(75th, 100th]
##1.3032618 -0.1126396 -0.2115265 -0.2347981

se_imp <- sqrt(diag(vcovHC(mod_imp, type = "HC0")))
se_imp

##Intercept PctImpervious_cat(25th, 50th]PctImpervious_cat(50th, 75th]PctImpervious_cat(75th, 100th]
##0.1501544 0.1597992 0.1506285 0.1510326

cbind(beta_imp- q*se_imp, beta_imp + q*se_imp)

##                [,1]      [,2]
## Intercept          1.0089646  1.59755911
## PctImpervious_cat(25th, 50th] -0.4258403  0.20056105
## PctImpervious_cat(50th, 75th] -0.5067528  0.08369990
## PctImpervious_cat(75th, 100th] -0.5308166  0.06122029

2*pnorm(abs(beta_imp/se_imp), lower.tail=FALSE)

##Intercept PctImpervious_cat(25th, 50th]PctImpervious_cat(50th, 75th]PctImpervious_cat(75th, 100th]
##3.975936e-18 4.808835e-01 1.602317e-01 1.200368e-01

mod_can<-lm(RRglm~PctCanopy_cat,data=dat2)
summary(mod_can)
## Call:
## lm(formula = RRglm ~ PctCanopy_cat, data = dat2)
##
## Residuals:
##  Min    1Q  Median    3Q   Max
## -1.27271 -0.14343 -0.03304  0.04569  2.85496
##
## Coefficients:
##              Estimate Std. Error t value Pr(>|t|)
## Intercept          1.08490  0.08249  13.152 <2e-16 ***
## PctCanopy_cat(25th, 50th]  0.02108  0.11666  0.181  0.857
## PctCanopy_cat(50th, 75th]  0.10559  0.11666  0.905  0.367

```

```

## PctCanopy_cat(75th, 100th] 0.18782 0.11666 1.610 0.110
##
## Signif. codes: 0 '***' 0.001 '**' 0.01 '*' 0.05 '.' 0.1 ' ' 1
##
## Residual standard error: 0.4593 on 120 degrees of freedom
## Multiple R-squared: 0.0264, Adjusted R-squared: 0.002063
## F-statistic: 1.085 on 3 and 120 DF, p-value: 0.3583

beta_can <- mod_can$coefficient
beta_can

##Intercept PctCanopy_cat(25th, 50th] PctCanopy_cat(50th, 75th] PctCanopy_cat(75th, 100th]
##1.08489884 0.02107986 0.10559209 0.18781586

se_can <- sqrt(diag(vcovHC(mod_can, type = "HCO")))
se_can

##Intercept PctCanopy_cat(25th, 50th] PctCanopy_cat(50th, 75th] PctCanopy_cat(75th, 100th]
##0.02255945 0.02554960 0.06352291 0.15056493

cbind(beta_can-q*se_can, beta_can + q*se_can)

##
##
## [,1] [,2]
## Intercept 1.04068313 1.12911455
## PctCanopy_cat(25th, 50th] -0.02899644 0.07115615
## PctCanopy_cat(50th, 75th] -0.01891053 0.23009471
## PctCanopy_cat(75th, 100th] -0.10728598 0.48291770

2*pnorm(abs(beta_can/se_can), lower.tail=FALSE)

##Intercept PctCanopy_cat(25th, 50th] PctCanopy_cat(50th, 75th] PctCanopy_cat(75th, 100th]
##0.00000000 0.40933964 0.09645909 0.21224803

mod_pov<-lm(RRglm~PctPoverty_cat,data=dat2)
summary(mod_pov)
## Call:
## lm(formula = RRglm ~ PctPoverty_cat, data = dat2)
##
## Residuals:
## Min 1Q Median 3Q Max
## -1.18563 -0.14985 -0.06272 0.00809 2.93094
##
## Coefficients:

```

```

##              Estimate Std. Error t value Pr(>|t|)
## Intercept          1.18563  0.08335  14.225 <2e-16 ***
## PctPoverty_cat(25th, 50th] -0.01901  0.11787  -0.161  0.872
## PctPoverty_cat(50th, 75th]  0.01111  0.11787   0.094  0.925
## PctPoverty_cat(75th, 100th] -0.08053  0.11787  -0.683  0.496
##
## Signif. codes:  0 '***' 0.001 '**' 0.01 '*' 0.05 '.' 0.1 ' ' 1
##
## Residual standard error: 0.4641 on 120 degrees of freedom
## Multiple R-squared:  0.005979, Adjusted R-squared: -0.01887
## F-statistic: 0.2406 on 3 and 120 DF, p-value: 0.8679

beta_pov <- mod_pov$coefficient
beta_pov

##Intercept PctPoverty_cat(25th, 50th] PctPoverty_cat(50th, 75th] PctPoverty_cat(75th, 100th]
##1.18562756 -0.01900809 0.01110782 -0.08052678

se_pov <- sqrt(diag(vcovHC(mod_pov, type = "HCO")))
se_pov

##Intercept PctPoverty_cat(25th, 50th] PctPoverty_cat(50th, 75th] PctPoverty_cat(75th, 100th]
##0.08831623 0.11197228 0.13875649 0.10344459

cbind(beta_pov- q*se_pov, beta_pov + q*se_pov)

##              [,1]      [,2]
## Intercept          1.0125309  1.3587242
## PctPoverty_cat(25th, 50th] -0.2384697  0.2004535
## PctPoverty_cat(50th, 75th] -0.2608499  0.2830655
## PctPoverty_cat(75th, 100th] -0.2832745  0.1222209

2*pnorm(abs(beta_pov/se_pov), lower.tail=FALSE)

##Intercept PctPoverty_cat(25th, 50th] PctPoverty_cat(50th, 75th] PctPoverty_cat(75th, 100th]
##4.327633e-41 8.652012e-01 9.361954e-01 4.363018e-01

mod_pop<-lm(RRglm~logPop,data=dat2)
summary(mod_pop)
## Call:
## lm(formula = RRglm ~ logPop, data = dat2)
##
## Residuals:

```

```
##   Min       1Q   Median     3Q      Max
## -1.29717 -0.11805 -0.03813  0.02739  2.89684
##
## Coefficients:
##           Estimate Std. Error t value Pr(>|t|)
## Intercept    1.42474  0.18380  7.752  3.04e-12 ***
## logPop      -0.03050  0.02092 -1.458  0.147
##
## Signif. codes:  0 '***' 0.001 '**' 0.01 '*' 0.05 '.' 0.1 ' ' 1
##
## Residual standard error: 0.4577 on 122 degrees of freedom
## Multiple R-squared:  0.01713, Adjusted R-squared:  0.009072
## F-statistic: 2.126 on 1 and 122 DF, p-value: 0.1474
```

```
beta_pop <- mod_pop$coefficient
beta_pop
```

```
##Intercept      logPop
##1.42473509    -0.03049894
```

```
se_pop <- sqrt(diag(vcovHC(mod_pop, type = "HC0")))
se_pop
```

```
##Intercept      logPop
##0.24885653     0.02473966
```

```
cbind(beta_pop- q*se_pop, beta_pop + q*se_pop)
```

```
##           [,1]      [,2]
## Intercept  0.93698524  1.91248493
## logPop    -0.07898778  0.01798989
```

```
2*pnorm(abs(beta_pop/se_pop), lower.tail=FALSE)
```

```
##Intercept      logPop
##1.033568e-08   2.176520e-01
```

```
mod_AgeL5<-lm(RRglm~PctAgeL5,data=dat2)
summary(mod_AgeL5)
```

```
## Call:
## lm(formula = RRglm ~ PctAgeL5, data = dat2)
```

```
##
## Residuals:
```

```
##      Min      1Q      Median      3Q      Max
## -1.21142 -0.12774 -0.05928  0.00587  2.93031
##
## Coefficients:
##           Estimate Std. Error t value Pr(>|t|)
## Intercept  1.29341   0.17357   7.452  1.46e-11 ***
## PctAgeL5   -0.02163   0.02808  -0.771   0.442
##
## Signif. codes:  0 '***' 0.001 '**' 0.01 '*' 0.05 '.' 0.1 ' ' 1
##
## Residual standard error: 0.4605 on 122 degrees of freedom
## Multiple R-squared:  0.004843, Adjusted R-squared: -0.003314
## F-statistic: 0.5937 on 1 and 122 DF, p-value: 0.4425
```

```
beta_AgeL5 <- mod_AgeL5$coefficient
beta_AgeL5
```

```
##Intercept      PctAgeL5
##1.29340613    -0.02163244
```

```
se_AgeL5 <- sqrt(diag(vcovHC(mod_AgeL5, type = "HCO")))
se_AgeL5
```

```
##Intercept      PctAgeL5
##0.21708223     0.03077152
```

```
cbind(beta_AgeL5- q*se_AgeL5, beta_AgeL5 + q*se_AgeL5)
```

```
##           [,1]      [,2]
## Intercept  0.8679328  1.71887948
## PctAgeL5  -0.0819435  0.03867863
```

```
2*pnorm(abs(beta_AgeL5/se_AgeL5), lower.tail=FALSE)
```

```
##Intercept      PctAgeL5
##2.551260e-09   4.820545e-01
```

```
mod_Age5_14<-lm(RRglm~PctAge5_14,data=dat2)
summary(mod_Age5_14)
```

```
## Call:
```

```
## lm(formula = RRglm ~ PctAge5_14, data = dat2)
```

```
##
```

```
## Residuals:
```

```

##      Min      1Q      Median      3Q      Max
## -1.16296 -0.15181 -0.06897  0.00055  2.96976
##
## Coefficients:
##              Estimate Std. Error t value Pr(>|t|)
## Intercept      1.02702  0.22742  4.516  1.47e-05 ***
## PctAge5_14     0.01028  0.01685  0.610  0.543
##
## Signif. codes:  0 '***' 0.001 '**' 0.01 '*' 0.05 '.' 0.1 ' ' 1
##
## Residual standard error: 0.4609 on 122 degrees of freedom
## Multiple R-squared:  0.003045, Adjusted R-squared: -0.005127
## F-statistic: 0.3726 on 1 and 122 DF, p-value: 0.5427

beta_Age5_14 <- mod_Age5_14$coefficient
beta_Age5_14

##Intercept      PctAge5_14
##1.02702249     0.01028236

se_Age5_14 <- sqrt(diag(vcovHC(mod_Age5_14, type = "HC0")))
se_Age5_14

##Intercept      PctAge5_14
##0.101703368    0.007096108

cbind(beta_Age5_14- q*se_Age5_14, beta_Age5_14 + q*se_Age5_14)

##              [,1]      [,2]
## Intercept    0.827687552  1.22635743
##PctAge5_14   -0.003625758  0.02419047

2*pnorm(abs(beta_Age5_14/se_Age5_14), lower.tail=FALSE)

##Intercept      PctAge5_14
##5.625675e-24   1.473338e-01

mod_Age15_44<-lm(RRglm~PctAge15_44,data=dat2)
summary(mod_Age15_44)
## Call:
## lm(formula = RRglm ~ PctAge15_44, data = dat2)
##
## Residuals:

```

```

##   Min       1Q   Median     3Q      Max
## -1.19062 -0.14166 -0.05979  0.00043  2.95715
##
## Coefficients:
##              Estimate Std. Error t value Pr(>|t|)
## Intercept      1.320402  0.274205  4.815  4.26e-06 ***
## PctAge15_44   -0.004061  0.007016 -0.579  0.564
##
## Signif. codes:  0 '***' 0.001 '**' 0.01 '*' 0.05 '.' 0.1 ' ' 1
##
## Residual standard error: 0.461 on 122 degrees of freedom
## Multiple R-squared:  0.002738, Adjusted R-squared: -0.005436
## F-statistic: 0.335 on 1 and 122 DF, p-value: 0.5638

beta_Age15_44 <- mod_Age15_44$coefficient
beta_Age15_44

##Intercept      PctAge15_44
##1.320402077   -0.004060702

se_Age15_44 <- sqrt(diag(vcovHC(mod_Age15_44, type = "HC0")))
se_Age15_44

## Intercept      PctAge15_44
##0.239300896    0.005361838

cbind(beta_Age15_44- q*se_Age15_44, beta_Age15_44 + q*se_Age15_44)

##              [,1]      [,2]
## Intercept    0.85138094  1.789423214
## PctAge15_44 -0.01456971  0.006448308

2*pnorm(abs(beta_Age15_44/se_Age15_44), lower.tail=FALSE)

##Intercept      PctAge15_44
##3.433710e-08   4.488499e-01

mod_Age45_64<-lm(RRglm~PctAge45_64,data=dat2)
summary(mod_Age45_64)
## Call:
## lm(formula = RRglm ~ PctAge45_64, data = dat2)
##
## Residuals:

```

```

##      Min      1Q      Median      3Q      Max
## -1.25300 -0.13119 -0.04012  0.02086  2.89873
##
## Coefficients:
##              Estimate Std. Error t value Pr(>|t|)
## Intercept      0.821572  0.254646  3.226  0.00161 **
## PctAge45_64    0.010933  0.008035  1.361  0.17611
##
## Signif. codes:  0 '***' 0.001 '**' 0.01 '*' 0.05 '.' 0.1 ' ' 1
##
## Residual standard error: 0.4582 on 122 degrees of freedom
## Multiple R-squared:  0.01495, Adjusted R-squared:  0.006876
## F-statistic: 1.852 on 1 and 122 DF, p-value: 0.1761

beta_Age45_64 <- mod_Age45_64$coefficient
beta_Age45_64

##Intercept      PctAge45_64
##0.82157207     0.01093322

se_Age45_64 <- sqrt(diag(vcovHC(mod_Age45_64, type = "HC0")))
se_Age45_64

##Intercept      PctAge45_64
##0.2687604      0.0097046

cbind(beta_Age45_64- q*se_Age45_64, beta_Age45_64 + q*se_Age45_64)

##              [,1]      [,2]
##Intercept      0.294811281  1.34833286
##PctAge45_64    -0.008087449  0.02995388

2*pnorm(abs(beta_Age45_64/se_Age45_64), lower.tail=FALSE)

## Intercept      PctAge45_64
## 0.002236437     0.259910973

mod_Age65_84<-lm(RRglm~PctAge65_84,data=dat2)
summary(mod_Age65_84)
## Call:
## lm(formula = RRglm ~ PctAge65_84, data = dat2)
##
## Residuals:

```

```

##   Min   1Q  Median   3Q   Max
## -1.15271 -0.13995 -0.07952  0.00201  2.94420
##
## Coefficients:
##              Estimate Std. Error t value Pr(>|t|)
## (Intercept)   1.30339  0.14483   9.000 3.66e-15 ***
## PctAge65_84  -0.01486  0.01475  -1.008  0.316
##
## Signif. codes:  0 '***' 0.001 '**' 0.01 '*' 0.05 '.' 0.1 ' ' 1
##
## Residual standard error: 0.4597 on 122 degrees of freedom
## Multiple R-squared:  0.008253, Adjusted R-squared:  0.0001242
## F-statistic: 1.015 on 1 and 122 DF, p-value: 0.3156

beta_Age65_84 <- mod_Age65_84$coefficient
beta_Age65_84

## Intercept      PctAge65_84
## 1.30339487    -0.01486033

se_Age65_84 <- sqrt(diag(vcovHC(mod_Age65_84, type = "HC0")))
se_Age65_84

## Intercept      PctAge65_84
## 0.106804051    0.009984258

cbind(beta_Age65_84- q*se_Age65_84, beta_Age65_84 + q*se_Age65_84)

##              [,1]      [,2]
## Intercept    1.09406277  1.512726962
## PctAge65_84 -0.03442912  0.004708454

2*pnorm(abs(beta_Age65_84/se_Age65_84), lower.tail=FALSE)

## Intercept      PctAge65_84
## 2.973470e-34    1.366517e-01

mod_AgeG85<-lm(RRglm~PctAgeG85,data=dat2)
summary(mod_AgeG85)
## Call:
## lm(formula = RRglm ~ PctAgeG85, data = dat2)
##
## Residuals:

```

```
##   Min   1Q  Median   3Q   Max
## -1.19843 -0.14868 -0.05873 0.01757 2.91617
##
## Coefficients:
##           Estimate   Std. Error  t value  Pr(>|t|)
## Intercept      1.24655    0.07856   15.868  <2e-16 ***
## PctAgeG85     -0.05941    0.04786   -1.241   0.217
## ---
## Signif. codes:  0 '***' 0.001 '**' 0.01 '*' 0.05 '.' 0.1 ' ' 1
##
## Residual standard error: 0.4587 on 122 degrees of freedom
## Multiple R-squared:  0.01247, Adjusted R-squared:  0.004379
## F-statistic: 1.541 on 1 and 122 DF, p-value: 0.2169
```

```
beta_AgeG85 <- mod_AgeG85$coefficient
beta_AgeG85
```

```
## Intercept      PctAgeG85
## 1.24655377    -0.05941194
```

```
se_AgeG85 <- sqrt(diag(vcovHC(mod_AgeG85, type = "HCO")))
se_AgeG85
```

```
## Intercept      PctAgeG85
## 0.08720122     0.03767876
```

```
cbind(beta_AgeG85- q*se_AgeG85, beta_AgeG85 + q*se_AgeG85)
```

```
##           [,1]      [,2]
## Intercept  1.0756425  1.41746502
## PctAgeG85 -0.1332609  0.01443708
```

```
2*pnorm(abs(beta_AgeG85/se_AgeG85), lower.tail=FALSE)
```

```
## Intercept      PctAgeG85
## 2.346290e-46    1.148411e-01
```

```
#####
### Model selection
#####
```

```
### helper function to split data into 10 folds
```

```
make_fold <- function(N, nfold=10){
```

```

index <- sample(N)
temp <- floor(N/nfold)
fold <- c(rep(1:nfold, temp), 1:(N-nfold*temp))
result <- list(index=index, fold=fold)
return(result)
}

```

function to predict for regsubsets object

```

mypredict <- function(object, newdata, id, ...){
  form <- as.formula(object$call[[2]])
  mat <- model.matrix(form, newdata)
  coefi <- coef(object, id = id)
  xvars <- names(coefi)
  out <- mat[,xvars] %*% coefi
  return(out)
}

```

CV and best subset selection for RRglm as outcome

```

p <- length(list_var1)
k <- 10
N <- nrow(BLSvic2)

```

```

myseed <- 20170215
set.seed(myseed)
folds <- make_fold(N = N)

```

Use bestglm, with AIC criteria

```

cv1_errors_bestglm <- cv2_errors_bestglm <- matrix(NA, nrow=k, ncol=p-1, dimnames=list(NULL, paste(1:(p-1))))

```

```

for(i in 1:k){
  test1 <- dat1[folds$index[folds$fold==i], ]
  train1 <- dat1[folds$index[folds$fold!=i], ]
  bestfit1 <- bestglm(train1, IC="AIC")
  out1 <- bestfit1$Subsets[-1, -c(1, 15, 16)]

```

```

test2 <- dat2[folds$index[folds$fold==i], ]
train2 <- dat2[folds$index[folds$fold!=i], ]

```

```

bestfit2 <- bestglm(train2, IC="AIC")
out2 <- bestfit2$Subsets[-1, -c(1, 15, 16)]

for(j in 1:(p-1)){
  varname1 <- names(out1)[which(out1[j,] == TRUE)]
  formula1 <- as.formula(paste("RRglm ~", varname1))
  mod1 <- lm(formula1, data=train1)
  pred1 <- predict(mod1, newdata=test1)
  cv1_errors_bestglm[i, j] <- mean( (test1$RRglm - pred1)^2, na.rm=TRUE)

  varname2 <- names(out2)[which(out2[j,] == TRUE)]
  formula2 <- as.formula(paste("RRglm ~", varname2))
  mod2 <- lm(formula2, data=train2)
  pred2 <- predict(mod2, newdata=test2)
  cv2_errors_bestglm[i, j] <- mean( (test2$RRglm - pred2)^2, na.rm=TRUE)
}
}

mean_cv1_errors_bestglm <- apply(cv1_errors_bestglm, 2, mean)
mean_cv2_errors_bestglm <- apply(cv2_errors_bestglm, 2, mean)

best_nvars1_bestglm <- which.min(mean_cv1_errors_bestglm)
best_nvars1_bestglm

## 3
## 3

best_nvars2_bestglm <- which.min(mean_cv2_errors_bestglm)
best_nvars2_bestglm

## 3
## 3

fullselection1_bestglm <- bestglm(dat1, IC="AIC")

subset1_bestglm <- fullselection1_bestglm$Subsets[-1, -c(1, 15, 16)]
varname1_bestglm <- names(subset1_bestglm)[which(subset1_bestglm[best_nvars1_bestglm,] == TRUE)]
formula1_bestglm <- as.formula(paste("RRglm ~", paste(varname1_bestglm, collapse=" + ")))
formula1_bestglm

## RRglm ~ PctImpervious_cat + logPop + MedIncome_cat

```

```

finalmod1_bestglm <- lm(formula1_bestglm, data=dat1)
summary(finalmod1_bestglm)
## Call:
## lm(formula = formula1_bestglm, data = dat1)
##
## Residuals:
##   Min     1Q   Median     3Q      Max
## -1.29187 -0.15255 -0.01161  0.06302  2.70531
##
## Coefficients:
##
##              Estimate Std. Error t value Pr(>|t|)
## Intercept          0.88760   0.30387   2.921  0.00419 **
## PctImpervious_cat(25th, 50th] -0.20542   0.14740  -1.394  0.16610
## PctImpervious_cat(50th, 75th] -0.39100   0.21037  -1.859  0.06562 .
## PctImpervious_cat(75th, 100th] -0.44432   0.26245  -1.693  0.09314 .
## logPop              0.05412   0.04750   1.139  0.25691
## MedIncome_cat(25th, 50th]   0.19071   0.12595   1.514  0.13268
## MedIncome_cat(50th, 75th]   0.06171   0.12963   0.476  0.63493
## MedIncome_cat(75th, 100th]  0.03806   0.13895   0.274  0.78464
##
## Signif. codes:  0 '***' 0.001 '**' 0.01 '*' 0.05 '.' 0.1 ' ' 1
##
## Residual standard error: 0.4549 on 116 degrees of freedom
## Multiple R-squared:  0.07659, Adjusted R-squared:  0.02087
## F-statistic: 1.375 on 7 and 116 DF, p-value: 0.2226

q <- qnorm(0.975)
beta1_bestglm <- finalmod1_bestglm$coefficient
beta1_bestglm

##Intercept PctImpervious_cat(25th, 50th]PctImpervious_cat(50th, 75th]PctImpervious_cat(75th, 100th]
##0.88759656   -0.20541574           -0.39099519           -0.44432200

##logPop MedIncome_cat(25th, 50th]MedIncome_cat(50th, 75th] MedIncome_cat(75th, 100th]
## 0.05411585   0.19071140           0.06171304           0.03806156

se1_bestglm <- sqrt(diag(vcovHC(finalmod1_bestglm, type = "HCO")))
se1_bestglm

##Intercept PctImpervious_cat(25th, 50th]PctImpervious_cat(50th, 75th]PctImpervious_cat(75th, 100th]

```

```
##0.27986372    0.19810793          0.24352819          0.27858786
##logPop MedIncome_cat(25th, 50th] MedIncome_cat(50th, 75th]MedIncome_cat(75th, 100th]
## 0.04458402    0.09746545          0.07903991          0.10228889
```

```
cbind(beta1_bestglm - q*se1_bestglm, beta1_bestglm + q*se1_bestglm)
```

```
##                [,1]      [,2]
## Intercept      0.3390737525  1.43611936
## PctImpervious_cat(25th, 50th] -0.5937001455  0.18286867
## PctImpervious_cat(50th, 75th] -0.8683016713  0.08631129
## PctImpervious_cat(75th, 100th ] -0.9903441674  0.10170018
## logPop          -0.0332672350  0.14149893
## MedIncome_cat(25th, 50th] -0.0003173625  0.38174017
## MedIncome_cat(50th, 75th] -0.0932023254  0.21662841
## MedIncome_cat(75th, 100th] -0.1624209867  0.23854411
```

```
2*pnorm(abs(beta1_bestglm/se1_bestglm), lower.tail=FALSE)
```

```
##Intercept PctImpervious_cat(25th, 50th]PctImpervious_cat(50th, 75th]PctImpervious_cat(75th, 100th]
##0.001516375    0.299788046          0.108374165          0.110732819
##logPop MedIncome_cat(25th, 50th]MedIncome_cat(50th, 75th] MedIncome_cat(75th, 100th]
##0.224826180    0.050381829          0.434929919          0.709819390
```

```
anova(lm(RRglm ~ 1, data=dat1), finalmod1_bestglm)
```

```
## Analysis of Variance Table
```

```
##
```

```
## Model 1: RRglm ~ 1
```

```
## Model 2: RRglm ~ PctImpervious_cat + logPop + MedIncome_cat
```

```
## Res.Df  RSS Df Sum of Sq  F Pr(>F)
```

```
## 1  123 25.999
```

```
## 2  116 24.008 7  1.9913 1.3745 0.2226
```

```
fullselection2_bestglm <- bestglm(dat2, IC="AIC")
```

```
subset2_bestglm <- fullselection2_bestglm$Subsets[-1, -c(1, 15, 16)]
```

```
varname2_bestglm <- names(subset2_bestglm)[which(subset2_bestglm[best_nvars2_bestglm,] == TRUE)]
```

```
formula2_bestglm <- as.formula(paste("RRglm ~", paste(varname2_bestglm, collapse=" + ")))
```

```
formula2_bestglm
```

```
## RRglm ~ PctAgeL5 + PctAge15_44 + PctAge65_84
```

```

finalmod2_bestglm <- lm(formula2_bestglm, data=dat2)
summary(finalmod2_bestglm)
## Call:
## lm(formula = formula2_bestglm, data = dat2)
##
## Residuals:
##   Min       1Q   Median       3Q      Max
## -1.28727 -0.13933 -0.02745  0.04372  2.80343
##
## Coefficients:
##              Estimate Std. Error t value Pr(>|t|)
## (Intercept)  2.229852  0.494518  4.509  1.53e-05 ***
## PctAgeL5     -0.056808  0.036167 -1.571  0.1189
## PctAge15_44 -0.008340  0.008357 -0.998  0.3203
## PctAge65_84 -0.042818  0.019953 -2.146  0.0339 *
##
## Signif. codes:  0 '***' 0.001 '**' 0.01 '*' 0.05 '.' 0.1 ' ' 1
##
## Residual standard error: 0.4556 on 120 degrees of freedom
## Multiple R-squared:  0.04212, Adjusted R-squared:  0.01818
## F-statistic: 1.759 on 3 and 120 DF, p-value: 0.1587

beta2_bestglm <- finalmod2_bestglm$coefficient
beta2_bestglm

##Intercept      PctAgeL5      PctAge15_44  PctAge65_84
##2.229851630 -0.056808363 -0.008340233 -0.042817759

se2_bestglm <- sqrt(diag(vcovHC(finalmod2_bestglm, type = "HCO")))
se2_bestglm

## Intercept      PctAgeL5      PctAge15_44  PctAge65_84
## 0.648528833  0.044928991  0.005125111  0.021958797

cbind(beta2_bestglm - q*se2_bestglm, beta2_bestglm + q*se2_bestglm)

##              [,1]      [,2]
## Intercept  0.95875848  3.5009447853
## PctAgeL5   -0.14486757  0.0312508410
## PctAge15_44 -0.01838527  0.0017047999
## PctAge65_84 -0.08585621  0.0002206923

```

```

2*pnorm(abs(beta2_bestglm/se2_bestglm), lower.tail=FALSE)

## Intercept      PctAgeL5      PctAge15_44 PctAge65_84
## 0.000585329 0.206085319 0.103667605 0.051186407

anova(lm(RRglm ~ 1, data=dat2), finalmod2_bestglm)

## Analysis of Variance Table
##
## Model 1: RRglm ~ 1
## Model 2: RRglm ~ PctAgeL5 + PctAge15_44 + PctAge65_84
## Res.Df  RSS Df Sum of Sq  F Pr(>F)
## 1  123 25.999
## 2  120 24.904 3  1.0951 1.759 0.1587

#####
### Moran's I Test
#####

### merge with polygons
vicgrid_BLS <- merge(vicgrid, BLSvic, by = "GRIDCODE")
vicgrid_BLS2 <- merge(vicgrid, BLSvic2, by = "GRIDCODE")

vic.nb <- poly2nb(vicgrid)
col.W <- nb2listw(vic.nb, style = "W", zero.policy = TRUE)

### use residuals from finalmod1_bestglm
res1_bestglm <- finalmod1_bestglm$residuals
resdat1_bestglm <- data.frame(GRIDCODE = BLSvic2$GRIDCODE, res = res1_bestglm)
vicgrid1_bestglm <- merge(vicgrid_BLS2, resdat1_bestglm, by="GRIDCODE")
moran.test(vicgrid1_bestglm$res, col.W, na.action=na.omit)
## Moran I statistic standard deviate = 0.15901, p-value = 0.4368
## alternative hypothesis: greater
## sample estimates:
## Moran I statistic  Expectation  Variance
## 4.226146e-05 -8.130081e-03 2.641612e-03

### use residuals from finalmod2_bestglm
res2_bestglm <- finalmod2_bestglm$residuals
resdat2_bestglm <- data.frame(GRIDCODE = BLSvic2$GRIDCODE, res = res2_bestglm)
vicgrid2_bestglm <- merge(vicgrid_BLS2, resdat2_bestglm, by="GRIDCODE")

```

```
moran.test(vicgrid2_bestglm$res, col.W, na.action=na.omit)
## Moran I statistic standard deviate = 0.21864, p-value = 0.4135
## alternative hypothesis: greater
## sample estimates:
## Moran I statistic   Expectation   Variance
## 0.003046099      -0.008130081    0.002613029
```